

Analysis and Modeling of Industrial Purified Terephthalic Acid Oxidation Process

Shengjing Mu, Hongye Su, Ruilan Liu, Yong Gu, Jian Chu

National Laboratory of Industrial Control Technology, Institute of Advanced Process Control, Zhejiang University, Yuquan Campus, Hangzhou, 310027, P.R.China

Abstract: A mathematic model to predict the concentration of 4-carboxy-benzaldehyde (4-CBA) for an industrial Purified Terephthalic Acid (PTA) oxidation unit is built in this paper. The model is based on a mechanism model from the results of bench-scale laboratory experiment and chemical reaction principle, which is structured into two series ideal CSTR models. Six plant factors are designed to correct the deviation between the laboratory model and the industrial practice. For the existing of substantial time delays between process variables and quality variable, the weighted moving average method is applied to make each variable be in same time slice. The analysis of process data by projection on latent variables of Partial Least Square (PLS) and analysis of Hotelling's T-squared statistic value of Principal Component Analysis (PCA) are gave to discriminate the operating data into normal operating part and load down and load up operating part. At the each operating part, the typical data are selected to regress the plant factors. The proposed model predictive result follows the tracks of the observed value quite well. Compared with the empirical Amoco model, the proposed model is regarded as to be more suitable to be applied to industrial online soft sensor.

Key Words: Purified Terephthalic acid (PTA) process, mechanism model, plant factor, Partial Least Square (PLS), Principal Component Analysis (PCA), time delay

1. INTRODUCTION

In this Purified Terephthalic acid (PTA) oxidation reaction, a proprietary process of Amoco Chemical Company is employed for the catalytic liquid phase air oxidation of paraxilene. More than 30 patents about PTA oxidation process and the design of its oxidation reactor have been proposed in the past decade (Li, et al., 2001). The research works about oxidation mechanism with high temperature and normal pressure also have obtained many progresses (Lindahl, et al., 1989, Ge, 1993, Wang, 2001). Lindahl, et al. (1989) gave a set of empirical

mathematical relationships between the oxygen uptake in the first crystallizer, the CO₂ in the vent gas from the reactor stage and 4-carboxy-benzaldehyde (4-CBA) content levels. But the empirical model needs a bulk of data to regress model parameters and often suitable to a limited operating region. Ge (1993) provided the experiment results of catalytic oxidation kinetics of acetic acid-p-xylene system in liquid phase qualitatively. Wang (2001) proposed a first principle model based on bench-scale laboratory results. It simulated the effect of reactive temperature, catalyst ingredient and concentration, residence time, vent oxygen concentration to the concentration of the

Corresponding author email: sjmu@iipc.zju.edu.cn

reactants. But the experimental model was only verified by few industrial data, and many of industrial application problems were not settled.

The paper proposes a practical mathematic model to predict the concentration of 4-carboxybenzaldehyde (4-CBA) for an industrial purified terephthalic acid (PTA) oxidation unit. The first principle model based on laboratory experiments is applied and modified according to the analysis of the process. The main works comprise: 1. obtaining 133 sets of process variables and corresponding quality variables by considering the time delay between them with weighted moving average method; 2. distinguishing the operating into normal operating and load down and load up operating by projection on latent variables of Partial Least Square (PLS) and analysis of Hotelling's T-squared statistic value of Principal Component Analysis (PCA); 3. configuring and regressing six plant factors to correct the deviation between the laboratory experiment and the industrial process. The model is composed of two series CSTR ideal models. The plant factors are regressed by several sets of typical industrial data. The predictive accuracy of the process model could satisfy the accuracy requirement of online soft sensor.

2. PTA OXIDATION PROCESS

Fig. 1 presents the oxidation reaction mechanism commonly used (Wang, 2001). The oxidation reaction sequence of PX generates three kinds of intermediates, p-tolualdehyde (TALD), p-toluic acid (P-T) and 4-carboxybenza-ldehyde (4-CBA).

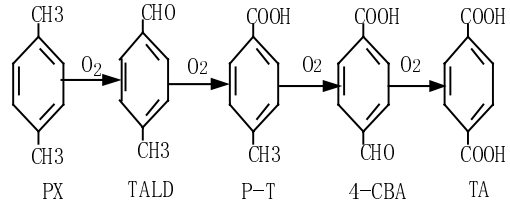


Fig. 1. The oxidation reaction process mechanism of PX

The industrial PTA oxidation process flowsheet is shown in Fig. 2. Paraxylene (PX), acetic acid solvent, promoter, and catalyst are continuously metered into feed mixing tank. The residence time is approximately 25 minutes. The mixed stream pumps the reactor, and the air are fed to the reactor through fourinlets. The oxidation reaction is conducted in two stages, first stage being the agitated oxidation reactor, while the second stage is the agitated first crystallizer. Exothermic heat of reaction is removed by condensing the boiling reaction solvent. A portion of this condensate is withdrawn to control the water concentration in the reactor, and the remainder is refluxed to the reactor.

Reactor effluent is depressurized and cooled to filtering conditions in a series of three crystallizing vessels (first crystallizer, second crystallizer and third crystallizer) for the secondary reaction and crystallization step. Air is fed to the first crystallizer for additional reaction, which used to do polishing oxidation of unreacted paraxylene from the reactor. Precipitated terephthalic acid (TA) is recovered by filtering and drying. The crude TA solids are conveyed to the purification section feed silos

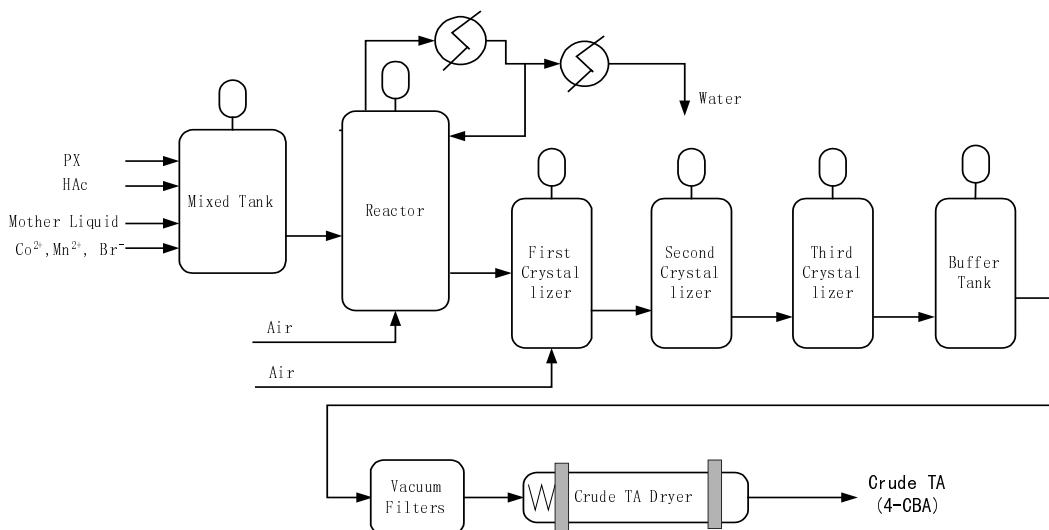


Fig. 2. Schematic layout of PTA Oxidation process

for additional processing as shown in Fig. 2.

Autoxidation of PX in acetic acid solvent with cobalt acetate, manganese acetate, and hydrobromic acid as catalysis proceeds by the following overall reaction to afford terephthalic acid in 95-96% molar yield. The combined yield of the intermediates (4-carboxybenzaldehyde, p-toluic acid and p-tolualdehyde) is about 3%. The detailed discussion about the oxidation mechanism of para-xylene can be found in Lindahl, et al. (1989), Ge (1993) and Wang (2001).

In the oxidation process, the concentration of 4-CBA is regarded as observer of the oxidation reactive progress. The 4-CBA content should be controlled in an interval. Excessive content level may lead to over-oxidation and loss more acetic acid, whereas low level represents under-oxidation and insufficient for PX convert to TA.

The concentration of 4-CBA is related with oxidation process. Therefore, the variables affect the oxidation process as well as the concentration of 4-CBA. In the oxidation reactor, the affect variables of the reactive system mostly

are the residence time of reaction, the ratio of PX to acetic acid, the ingredient and the concentration of catalyst, reaction temperature and pressure, the partial pressure of oxygen and water content in the reactor. After the comparison of these variables and process variables, 10 process variables are selected as input variables of the model, which shown in Table 1.

The schematic layout of PTA oxidation process in Fig. 2 shows that there are exist substantial time delay between the different process variables and the quality variable. Every tank has residence time from 15 minutes to 71 minutes. The total time delay of the process is about 200 minutes. The sample frequency of 4-CBA from the crude TA dryer is 3 times a day by laboratory. While the process data pick periodic is 30 seconds by DCS.

The preliminary work of process modeling is to collect the process data and corresponding quality data as many as possible. Here the ‘corresponding’ mean both the time delay and sample frequency of the two kinds of data are considered.

Table 1. The all variables of the process model.

No.	Variable	Time delay(min)	Sample frequency
<i>Inputs</i>			
1	Paraxylene to feed mixing tank	205	30 s
2	Feed to reactor	180	30 s
3	Catalyst concentration	185	30 s
4	Reactor temperature	110	30 s
5	Level of reactor	110	30 s
6	Reactor condenser to water withdraw	95	30 s
7	Vent O ₂ concentration from the reactor	95	30 s
8	Total water withdrawal	90	30 s
9	First crystallizer temperature	75	30 s
10	Vent O ₂ concentration from the first crystallizer	70	30 s
<i>Output</i>			
11	4-CBA concentration in the crude TA	0	8 hours

3. ANALYSIS AND MODELING OF INDUSTRIAL PTA OXIDATION PROCCESS

According to the industrial process, the model is composed of two series CSTR ideal models. The two ideal CSTR models denote the oxidation reactor and the first crystallizer, respectively. Each of them follows with the mechanism model developed by Wang (Wang, 2001). The feed

component of the first crystallizer is the effluent of the oxidation reactor.

Due to many factors, the plant data contain much gross error and not corresponded to each other well. Some for the measure instruments are often not well calibrated, for the process is not stable enough or the inaccuracy of quality data caused by artificial sample and analysis. In order to

utilize plant data to build the industrial process model, it is necessary to screen the data using statistical methods. By these techniques some of the inherent characteristics of the data can be incorporated into the model thereby, increasing the model accuracy.

3.1 Preprocessing industrial data

For the oxidation process comprises nearly 10 tanks shown at Fig. 2, the residence time of the all tanks is about 200 minutes. Therefore it is reasonable to expect that not the current values of these variables, but more so the historical values of the variables over the last 200 minutes are likely to have a profound effect on the output variables at the present time. To take care of the historical effect of these variables a weighted moving average method is used to define the model input variables (Radhakrishnan, et al. 2000)

$$X(t) = 0.05x(t - 2t_d) + 0.1x(t - 1.5t_d) + \\ 0.2x(t - 1.2t_d) + 0.4x(t - t_d) + \\ 0.2x(t - 0.5t_d) + 0.05x(t - 0.2t_d) \quad (1)$$

where $X(t)$ is the value at time t , $x(t-i)$ is the value at time $t-i$ of each input variables and t_d is time delay value of the variable, which is given in Table 1.

That is, the process variables at time t are the combination values of their historical data at time point $0.2t_d$, $0.5t_d$, t_d , $1.2t_d$, $1.5t_d$ and $2t_d$ before current. All of the process variables were defined in this manner as the input of the model. The weights values were decided on the basis of a residence time distribution study from the investigation on the operators and engineers and the analysis of process history data.

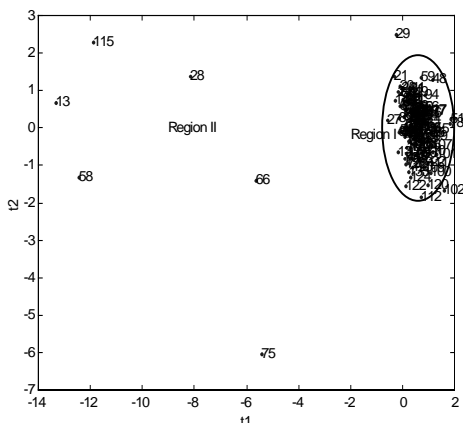


Fig. 3. Projection on latent variables determined by PLS of PTA oxidation process data

3.2 Analyzing the oxidation process

PLS and PCA are used to extract the information in the data by projecting them onto low dimensional spaces defined by the latent variables or principal components. For they are capable of tracking the progress of process and detecting the occurrence of observable upsets, PLS and PCA are widely applied in process analysis, monitor, fault diagnosis and statistical process control (Kourti, et al., 1995, MacGregor, et al. 1995).

The projection of the first two latent variables of PLS and Hotelling's T-squared statistic value of PCA to analysis historical data are illustrated in Fig. 3 and Fig. 4 from 133 sets of data of industrial PTA oxidation process.

It is obviously that there are two operating regions of the industrial data involved. Region I has the most number of points and the highest density, which belong to normal operating region and identified by the factory. Region II is a little away from region I and includes 6 points. This region is characterized as periodically load down and load up process for purging the dryer operation and adjusting the buffer tank, which the operating region is widely compared with region I.

The two operating regions have significant differences intrinsically. Thus, it is reasonable to divide the process model into two parts: normal operating part and load down and load up operating part, and be treated in different plant factors.

3.3 Setting the plant factors

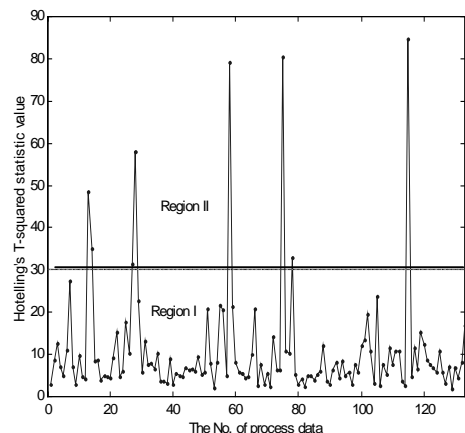


Fig. 4. Hotelling's T^2 statistic value determined by PCA of PTA oxidation process data

In the PTA oxidation process, many other factors are also effect the reaction but be hard to described in the mathematical model. For instance, the design of feed inlet of air flow, the existing of foam in the vapor phase, the effect of crystallized product to main oxidation reaction, the occurrence of subsidiary reaction and its product, the effects of other process parameters from the second crystallizer to the dryer sampling valve, etc.

To correct the deviation between the laboratory condition and industrial condition, six plant factors are set in the principle model. They correct the oxidation reactor's reactive kinetics parameters, k , the residence time, r , the feed concentration of PX, and the first crystallizer's reactive kinetics parameters, k , the residence time, r and the final discharge concentration of 4-CBA, respectively.

3.4 Regressing the plant factors

In this section, 6 sets of normal operating data from 127 total and 3 sets of load down and load up operating data from 6 total are selected as standard industrial process data to regress the two sets of plant factors, respectively. The regression algorithm is the modified Levenberg -Marquardt algorithm (Gao, 1995). It uses differential approximate the Jacobian matrix and the initial damped factor set to 40000, the adjust coefficient set to 2. To control the rate of convergence not less than a certain value, the damped factor should be larger than a threshold value. The enlarging damped factor procedure is limited to run 2 times continuously at one time and the initial value is set to initial damped factor at every time the procedure be called.

The result of plant factor regression is given in the table 2. After obtained the plant factors, the model is determined and able to predict the concentration of 4-CBA in the crude TA as a kernel part of on-line soft sensor.

Table 2. The two sets of plant factors regress results from each operating data.

	F1	F2	F3	F4	F5	F6
Normal operating	1.5911	0.8701	0.9838	0.1215	1.2705	0.3529
Load down and load up operating	1.1807	0.7677	0.5197	0.6395	1.0532	0.8768

4. RESULTS & DISCUSSION

The comparison of predictive results of the proposed model, Amoco empirical model (Lindahl, et al., 1989) and observed concentration of 4-CBA is given in Fig. 5. It is obviously illustrate that the predictive result of the proposed model follows to the tracks of the observed value quite well, especially at the normal operating part, whereas the predictive result of Amoco model only lie near the mean value of observed in normal operating region and can't well follow the observed change trend. This feature is important in applying to industrial online soft sensor, which the qualitative tendency is the preference. Though the predictive mean error of our model is $\pm 1.54\%$ and the maximum error is $\pm 6.03\%$, which are both a little worse than those of the Amoco model, $\pm 1.49\%$ and $\pm 4.67\%$.

At the points 7, 88 and 105, the observed quality value is badly higher than its neighbors. But its associated process variables have not marked changes compared with others. Similarly, the observed values at points 25, 26, 54 and 65 are

less than the corresponding points of the model predict values extraordinary. Thus, these points can be regarded as outliers that their process data are anomalous. The predict result of load down and load up operating part are not very well as that of the normal operating part, which contributes to most predictive error for the whole MSE, because it is not operated at steady state that both the process variables and their residence time are under largely dynamic change. But the predictive trend of load down and load up operating is quite well, which was also confirmed by the engineers.

On the whole, the proposed model predictive accuracy is satisfied with the requirement of online soft sensor.

5. CONCLUSION

This paper proposed a practical mathematic model to predict the concentration of 4-CBA in PTA oxidation process. The model is based on a first principle model and modified according to the industrial practice. Several technologies are

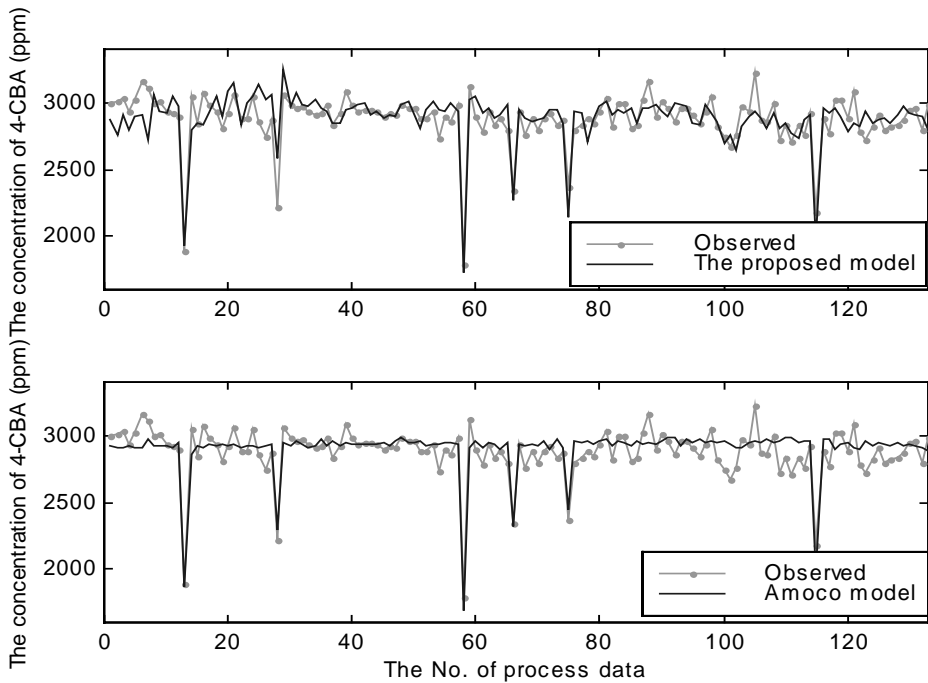


Fig. 5. The results comparison among the proposed model, Amoco empirical model and the observed values.

applied to cope with the problems in process data. Firstly, considering the exact estimation of the time delay between variables and quality variable is difficult, a weighted moving average method is used to combine 6 values at different time point from the 0.2 times estimated time delay to double time delay in the past as the model input variables. Then the projection on latent variables and Hotelling's T-squared statistic are made to identify two operating regions, which are also confirmed by the engineers. For many of factors in the industrial process are hard to considered in the mathematics model, six plant factors are used to correct the deviation between the laboratory model and the industrial process model. Robust nonlinear least square method, modified Levenberg-Marquardt method is applied to regress the six plant factors. Finally, the satisfactory predict results prove that the proposed model is inspiring in applying to industrial online soft sensor.

ACKNOWLEDGEMENT

This work is supported by The National Outstanding Youth Science Foundation of China (NSFC: 60025308).

REFERENCES

Li X. Xie G., Hua W. (2001), Key problems and

research program for PTA process domestic development, *Polyester Industry*, Chinese, 14(1):1-7.

Lindahl H. A., et al. (1989), Method and apparatus for controlling the manufacture of terephthalic acid to control the level and variability of the contaminant content and the optical density, *US Patent*, 4835307.

Wang L. J. (2001), Studies on the Kinetics of p-Xylene oxidation and the reactor simulation, Dissertation for Master Degree, Zhejiang University, Chinese.

Ge X.D. (1993), Studies on Catalytic Oxidation Kinetics of Acetic Acid-p-Xylene System in Liquid Phase, *Petrochemical Technology*, Chinese, 11:715.

Radhakrishnan V.R., Mahamed A.R. (2000), Neural networks for the identification and control of blast furnace hot metal quality, *Journal of process control*, 10(6): 509-524.

Kourti, T., Nomikos, P. and MacGregor, J.F. (1995). Analysis, Monitoring and Fault Diagnosis of Batch Processes Using Multiblock and Multiway PLS. *Journal of Process Control*, No. 5, pp. 277-284.

MacGregor J.F. and Kourti T. (1995), Statistical process control of multivariate processes, *Control Engineering Practice*, 3 (3) 403-414.

Gao H. (1995), *Statistical Computer*, pp380-391, Peking University Press, Beijing, Chinese.

ANALYSING THE START UP OF REACTIVE DISTILLATION COLUMNS

Frauke Reepmeyer, Jens-Uwe Repke, Günter Wozny

Technical University Berlin, Dep. of Process Dynamics and Operation
Sekr. KWT-9, Str. d.17.Juni 135, 10623 Berlin, Germany

Abstract: In this paper a simulation model developed for the start up process of a cold and empty reactive distillation (RD) column is presented. The rigorous model is experimentally validated with data from a pilot plant at the department. The sample reaction is a transesterification of a fatty methylester with isopropanol. With the validated model, different start up strategies, known from conventional distillation have been applied. It was found, that the total reflux strategy cannot be recommended for RD processes. Mathematical optimization of the control variables heating duty, reflux and feed flowrate did not show significant savings in start up time. Alternative strategies utilizing product recycle flows and initial column charges are presented. With these strategies about 80% of the necessary start up time could be saved. *Copyright © 2003 IFAC*

Keywords: reactive distillation, start up, dynamic models, simulation, dynamic optimisation

1. INTRODCUTION

In recent years the integration of reaction and distillation in one process gained industrial and academic interest. The combination of two processes in one piece of equipment can help saving enormous investment and operating costs. The industrial application of reactive distillation processes ranges from esterification (like methyl-, ethyl and butyl acetate) to fuel additives (MTBE, ETBE, TAME) and some alkylations.

With equilibrium limited reactions the thermal separation of the products from the reaction zone can increase the yield of the desired components. Exothermal reaction can contribute to the energy demand of a distillation. This makes reactive distillation a favourable process alternative.

The complexity of the process increases with the interaction of reaction and separation. This requires a better knowledge of the process and the kinetic activities. The steady state process synthesis and simulation for reactive distillation has widely been examined. A comprehensive overview is given by Doherty and Buzad (1992) and Taylor and Krishna (2000).

Exo- and endothermic reactions and changes in feed flows and compositions can have a big impact on the yield in the reactive zone and the required product quality. It is therefore necessary to also analyse the dynamic behaviour of reactive distillation processes, which gained attention just recently. As sample processes the production of acetates with different alcohols were used by Alejski and Duprat (1996) or

Scenna et al. (1998). But these papers all focus on the dynamic behaviour near a known operating point based on a known steady state.

The start up of each distillation column and especially an RD column is a time and energy consuming process. In contrast to distillation without reaction, the off-spec product produced during start up can mostly not be recycled back to the feed stream but most costly be disposed. Also the control of a start up process is very challenging. Almost all process variables change rapidly in value, control variables like heating power, reflux ratio or feed flow have to be switched at least once, but mostly several times to reach steady state. Different start up strategies can yield different, undesired steady states. Processes that show multiplicities and their analysis can be found at Güttinger (1998) and Scenna and Benz (2003). In these papers, the column does not start from a cold and empty state, but from a defined state, with trays filled an warm. To have consistent and physically sound starting values for a process, it is necessary to simulate the complete start up process. In the paper we introduce a rigorous model to simulate the dynamic behaviour of a column from the cold and empty state. The model is validated with experimental data from a pilot plant with a reaction of fatty methylester to isopropylester. Then start up strategies known from conventional distillation are presented and applied to RD. Alternative strategies to minimize the start up time are developed with the aid of the rigorous simulation model.

2. START UP OF REACTIVE COLUMNS

The start up procedure for distillation columns without reaction has already been examined. Kister (1979) describes problems with column start ups. Eden et al. (2000) developed a procedure for generating start up sequences utilizing process knowledge for heat integrated columns. Löwe (2001) developed an optimised strategy for the start up of an energy integrated column system and validated the results. Gani et al. (1987), Gani et al. (1998) published various papers on dynamic simulation of distillation columns with the total reflux strategy. The strategy that is recommended for most of the column start up processes is the total reflux operation.

In the following four strategies that are used are explained and the classifying parameters are explained:

- 1) Conventional strategy: The empty and cold column is filled with feed, than all control variables (mainly heating power, reflux rate, feed composition and rate) are set to their steady state values.
- 2) Total reflux: The column is filled with feed. Heating begins, if the first distillate reaches the reflux drum, all material is refluxed back into the column. No distillate is taken from the top.
- 3) Total distillate removal: during the start up the distillate is completely taken away at the top, there is no reflux stream back into the column.
- 4) Improved strategy (developed for heat integrated columns): reflux and reboiler heat duty are set to approximately 1.3 times their steady state value.

The time, where the control variables are switched for strategy 2) to 4) is calculated via the so called MT-function developed by Yasuoka et al. (1987) for distillation without reaction.

$$MT = \sum_{\text{trays}} (T_{\text{tray, current}} - T_{\text{steady state}}) = \min \quad (1)$$

The MT function is the sum over all trays of the deviations of the actual measured temperature profile to steady state profile, therefore it can be seen as a measure for the distance to steady state. If the function reaches a minimum, the variables should be adjusted to steady state values. With the total distillate removal strategy using the MT function as an indicator for switching, the time for start up of distillation without reaction could be reduced by up to 90% (Kruse et al. (1996); Flender (1999)).

2.1. Modelling and Simulation

To simulate a start up procedure from the cold and empty state to a steady state point a description with just one set of equations is not enough. During the fill up and heating, the trays are not at physical or chemical equilibrium. Therefore it is necessary to have two sets of equations that are active at different

times during the dynamic simulation. The first set is active during the fill up and heating of the column to the boiling point. Once the boiling point of a tray is reached, the second set of equations is activated.

The assumptions made within the overall model are:

- the reaction only takes place in the liquid phase (homogeneous catalysis with sulfuric acid)
- vapour and liquid phase are in phase equilibrium
- vapour phase shows ideal behavior (operation at ambient pressure)

The start up process for a tray is demonstrated in figure 1. In Phase I the tray is empty, cold and at ambient pressure. Feed fills the tray until liquid leaves the stage to the stage below. In phase III vapor from the below stage is entering the stage and heating it up until in phase IV the mixture's bubble pressure reaches the set pressure of 1 bar. The equations are then switched to phase equilibrium. In phase V the stage pressure is higher than the pressure from the stage above, vapor is leaving the stage. In phase VI the stage is operating at steady state. In phases I to IV the first set of equations is active. The switching point is reached exactly if $p_{\text{bub}} = p_{\text{set}}$. Then the phase equilibrium equation is applied.

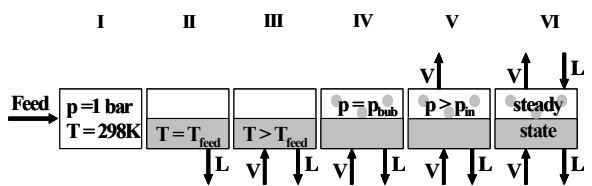


Fig. 1: different states of sample tray during start up

Additionally to the known equations (component, mass and energy balances, Francis weir formula), that are valid from phase I to phase VI, equation 2 and 3 have to be switched if phase IV is reached. For the fill up phase (I-IV), the vapour holdup is set to zero and the vapour compositions are equal to the liquid compositions. Further the pressure is fixed at arbitrarily 1 bar. Once the bubble pressure of the mixture on a tray is reached ($p_{\text{bub}} \geq p_{\text{tray}}$), the equations are switched to

$$M_{\text{Tot,vap}} = 0 \rightarrow V_{\text{tray}} = M_{\text{Tot,vap}} \cdot v^v + M_{\text{Tot,liq}} \cdot v^l \quad (2)$$

$$y_i = x_i \rightarrow y_i \cdot p_{\text{tray}} = \gamma_i \cdot x_i \cdot p_{\text{vap}}^i \quad (3)$$

The reaction rate is captured with a kinetic approach.

$$r_A = k_{\text{for}} \cdot x_A \cdot x_B - k_{\text{back}} \cdot x_C \cdot x_D \quad (4)$$

The sample reaction is a second order reaction from the type $A + B \leftrightarrow C + D$. A detailed listing of the describing equations can be found in Reepmeyer et al. (2003).

2.2. Experimental Validation

For the validation of the rigorous model to simulate the start up of a reactive distillation column from the cold and empty state, experiments with the pilot plant

at TU Berlin have been conducted. As a sample reaction the transesterification of a fatty methyl ester (ME) with isopropanol (IPA) to isopropylester (IPE) and methanol (MeOH) has been chosen. The data of the process are summarized in table 1.

Tab. 1: data for pilot plant at department

number of trays	28	holdup reboiler [l]	5.7
tray holdup [l]	0.3	reflux flow [l/h]	2.3
feed flow ME [l/h]	4	feed flow IPA [l/h]	6
ME temp. [°C]	80	IPA temp. [°C]	130
tray diameter [m]	0.1	tray spacing [m]	0.18

The column has two feeds, one at the top, where the high boiling methylester (ME) is inserted and one at the bottom, where the lowboiling isopropanol (IPA) is prevaporized. Figure 2 shows the comparison of the dynamic temperature profile from the cold and empty state to the steady state point. As can be seen from the figure, the dynamic characteristics of the temperature are well captured. The time were the first vapour reaches the top tray (about 180 mins) can be well predicted by the simulation.

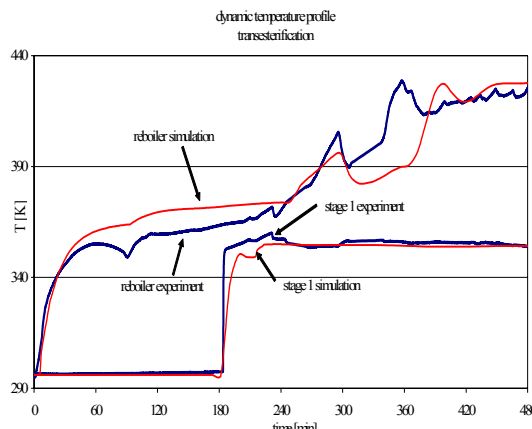


Fig. 2: dynamic validation: experiment vs. simulation for transesterification

But it is important to not only match the temperature profile, but also the dynamic changes in composition to be sure, the precise steady state desired is reached. Especially for RD, the temperature profile is not sufficient to describe a steady state. Therefore during the experiments liquid samples over the column height have been taken. The samples have been diluted with isoctan and have been analysed with a gas chromatograph. First, the steady state profile over the column height is compared to the simulation data. Figure 3 shows the simulation data in lines and the experimental data in dots. It can be stated, that simulation and experimental data show a pretty good fit. The highest deviation for the reboiler methylester concentration is below 10 mole%.

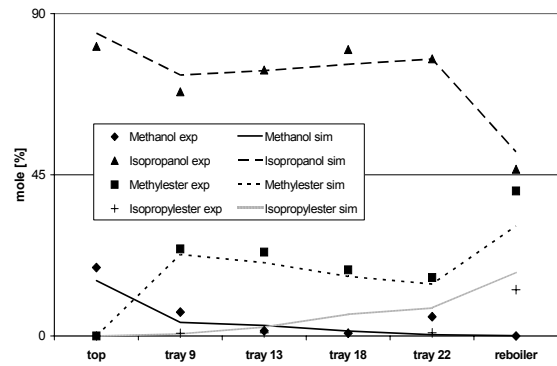


Fig. 3: steady state validation: concentration profile

The following figure 4 shows a comparison of the dynamic concentration profile for simulation and experiment for the reboiler.

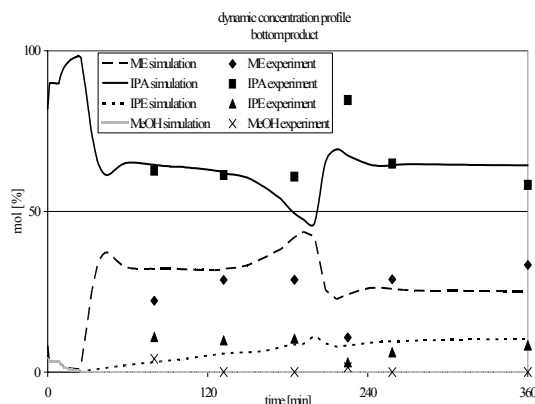


Fig. 4: dynamic validation: concentration profile

As can be seen, the dynamic trend of the concentration is well simulated. The highest deviation between experiment and simulation is 12%. The fit between simulation data and experimental data is satisfactory. It has been shown that the simulated temperature and concentration profiles resemble the experimental data in the steady state as well as in the dynamic start up phase. With this now experimentally validated model, the different start up strategies are calculated.

2.3. Start up times

With the now validated model, start up times for the process are calculated. First the strategies known from distillation without reaction are tested. Table 2 shows the results.

Tab. 2: Comparison of start up times

strategy	start up time [min]
conventional	180
total reflux	260
total distillate removal	182
improved	191

The start up times show, that the strategy of total reflux, recommended for distillation without reaction takes in comparison the longest start up time. The conventional strategy is the best out of these four alternatives.

This sample process of a transesterification has shown, that it is possible to predict the dynamic behavior of a RD start up process with the presented rigoros model. Now the model is applied to a known process, the production of ethyl acetate.

2.4. Ethyl acetate process

The production of ethyl acetate from acetic acid and ethanol has been investigated by several authors like Kenig et al. (2001), Suzuki et al. (1971), Alejski and Duprat (1996) or Lee and Dudukovic (1998). Most of them rely on the following process design.

Tab. 3: ethyl acetate process from Lee and Dudukovic (1998)

number of trays	13	reflux ratio	10
feed tray	6	feed [mol/s]	1.076
diameter [m]	0.6	holdup reb [l]	10
holdup tray [l]	3	weir height [m]	0.05
feed composition (acetic acid, ethanol, water, ethylacetate)	0.4963, 0.4808, 0.0229, 0		

With the model the start up times for this process have been calculated. The following table summarizes the results for the four mentioned strategies.

Tab. 4: start up time: esterification

strategy	start up time [min]
conventional	175
total reflux	225
total distillate removal	183
improved strategy	191

Here the same conclusions can be made as with the transesterification. The total reflux strategy takes the longest time to reach steady state. Therefore it is not suited for reactive distillation processes. The following chapters all base on the esterification as a sample reaction.

3. ALTERNATIVE START UP STRATEGIES

As could be seen from the calculations utilizing the start up strategies for conventional distillation, not much start up time could be saved. Mathematical optimization of the rigoros model, with control variables heating duty, reflux and feed flow and objective function start up time, do not show promise,

because the results would lie between the strategy of total reflux and total distillate removal. Even multiple switching in control parameter sets would not yield significant saving of start up time.

Therefore different procedures have to be developed, starting from different conditions breaking new ground instead of optimizing control variables reflux, heating and feed flow rate. In the following two examples are presented.

- initial charge of the column stages with feed stock, bottom or top product or one reactant in excess
- recycling of top or bottom product during the start up phase

As a measure for reaching the steady state, the MX function for top and bottom product is taken here. The MX function is based on the MT function explained earlier, taking into account the deviation of the top product compositions from the actual point in time to the steady state. The same is done for the bottom product.

$$MX_{Top} = \sum_{\text{components}} \left| (x_{i,top,current} - x_{i,top,steadystate}) \right| \quad (5)$$

If the $MX < 0.01$, the start up period is defined to be finished.

3.1. DIFFERENT INITIAL COLUMN CHARGES

In conventional start up the column is first filled with the feed. Opposite to this, it is possible to charge the column not with feed, but with liquid having a different composition. The following figure 5 shows a simulation of cases for ethyl acetate production with different initial charges. In the diagramm the MX function over time is drawn. Five different charges have been calculated. For the feed composition this is 49.63% acetic acid and 48.08% ethanol, for the top and bottom product it is the steady state composition of the two streams and for acetic acid and ethanol, it is pure educt.

As can be seen from the figure and also from the table showing the start up times, a significant amount of time can be saved, if the low boiler (in this case ethylacetate and ethanol) is initially charged. With pure ethanol as charge, the start up time reduces by 23%, and even more (82%) if the top product is charged to the column. In this column two numbers are listed, because if top product is charged, obviously the MX function for the bottom product takes longer to reach steady state (1.07 h).

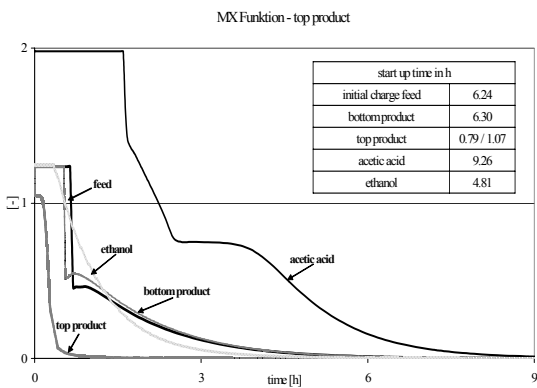


Fig. 5: MX_{Top} function for different initial charges

Therefore it is usefull to save some of the top product to recharge the column before the next start up. In the next step a cost optimization has to be executed to see, if the savings in time and off-spec product can compensate the losses in top product. With this significant savings in start up time, the initial charging with top product should be the strategy of choice, if the desired product is the low boiler.

The same set up has been simulated for the transesterification of methylester as in the experiments. Here four different initial charges have been tested. Initially charged with pure methylester and pure isopropanol and charged with bottom product of molar composition ME 52.2%, IPA 34.7%, IPE 12.7% and MeOH 0.4% and with top product of molar composition [0,87.1%, 0, 12.9%]. The required start up times are summarized in the following table

Tab. 5: start up times for initial charges

initially charged with	start up time [h]
pure methylester	5.08
pure isopropanol	5.10
top product	5.23
bottom product	5.27

It can be seen, that the strategy that could save significant amounts of start up time for the ethylacetate process is not the first choice for the transesterification process. The relative volatilities of the products and the kinetics of the reaction have a significant influence in the choice of a sensible start up strategy.

3.2. Recycle of top and bottom product

Another alternative to shorten the start up time of an reactive distillation process is to recycle top and bottom product, that is off spec. This also saves the expensive disposal.

In these simulations, a splitter, that splits the product stream (splitfactor = product/recyclestream) and a

mixer, that mixes the recycle stream with the feed are introduced. The first diagramm shows the recycling of the bottom product with different split factors continuing for different times again for the ethylacetate process.

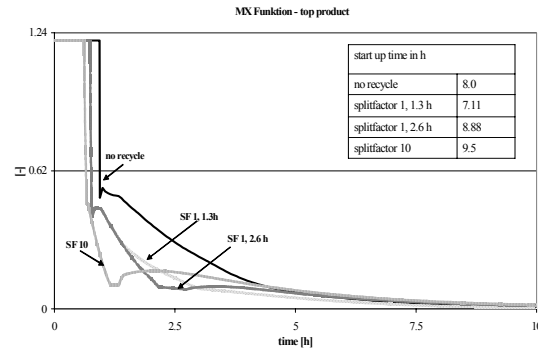


Fig. 6: MX_{Top} function for bottom product recycle

Figure 6 shows, that a moderate recycle of bottom product can save about 12% start up time. A recycle of more bottom product yields a steeper descent of the MX function, but after switching back to regular feed, the MX function shows an increase again, which prolongs the start up time for 1.5 h.

If the top product is recycle, the MX function of the bottom product shows no influence. The start up times for different splitfactors and recyclce times do not show significant differences. Therefore this strategy should not be chosen for the start up of a reactive distillation column.

4. CONCLUSIONS

A rigorous simulation model has been presented, that can capture the dynamic behavior of a RD column starting from a cold and empty state. This model has been validated with steady state and dynamic data for a transesterification of a methylester. The match between experimental data and simulation data is satisfactory.

The validated model has been used to calculate start up times for two different processes, one esterification and one transesterification, utilizing strategies known from conventional distillation without reaction. It has been shown, that these strategies do not yield significant savings in start up time. The industrially favoured strategy of total reflux takes the longest start up time for reactive distillation.

Alternative strategies to reduce the necessary start up time have been developed. The investigation of these strategies showed, that a saving of about 82% of the start up time for the ethylacetate process could be achieved, if the column is initially charged with top product. About 23% start up time could be saved, if the low boiling educt is initially charged to the column. Recycling of the bottom product could save about 12% of the start up time whereas a recycling of

top product did not yield in any savings. In contrast to this the transesterification did not show significant start up time reduction for initial top product charging. The relative volatilities of the components as well the kinetic contact are critical for the correct choice of strategies.

5. ACKNOWLEDGEMENT

Financial support from the AIF, grant No. 12789N/1 is gratefully acknowledged.

6. NOMENCLATURE

D,L,V,B,F	mol/s	Distillate, liquid, vapour, bottom and feed stream
F _V , F _L	mol/sec	vapour, liquid flow
HU _B	mol	liquid holdup
k _{far} , k _{back}	mol/s	frequency factor
K	-	phase equilibrium constant
MT, MX _{Top}		MT function, MX function for top product
M _{Tot,vap} , M _{Tot,liq}	mol	vapour, liquid holdup on tray
p _{vap} ⁱ , p _{tray}	bar	vapour pressure component i, pressure of tray
r _A	mol/s	reaction rate component A
T	K, °C	temperature
V _{tray} ^v , V _{tray} ^l	m ³	tray volume
x _{A,XB,XC,XD}	mol/mol	liquid mol fraction of components
y _i	mol/mol	vapour mol fraction
Δ _{Level}	m	level of liquid over weir
Δp	bar	pressure drop between two adjacent trays
γ _l	-	liquid activiy coefficient

REFERENCES

- Alejski, K. and Duprat, F. (1996). Dynamic Simulation of the multicomponent reactive Distillation. *Chemical Engineering Science*, **51**, pp. 4237-4252
- Bock, H. (1999). Theoretische und experimentelle Analyse der Reaktivrektifikation., VDI Verlag, Düsseldorf, ISBN 3-18-358803-x
- Doherty, M. and Buzad, G. (1992). Reactive distillation by design. *Chemical Engineering Research and Design: Transactions of the Institution of Chemical Engineers: Part A*, **70**, pp. 448-457
- Eden, M., Koggersbol, A. and Hallager, L. (2000). Dynamics and control during startup of heat integrated distillation column. *Computers and Chemical Engineering*, **24**, pp. 1091-1097
- Flender, Matthias (1999). Zeitoptimale Strategien für Anfahr- und Produktwechselvorgänge an Rektifizieranlagen., VDI Verlag GmbH, Düsseldorf, ISBN 3-18-361009-5
- Gani, R., Jepsen, T. and Perez-Cisneros, E. (1998). A generalized Reactive separation Unit Model. Modelling and simulation aspects. *Computers and Chemical Engineering*, **22** (Supp), pp. S363-S370
- Gani, R., Ruiz, C. and Cameron, I. (1987). Studies in the Dynamic of Startup and shutdown Operations of Distillation Columns. *Computers and Chemical Engineering*, pp. 26-30
- Güttinger, T.E. (1998). Multiple Steady States in Azeotropic and Reactive Distillation. Thesis (PhD). ETH Zürich
- Kenig, E.Y., Bäder, H. and Gorak, A. u.a. (2001). Investigation of ethyl acetate reactive distillation process. *Chemical Engineering Science*, **56**, pp. 6185-6193
- Kister, H.Z. (1979). When Tower Startup has Problems. *Hydrocarbon Processing*, **50** (2), pp. 89-94
- Kruse, Ch., Fieg, G. and Wozny, G. (1996). A new time-optimal strategy for column startup and product changeover. *Journal of Process Control*, **6** (2-3), pp. 187-193
- Lee and Dudukovic (1998) Lee, J.-H. and Dudukovic, M.P. (1998). Comparison of the equilibrium and nonequilibrium models for a multi-component reactive distillation column. *Computers and Chemical Engineering*, **23**, pp. 159-172
- Löwe, K. (2001). Theoretische und experimentelle Untersuchungen über das Anfahren und die Prozessführung energetisch und stofflich gekoppelter Destillationskolonnen., VDI Verlag, Düsseldorf, ISBN 3-18-367803-9
- Reepmeyer, F., Repke, J.-U. and Wozny, G. (2003). Analysis of the Start Up Process for Reactive Distillation. *Chemical Engineering & Technology*, **26**, pp. 81-86
- Scenna, N., Ruiz, C. and Benz, S. (1998). Dynamic simulation of start up procedures of reactive distillation columns. *Computers and Chemical Engineering* (22), pp. S719-S722
- Scenna, N.J. and Benz, S.J. (2003). Start up Operation of Reactive Columns with Mulitple Steady States: The Thylene Glycol Case. *Ind. Eng. Chem. Res.* (42), pp. 873-882
- Suzuki, S., Yagi, H. and Komatsu, H. (1971). Calculation of multicomponent distillation accompanied by a chemical reaction. *Journal of Chemical Engineering of Japan*, **4** (1), pp. 26-33
- Taylor, R. and Krishna, R. (2000). Modelling reactive distillation. *Chemical Engineering Science*, **55**, pp. 5183-5229
- Yasuoka, H., Nakanishi, E. and Kunigita, E. (1987). Design of an On-Line Startup System for Distillation Column Based on a simple algorithm. *International Chemical Engineering*, **27** (3), pp. 466-472

PLANTWIDE ECONOMICAL DYNAMIC OPTIMIZATION: APPLICATION ON A BOREALIS BORSTAR PROCESS MODEL

**Wim Van Brempt, Peter Van Overschee , Ton Backx, Øivind Moen,
Costas Kiparissides, Christos Chatzidoukas**

Wim Van Brempt, Peter Van Overschee

IPCOs, Technologilaan 11/0101, 3001 Heverlee, Belgium

Wim.VanBrempt@ipcos.com Peter.VanOverschee@ipcos.com

Ton Backx

IPCOs, Bosscheweg 145a, 5282 WV Boxtel, The Netherlands

Ton.Backx@ipcos.com

Øivind Moen

Borealis, 3960 Stathelle Norway

Oivind.Moen@borealisgroup.com

Costas Kiparissides, Christos Chatzidoukas

Department of Chemical Engineering and Chemical Process Engineering

Aristotle University of Thessaloniki,P.O. Box 472, 54006 Thessaloniki, Greece

cypress@alexandros.cperi.certh.gr

Abstract: A novel plantwide dynamic optimizer PathFinder has been applied to a dynamic model of a Borealis Borstar process. PathFinder optimizes dynamic paths subject to a merely economical criterion. Introduction of process constraints allows for a gradual migration from the currently used transition towards a more optimal transition. Special care has been taken to integrate the optimizer with on-line control tools. The results show a significant improvement in added value during a grade transition.

Keywords: Plantwide, Optimal trajectory, Optimization, Grade Transition, Chemical industry

1. INTRODUCTION

The chemical process industry is facing a huge problem to increase their capital productivity. A solution to this problem is demand driven process operation. This implies that exactly these products can be produced that have market demand and take price advantage of a scarce market. Flexible operation of production is therefore required [Backx, *et al.*, 1998].

A new integrated process control and transition optimization technology is needed for this purpose.

The idea of optimization of grade transitions has been introduced by McAuley [McAuley and

MacGregor, 1992]. Based on rigorous dynamic models optimal open-loop paths are calculated. The cost function has been improved into a more straightforward economical framework [Van der Schot et al, 1999]. The introduction of an economic objective function introduces strong non-linearities resulting in a strong increase in model evaluations. Special effort is paid to reduce the number of model evaluations to make the optimization feasible within a realistic timeframe. The PathFinder rigorous model based dynamic optimizer has been developed for these purposes. An application on a Borealis Borstar process is discussed. The paper is organized along the following four Sections:

- In Section 2 the formulation of the plantwide economic optimization criterion is given.
- Subsequently, in Section 3 a framework for on-line implementation of the optimized paths is discussed.
- In Section 4 relevant aspects of the Borstar process are described.
- Finally, Section 5 describes the application of PathFinder on a Borealis Borstar process.

2. PLANTWIDE DYNAMICAL ECONOMICAL OPTIMIZATION

PathFinder is a generic framework for plantwide economical dynamic optimization.

An economical balance is being calculated for the entire process over a finite time horizon. For this purpose the revenues and costs are assigned to various economical flows entering and leaving the process (Figure 1).

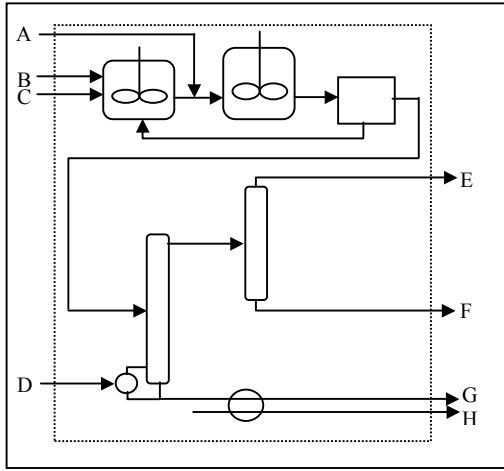


Figure 1 Example of the Generic Plantwide Economic Process Framework

In general, three types of flows characterize a process:

- Economical flows that are consumed by the process. In most cases these will correspond to the use of raw material (Figure 1, flow A, B and C), but also the use of utilities (cooling water, steam (Figure 1, flow D), electricity...) can be accounted for as well. These flows are characterized by a fixed price per unit consumption.

- Economical flows that are generated by the process, under a fixed price condition per generated unit. Typical examples are material

flows of reaction side products that can be sold but where the quality of the generated product is not determined fully inside the process (Figure 1, flow G). The price can be negative if side products result that must be reworked afterwards as waste material. Also non-material flows such as generated steam (Figure 1, flow H) or electricity can be accounted for in the same fashion.

- Economical flows corresponding to material or energy flows where the generated value depends on the value of a set of quality variables. Typical examples are reaction end products that must comply with given customers requirements, distillation tower top and bottom products that must satisfy purity demands (Figure 1, flow E and F) ...

It is key for an economical framework that the prices that must be accounted for in the last class of economical flows have a discrete nature. Products meeting a set of specifications have high economical value, while products that are outside the specification range ('off spec') show a value drop.

As such, the economic criterion to be optimized is given by the added value over a fixed time horizon T.

$$AddedValue =$$

$$\begin{aligned} & - \int_0^T \sum_i^L Inflow_i(t) price_i dt \\ & + \int_0^T \sum_i^M Outflow_i(t) price_i dt \\ & + \int_0^T \sum_i^N Productflow_i(t) price_i (QPar_1(t), QPar_2(t), \dots) dt \end{aligned}$$

Within PathFinder various specifications (also called 'grades') can be introduced for each of the existing product flows (Figure 2). A grade consists of a set of quality parameters, which form bounded regions by the introduction of inequalities.

Based on the given economical criterion, one can calculate improved dynamical paths to move from one operation point to another. As such it can be used to calculate economically optimal grade changes, production load changes, start-up and shut down procedures...

Economically optimal grade change trajectories reduce the transition cost and thus make it easier to operate the process in accordance with market

demand. It also enables a flexible process operation strategy that is no longer coupled to a fixed grade slate, but that allows shortcuts between most of the grades in the grade slate.

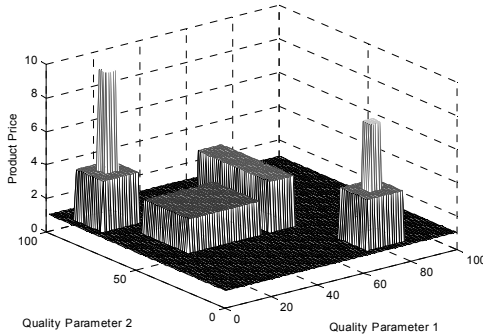


Figure 2 PathFinder's multigrade set-up

It can readily be understood that this economic formulation leads to different optimal trajectories if the market conditions change from an unsaturated market condition towards a closed market. In an unsaturated market raw material and utility consumption will be less penalized since the on-spec product will typically generate significantly more benefits compared to the production costs. On the other hand, in a closed market, the optimizer will automatically strive for cost reduction, since the on-off spec price difference will not be as large.

The optimizer searches for the optimal process manipulations, such that the resulting trajectory is economically optimal. It is clear that a dynamic process model is needed to enable the calculation of the Added Value given the applied process manipulations. The nonlinear dynamic model equations (set of DAE's) have to be integrated over the time horizon given by the input manipulations.

Constraints are added to the optimization problem, restricting the optimization freedom.

The reasons for the introduction of these constraints (Path Constraints and Rate of Change constraints on MV's and CV's) are:

- Guarantee a safe and feasible operation during the transition.
- Constrain the optimizer freedom such that the new trajectory doesn't differ too much from the initial trajectory.

The last reason is important when one has no blindfolded confidence in the process model.

Adding constraints will allow one to migrate gradually from a well-known recipe to a new recipe.

PathFinder is a robust and fast solution for the above optimization problem. Though the objective function is strongly non-linear, due to the discontinuous price function, typically 5 up to 10 trajectory simulations and model linearizations are needed for the cases that have been analyzed (compared to 500 up to 1000 model evaluations with a SQP optimization scheme). These model evaluations are the bottleneck for a faster calculation time. In [Van Brempt, *et al.*, 2001] relevant implementation topics are discussed.

3. INTEGRATED TRAJECTORY CONTROL AND OPTIMIZATION TECHNOLOGY

The manifest reduction that has been achieved in the number of required model evaluations, makes *off-line* economical plantwide dynamical optimization feasible. However, given the currently available computing power, *on-line* economical plantwide dynamical optimization will not be feasible for most industrial problems.

Therefore, a general framework has been set up in order to cope with the challenge to integrate dynamic optimization and on-line control [Van Brempt, *et al.*, 2000]. The key idea is explained in Figure 3.

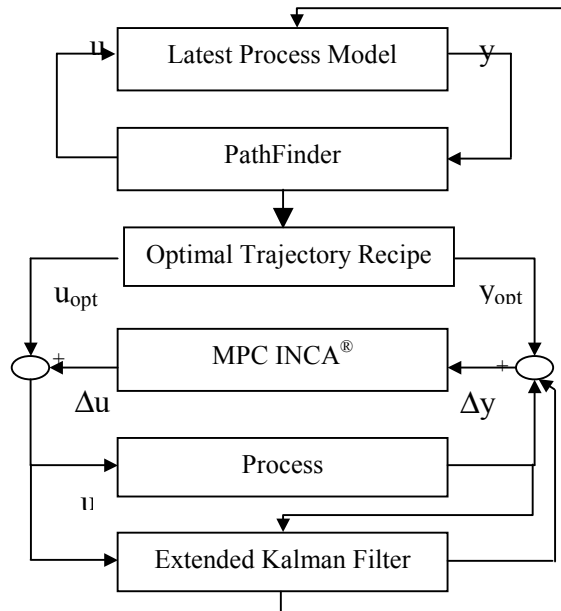


Figure 3 Integration of MPC control technology and optimization technology

PathFinder calculates off-line optimal dynamic economically paths based on the non-linear rigorous dynamic process model. These manipulated and controlled variable trajectories are as such applied to the process. The on-line controller corrects only for the deviations Δu and Δy ('delta mode') from the process input-output setpoints u_{opt} and y_{opt} that are given by the optimizer. These deviations will occur due to model-plant mismatch and due to disturbances entering the process.

The delta-mode guarantees a best of both worlds operation. The trajectory has generally been carefully designed with the knowledge of the non-linear process. It would be a pity to have this result overridden by a linear model controller. Therefore this trajectory is applied as such to the process. It puts a curb onto the controller, and the controller is allowed to shift the deviations of the input-output trajectory ($u_{\text{opt}}, y_{\text{opt}}$) between the controller input and output. It does not only try to follow as closely the output trajectory, but makes a compromise between deviations from the output trajectory and from the input trajectory.

As explained in the previous section, the long trajectory simulation time determines the optimization calculation time. In practice the optimizer will therefore still need a considerable time to calculate a new trajectory. Therefore PathFinder is started some time before the trajectory has to be initiated, with up-to-date market conditions that can be uploaded from an ERP environment.

In order to reduce plant-model mismatch, PathFinder will use the latest instance of the rigorous model that is known, with the latest state updates in case an Extended Kalman Filter is available. Once the optimal trajectory is calculated and acknowledged, it is sent to the controller environment (Figure 3).

4. THE BORSTAR PROCESS

Development in polymer materials is nowadays geared towards increased strength, resulting in less thickness for films, pipe and container walls. This results in a clear reduction in weight, transport cost and material usage, as such giving less harm to the environment.

Less taste and odor is also an issue for polymer materials, as is the speed of processing the polymer materials, which allows faster

production for end user applications. This requires more tailoring of the molecules. A bimodal molecular weight distribution is often used as it is a tailored distribution of the incorporation of co-monomers. Figure 4 shows how end polymer properties are affected by the molecular weight of the polymer molecules.

There are basically two routes to tailor-make a polymer; either to tailor the catalyst used in the production of the polymer and/or tailor the polymerization process. Both routes are extensively used. The following description will describe the up-to-date approach of modifying the polymer by the process route.

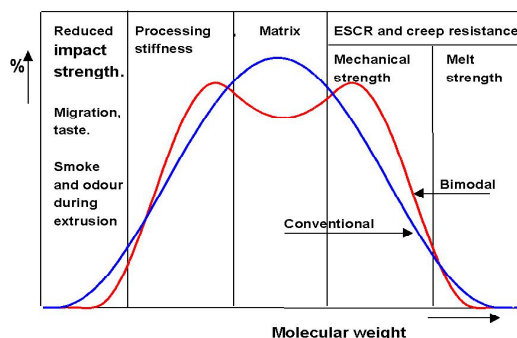


Figure 4 Molecular weight distribution can be more easily adapted with bimodal than unimodal materials to meet the property needs of the end application.

The polymer that is being produced depends not merely on the kinetic properties of the catalyst, but also on the temperature, pressure and duration of polymerization as well as on the concentration of the polymer and monomer involved in the reactions. The polymerization process used to produce the material controls the latter. There have been strong developments in this field to enable wide variations in the properties of the final polymer. Figure 5 shows the process for producing bimodal molecular weight distributed polymer as well as wide variation in co-polymer incorporation.

The Borstar process consists of at least three reactors. One pre-polymerization reactor is used to start the catalytic polymerization process in a controlled manner as well as developing the desired particle morphology. The subsequent loop reactor produces the low molecular weight polymer. Propane is used as the diluent. Operating the reactor above the critical thermodynamic point gives a very low solubility

of PE in the diluent. The probability of fouling is hence greatly reduced compared with process using other diluent. The loop reactor can therefore produce polymer with larger variation in density than a number of other processes. The high molecular weight part of the polymer is produced in the fluidized bed reactor following the loop reactor.

An extra versatility of the combined Borstar process comes also with the ease of varying the co-monomer content in each reactor and thereby tailor-making the co-monomer distribution of the final polymer. Various polyethylene grades can be produced on the same process using a carefully chosen set of flow, temperature and pressure setpoints (SPi) that we will refer to as a “recipe”. A given polyethylene grade will be characterized by a specified density and melt index.

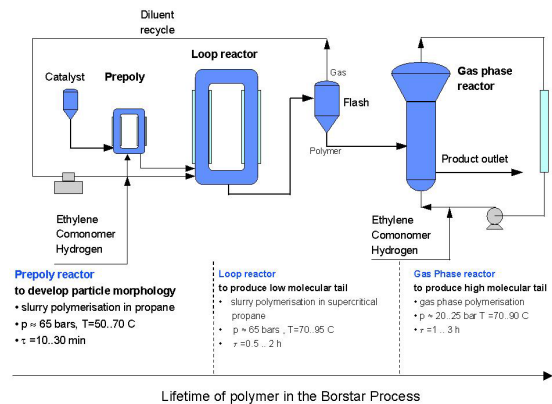


Figure 5. The Borstar process for producing bimodal MWD polymer as well as variation in co-polymer distribution.

When changing from one polymer grade to another polymer grade, setpoints must be moved from one recipe to the other, driving the process through a zone where off-specification product is made. Typically the transition path for recipe setpoints will be selected to minimize production of low value off-spec product.

Borealis developed a rigorous dynamic model for the Borstar process. This model is used to demonstrate the application of PathFinder.

5. APPLICATION OF PATHFINDER ON THE BORSTAR PROCESS

PathFinder's optimization technology is applied on a model of the Borstar process in order to

optimize the transition from one specific polymer grade to another grade.

In Figure 6 optimized trajectories are shown for both quality variables. Notice that in both situations the off-spec time has considerably been shortened to about a half of the original off-spec time. Also observe that the optimizer fully exploits the dynamical behavior of the process within the freedom of the entire specification band to optimize the transition. A typical optimizer behavior results for the density variable: the process first moves away from the desired spec, changes direction within the specification band, and takes full speed to go to the other grade. Upon arriving in the second grade specification, the process enters with full speed into the specification zone, bumps against the opposite boundary, and swings back without leaving the specification boundary.

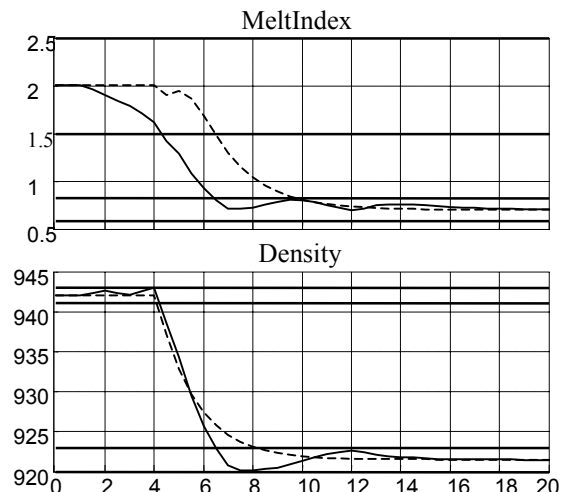


Figure 6 Trajectories for quality variables Density and Melt Index (together with specification boundaries): initial trajectory (---, final trajectory (solid).

In Figure 7 some MV trajectories are shown. The production setpoint controls the ethylene inflow using a PI controller. One can easily notice the move times in the trajectories, i.e. the timestamps where the optimizer is allowed to change the MV values. In between these values, the MV values are kept constant. In total an optimization problem with 174 move times (degrees of freedom) was solved. Observe also that the original trajectory was a rather quasi steady state transition, while the new trajectories are fully dynamic.

In Figure 8 the economical added value is shown in function of time. During Off-Spec the

added value drops due to the fact that only a lower price can be achieved for the end product. The optimized trajectory shows a much shorter dip due to the fact that the off-spec time is shortened considerably.

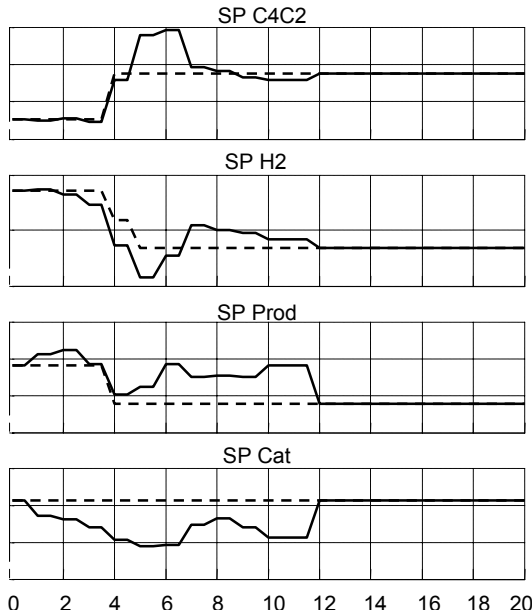


Figure 7 Manipulated Variable Trajectories (initial trajectory (---), Optimized (solid)).

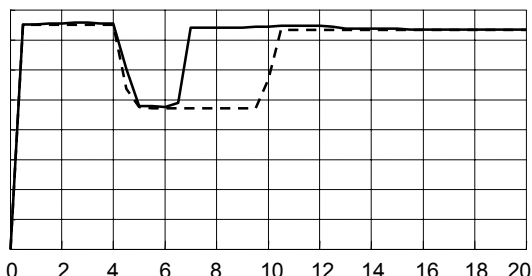


Figure 8 Added value: initial trajectory (---), optimized (solid).

6. CONCLUSION

A plant wide dynamical optimization tool has been developed for optimization of a straightforward economical criterion. Several types of constraints can be introduced, such that a safe operation can always be guaranteed and such that a gradual migration from a known recipe to a renewed recipe is obtained.

PathFinder has especially been laid out to increase optimization speed by limiting the number of necessary model evaluations. The

optimizer is seamlessly integrated with a model predictive control technology such that on-line implementation of the optimized paths becomes feasible.

PathFinder has been successfully applied on a grade transition problem for the Borstar process. The results showed considerable shortening of the off-spec time as well as a reduction of the overall cost of a grade transition.

7. ACKNOWLEDGEMENTS

This work is supported by the European Community project polyPROMS (GRD1-2000-25555): Development of Advanced Polymerization Process Modeling, Simulation, Design and Optimization Tools. The scientific responsibility is assumed by its authors.

REFERENCES

- Backx, T., O. Bosgra and W. Marquardt (2000). Integration of Model Predictive Control and Optimization of Processes, proc. AdChem 2000, June 2000, Pisa, Italy
- Backx, T., O. Bosgra and W. Marquardt, (1998). Towards intentional dynamics in supply chain conscious process operations, proc. FOCAPO 1998, 5-7 July 1998, Snowbird Resort, Utah, USA
- Van der Schot, J.J., R.L. Tousain, A.C.P.M. Backx and O.H. Bosgra (1999). SSQP for the solution of large scale dynamic-economic optimization problems, proc. ESCAPE 1999, June 1999, Budapest, Hungary
- McAuley, K.B., 1991
Modelling, Estimation and Control of Product Properties in a Gas Phase Polyethylene Reactor, Ph.D. Thesis.
McMaster University, 1991
- McAuley, K.B. and MacGregor, J.F., 1992
Optimal Grade Change Transitions in a Gas Phase Polyethylene Reactor, AIChE Journal, October 1992, Vol. 38, No 10, pp 1564-1575
- Van Brempt W., Backx T., Ludlage J., Van Overschee P., De Moor B., Tousain R. (2000). A high performance model predictive controller: application on a polyethylene gas phase reactor, proc. AdChem 2000, June 2000, Pisa, Italy
- Van Brempt W., Backx T., Ludlage J., Van Overschee P.. 2001
Optimal Trajectories for Grade Change Control: application on a polyethylene gas phase reactor, Preprints DYCOPS6, June 2001, Cheju Island, South Korea

FUZZY NEURAL NETWORK FOR PREDICTING 4-CBA CONCENTRATION OF PTA PROCESS

Ruilan LIU, YueXuan Wang, Hongye SU, Shengjing MU, Yongyou HU, Weiquan CHEN, Jian CHU

National Laboratory of Industrial Control Technology, Institute of Advanced Process Control, Zhejiang University, Yuquan Campus, Hangzhou, 310027, P.R. China

*Corresponding Author email: rlliu@iipc.zju.edu.cn

Abstract: A fuzzy neural network model has been developed to predict the 4-CBA concentration of the oxidation unit in PTA process. Several technologies are used to deal with the process data before modeling. Suitable input variables set has been selected according to prior knowledge, experience and fuzzy curve method. Dead time delay has been considered in the fuzzy neural network model. The simulation results show that the model of the fuzzy neural network is better than that of AMOCO in prediction precision.

Key words: Purified Terephthalic acid (PTA), 4-CBA ,Fuzzy Neural Network, Fuzzy Curve, Soft Sensor

1. INTRODUCTION

PTA (Purified Terephthalic Acid) is the necessary material used widely in textile and packaging industries. It is made by purifying the TA (Terephthalic Acid) which is produced by oxidizing PX(para-xylene) with the catalyster. The Catalytic Oxidation process of the PX is shown in figure 1. There are some mediproducts such as P-T(P-Toluic Acid) and 4-CBA (4-Carboxybenzaldehyde) in TA.

Concentration of 4-CBA is the main impurity and the important quality indicator. Reference (Cao,G,et al.1994) shows that the lower the 4-CBA concentration the more energy cost. So it is important to control the 4-CBA concentration of the oxidation unit on-line for saving energy and ensuring

the purity of PTA.

In practice the 4-CBA concentration is sampled three times each day and measured by spectroscopic analysis. Since spectroscopic analysis is a laboratory technique with obvious time delay, the analysis values of the 4-CBA concentration are not available for timely control adjustment if required. An alternative method is to build a soft sensor for on-line control of the 4-CBA concentration. In soft sensor technique the 4-CBA concentration is inferred from the other measured process variables such as temperatures, pressures, flows and their relationship.

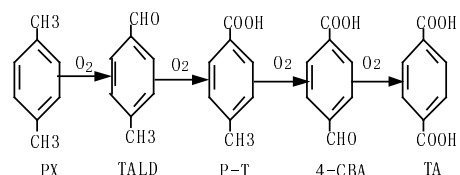


Fig. 1. The catalytic oxidation process of the PX

*This work is supported by The National Outstanding Youth Science Foundation of China (NSFC:60025308)

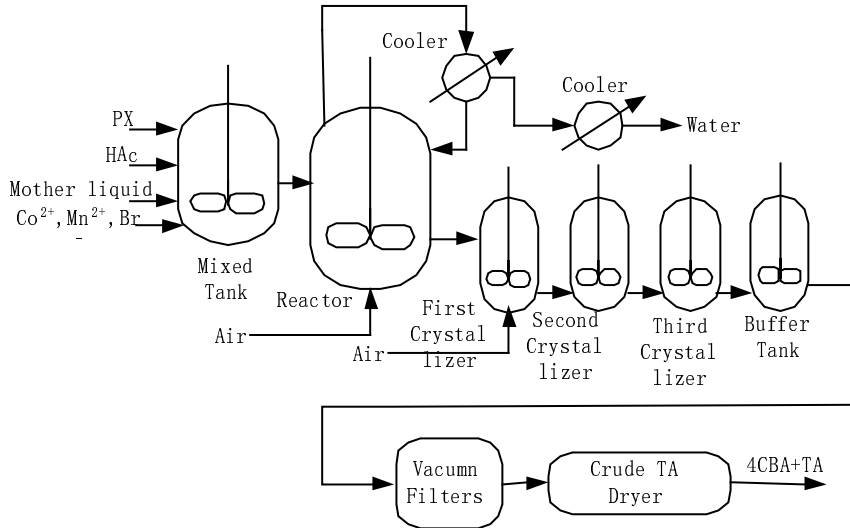


Fig. 2. Schematic diagram of the industry PTA oxidation process

The relationship between the measured process variables and 4-CBA concentration is modeled by a suitable technique.

Schematic diagram of the industry PTA oxidation process is shown in figure 2. The PTA oxidation process is very complex including heat transfer, mass transfer and solid crystal in gas and liquids phase. A complex dynamic model (Cao,G,*et al.* 1994) about the PX oxidation process has been proposed firstly. However this model is highly nonlinear and its parameters have uncertainty. In order to forecast the 4-CBA concentration, some famous chemistry corporations have also developed different empirical regression models with patent rights (Harold,A.L.,*et al.*1989). But the empirical models are only suitable to a limited operation region. In the present work fuzzy neural network based soft sensor is proposed to model the nonlinear relationship between the 4-CBA concentration and the measured process variables and accordingly predict the 4-CBA concentration in a timely manner.

The organization of the paper is as follows. Section 2 presents the architecture of the fuzzy neural network. Section 3 deals with a few practical issues including variable selection, dead time determination and data filtering. Section 4 presents simulation results. The final section gives conclusion.

2. FUZZY NEURAL NETWORK

The architecture of four layer fuzzy neural network with m inputs and one output is shown in figure 3, The four layers are input layer, fuzzification layer, inference layer and defuzzification layer respectively. There are m neurons connected with m input variables in the first layer, $m \times R$ neurons in the fuzzification layer, R neurons in the inference layer and one neuron in the output layer. Each m neurons in the fuzzification layer represents the premise part

of one fuzzy rule, so there are R rules in total. The i th IF-THEN rule is,

R^i :IF x_1 is $A_{i,1}$ and ... and x_j is $A_{i,j}$ and ... and x_m is $A_{i,m}$

THEN y is B_i

Where x_j is an input variable;

y is an output variable;

$A_{i,j}$ is a fuzzy set that characterized by the membership function $\mu_{A_{i,j}}(x_j)$;

B_i is a fuzzy set that characterized by the membership function $\mu_{B_i}(y)$;

Gaussian-type membership functions are used to calculate the values of $A_{i,j}$ and B_i as follows,

$$A_{i,j} = \mu_{A_{i,j}}(x_j) = \exp\left(-\frac{(x_j - a_{i,j})^2}{c_{i,j}}\right) \quad (1)$$

$$B_i = \mu_{B_i}(y) = \exp\left(-\frac{(y - b_i)^2}{d_i}\right) \quad (2)$$

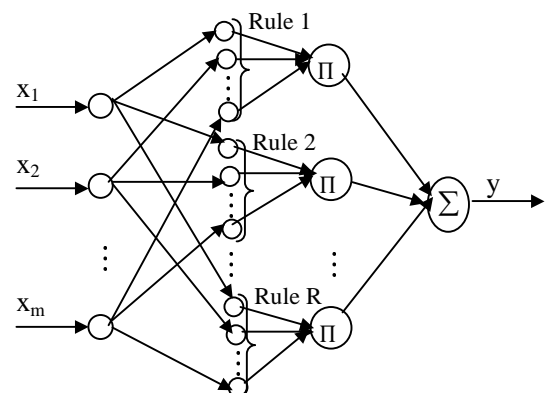


Fig. 3. The architecture of fuzzy neural network

where $a_{i,j}$, $c_{i,j}$, $i = 1, 2 \dots R$; $j = 1, 2 \dots m$ represent the center and width of input membership functions respectively. b_i and d_i represent the center and width of output membership function respectively. On the basis of multiplicative inference, we get

$$w_i = \prod_{j=1}^m \mu A_{i,j} \quad (3)$$

The inference result coming from R rules follows a standard center of gravity formula,

$$y_{out} = \left(\sum_{i=1}^R d_i b_i w_i \right) / \left(\sum_{i=1}^R d_i w_i \right) \quad (4)$$

the learning of FNN is accomplished by adjusting the input/output widths and centers of membership functions and follows gradient descent algorithm. in this study, we use an Euclidean distance, that is

$$E = \frac{1}{2} (y_{out} - y)^2 \quad (5)$$

where E is the error;

y_{out} is the actual output value;

y is the target output value.

We only take $a_{i,j}$ as an example for brevity. Using the BP (BackPropagation) algorithm, the following update formula can be derived

$$a_{i,j}(k+1) = a_{i,j}(k) - \eta \frac{\partial E}{\partial a_{i,j}} + \alpha(a_{i,j}(k) - a_{i,j}(k-1)) \quad (6)$$

$$\frac{\partial E}{\partial a_{i,j}} = \frac{\partial E}{\partial y_{out}} \frac{\partial y_{out}}{\partial w_i} \frac{\partial w_i}{\partial \mu A_{i,j}} \frac{\partial \mu A_{i,j}}{\partial a_{i,j}} \quad (7)$$

where η is the learning rate;

α represents the momentum coefficient.

It is important to initialize the parameters of fuzzy neural network because BP algorithm is sensitive to the initial parameters. In order to select a suitable parameters fuzzy C means clustering (FCM) algorithm (D.A.Linkens,Min-You Chen,1999) is applied to initialize the parameters. The centers of membership function, $a_{i,j}, b_i$, are initialized by the fuzzy clusters' centers; the initial width $c_{i,j}$ is given as follows,

$$c_{i,j} = \beta \times \text{sqrt} \left(\frac{\sum_{k=1}^N U_{i,k} (x_{k,i} - a_{i,j})^2}{\sum_{k=1}^N U_{i,k}} \right) \quad (8)$$

where U is the final fuzzy partition matrix calculated by FCM algorithm.

β is a constant.

d_i is initialized in the same way as $c_{i,j}$.

3. INPUT VARIABLES SELECTION AND DATA SET COLLECTION

3.1 Preliminary Selection of Process Variables

Hundreds of process variables affecting the 4_CBA concentration are recorded respectively one time per 30 seconds by the DCS system in PTA process. The selection of an appropriate subset from these variables is important. Too many unimportant variables included in the soft sensor model will lead to the difficulty of training and usage. On the other hand the model's accuracy can not be guaranteed if some important variables are not included.

According to prior knowledge and experience, ten variables are preliminarily selected including flow rates, reaction pressures, temperature, resident time, solvent ratio in the reactor and catalyzer liquid level. These ten process variables are measured in the reactor and the first crystallizer. Fuzzy curve method (Lin and Cunningham,1995) is applied to select the final variable subset in section 3.4.

3.2 Dead Time Determination

Dead time is the delay between the time when the value of a process variable changes and the time when the dependent variable begins to change in response which dependent on the structure and scale of the production equipment. It is obvious that the larger the scale of the production equipment and the longer the distance of materials transportation the longer the delay of dead time.

The schematic diagram of PTA oxidation process in figure 2 shows that the production equipment is of a large scale, so there are long dead time delays between the process variables and 4-CBA concentration. The different dead time of every process variable results from the fact that every tank has different residence time from 15 to 72 minutes and every sensor has its different position. Analysis indicated that the maximum dead time of the process variables is about 200 minutes while the minimum dead time is only about 70 minutes.

3.3 Data Collection and Preprocessing

As mentioned above, 4_CBA concentration is sampled only three times while the process variables are recorded about three thousand times each day. In other words, three samples at most are collected for training fuzzy neural network each day. The data set with 216 samples was collected according to the dead times of process variables and the sample time

of 4-CBA concentration. That is

$$X = [x_1(t - \tau_1) \quad x_2(t - \tau_2) \quad \cdots \quad x_{10}(t - \tau_{10})] \quad (9)$$

$$Y = [y(t)] \quad (10)$$

Where X and Y represent process variables values and 4-CBA concentration collected, respectively, τ_i , $i=1,2,\dots,10$, is the dead time of the i th process variable.

When data sets were collected, weighted moving average filtering method (Radhakrishnan V.R., Mahamed A.R. ,2000) is adopted to filter noise of the process data.

3.4 Reduce the Input Variables Using Fuzzy Curves method

The fuzzy curves method (Lin and Cunningham,1995) uses fuzzy logic to establish the relationship between the input variables and the output variable to identify the significant inputs. Suppose a multiple-input, single-output system has m inputs $X = [x_1 \quad x_2 \quad \cdots \quad x_m]$ and one output $Y = [y]$, We have N training data points. The algorithm is described briefly as follows,

- 1) Calculate the fuzzy membership function for the input variable x_i defined by

$$\Phi_{i,k}(x_i) = \exp\left(-\frac{(x_{i,k} - x_i)^2}{b}\right) \quad (11)$$

where $i = 1, \dots, m$; $k = 1, \dots, N$;

$$b = 0.2 \times (\max(x_i) - \min(x_i))$$

- 2) Use centroid defuzzification to calculate the fuzzy curve c_i for each input variable x_i by

$$c_i(x_i) = \frac{\sum_{k=1}^N \phi_{i,k}(x_i) \cdot y_k}{\sum_{k=1}^N \phi_{i,k}(x_i)} \quad (12)$$

- 3) Calculate the range of each fuzzy curve by $R_i = \text{Max}(C_i(x_i)) - \text{Min}(C_i(x_i))$, the larger the R_i , the more important the corresponding variable x_i .

According to the approach the ranges of the fuzzy curves c_i in the PTA process, $i=1,2,\dots,10$, are shown in table 1.

As shown in table 1, the range of the fuzzy curve for x_7 and x_9 is smaller than that of other variables. We delete these two variables for simplifying the model. However this does not mean that these two variables have no effect on the concentration of 4-CBA. It is just because that the range of these two variables is too small to produce any obvious error in the model prediction.

Table 1 The range of the fuzzy curves in PTA process

Input variables	The Range of c_i	Input variables	The Range of c_i
x_1	0.6188	x_6	0.5542
x_2	0.6030	x_7	0.0928
x_3	0.5822	x_8	0.4863
x_4	0.3318	x_9	0.1097
x_5	0.4921	x_{10}	0.3596

4. SIMULATION RESULTS

The data set with 216 samples is divided into two sets, one set has 150 samples used for training, the other set has 66 samples used for testing. After training FNN with different number of fuzzy rules, it is found that the most suitable number is 5. The training and testing relative errors after 250 iterations are shown in Fig 4. For comparison, the empirical nonlinear regression model of AMOCO is applied to the same data set. Under the same condition as in the FNN approach, the training and testing relative error are also given in Fig 4. Table 2 lists the two models' performances including maximum relative error, minimum relative error and root-mean-square-error (RMSE) in detail. It can be seen that not only the training results of the FNN model are better than that of the AMOCO model but also the better generalization results on the testing data.

The comparison of the predicted values of the two different models and the actual 4-CBAconcentration is given in Fig. 5. It can be seen that the FNN model has better prediction capability in the change trend of 4-CBA concentration while the AMOCO model just predicts the average of it.

Table 2 Training and testing performance for 4-CBA concentration using the FNN method and AMOCO model

Model	Training set			Testing set		
	max.rel.Error	min.rel.Error	RMSE	max.rel.Error	min.rel.Error	RMSE
FNN	0.0813	-0.0576	0.0248	0.0923	-0.0845	0.0342
AMOCO	0.1109	-0.0846	0.0357	0.0941	-0.0887	0.0373

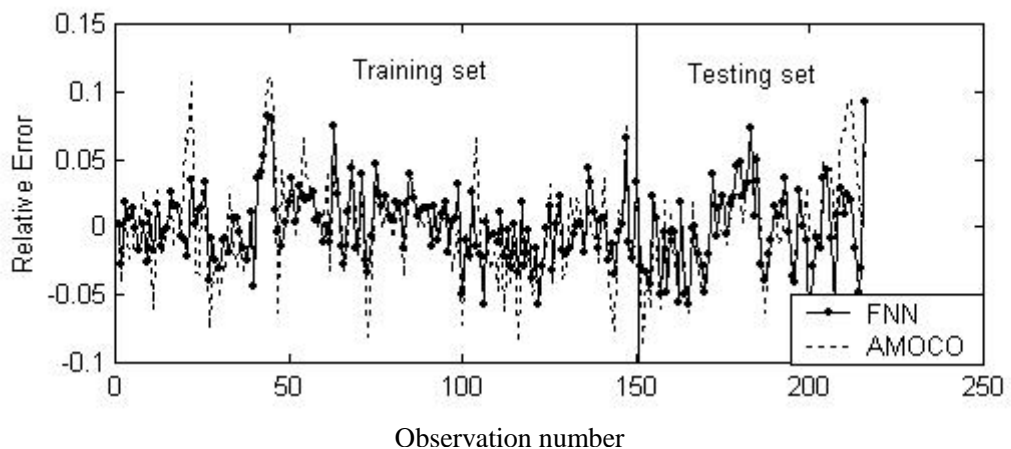


Fig. 4. Predicted relative errors for 4-CBA concentration using the fuzzy neural network model and AMOCO nonlinear regression model .

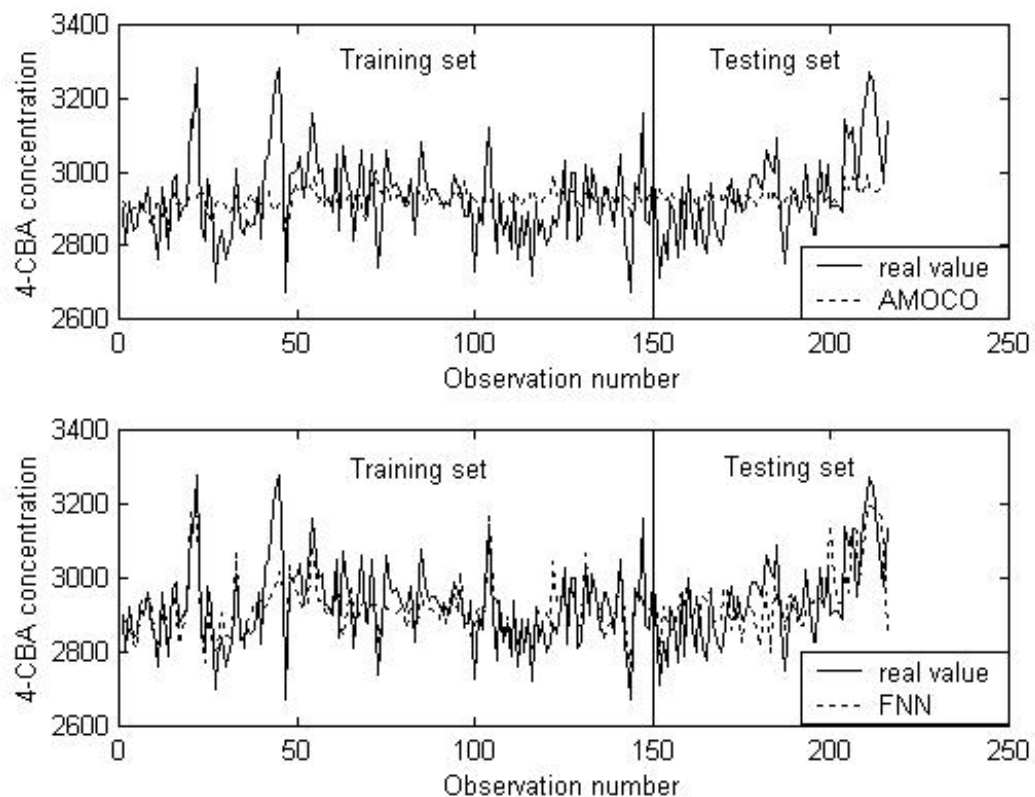


Fig. 5. Actual and predicted results of 4 CBA-concentration

5. CONCLUSION

In this paper, a fuzzy neural network model has been applied to predict the concentration of 4-CBA of the oxidation unit in PTA process. Several technologies are used to deal with the process data before modeling. Suitable input variable subset has been selected according to the prior knowledge and experience and fuzzy curve method. Dead time has been considered into the fuzzy neural network model.

The simulation results show that the model of the fuzzy neural network is better than AMOCO model in prediction precision.

REFERENCES

- Yinghua Lin,George A. Cunningham (1995) A new approach to fuzzy-neural system modeling. *IEEE Transactions on Fuzzy Systems*, Vol 3.No 2. MAY 1995.pp:190-198.
- Cao,G,et al(1994). Kinetics of p-Xylene Liqui-Phase Catalytic Oxidation *AICHE J* **40** pp:1156.
- Harold,A.L,et al(1989). Method and Apparatus for

- Controlling the Manufacture of Terephthalic Acid to Control the Level and Variability of the contaminant content and the Optical Density. U.S. Patent: 4835307.
- D.A.Linkens,Min-You Chen(1999) Input selection and partition validation for fuzzy modelling using neural network *Fuzzy Sets and Systems* **107** pp:299-308.
- Radhakrishnan V.R., Mahamed A.R. (2000), Neural networks for the identification and control of blast furnace hot metal quality, *Journal of process control*, **10** (6), pp: 509-524.

DESIGNING NEUROFUZZY SYSTEM BASED ON IMPROVED CART ALGORITHM

Jia Li Li Erguo and Yu Jinshou

*Research Institute of Automation, East China University of Science and Technology,
Meilong Road 130, Shanghai, 200237, People's Republic of China ,
Tel.: +86-021-64253399; Fax: +86-021-64253399; Email address: jli75@263.net*

Abstract: In this paper, a neuro-fuzzy system based on improved CART algorithm (ICART) is presented, in which the ICART algorithm is used to design neuro-fuzzy system. It is worth noting that ICART algorithm partitions the input space into tree structure adaptively, which avoids the curse of dimensionality (number of rules goes up exponentially with number of input variables). Moreover, it adopts density function to construct the local model for every node in order to overcome the discontinuous boundaries existed in CART algorithm. To illustrate the validity of the proposed method, a practical application are done. *Copyright © 2003 IFAC*

Keywords: decision trees; CART algorithm; ICART algorithm; neurofuzzy system; hydrocracking processing

1 . INTRODUCTION

According to the published papers about neuro-fuzzy system, there are still important open problems in the neuro-fuzzy system. At first, most of the current neuro-fuzzy approaches address parametric identification or learning only. In general, the designer chooses membership functions shape and the respective parameters are adjusted Mauricio (1999). Secondly, for some neuro-fuzzy systems, e.g., the fuzzy inference network in Wang (1994), the self-organizing neural-network-based fuzzy system in Yin (1999), neuro-fuzzy networks in Mauricio (1999), fuzzy neural networks in Meng (2000), etc., the number of partitions or the cluster radius is determined by the user, which can't guaranteed a optimal fuzzy system. In addition, extracting significant input variables among all possible input candidates is another challenging problems in fuzzy structure identification.

Considering above disadvantages, decision tree is another useful tool to construct the neuro-fuzzy system and choose the input variables, which is currently the most highly developed technique for

partition. It is generated from training data in a top-down, general-to-specific direction. The initial state of a decision tree is the root node that is assigned all the examples from the training set. If it is the case that all examples belong to the same class, then no further decisions need to be made to partition the examples, and the solution is complete. If examples at this node belong to two or more classes, then a test is made at the node that will result in a split. The process is recursively repeated for each of the new intermediate nodes until a completely discriminating tree is obtained. Obviously, the advantages are decision tree's understandable representation and adaptability to the inference Serge (2001). There are many methods have been used for modeling decision tree, such as ID3 and ID4 using entropy criteria for splitting nodes, SLIQ utilizing data structures and processing methods to build decision tree, CART utilizing the GINI for splitting nodes and so on. However, in these methods, classification and regression trees (CART) has been in extensive use, which was developed to analyze categorical and continuous data using exhaustive searches and computer intensive testing to select a

decision tree by Breiman in 1984. Crawford (1989) states that in cases where data is “noisy”, CART is “a remarkably sophisticated tool for concept induction”. Jang et al. (1997), based on CART algorithm, propose a quick method to solve the problem of the fuzzy rule generation. This method generates a tree partition of the input space, which relieves the problem of curse of dimensionality (number of rules goes up exponentially with number of inputs) associated with grid partition. Moreover, the method combines CART with artificial neuro-fuzzy inference system (ANFIS) approach to complete the task of fuzzy modeling and provides a new approach for neuro-fuzzy designing. There are no similar articles appeared in recent years.

After deeply researching the CART algorithm, an improved CART algorithm, abbreviated as ICART algorithm, adopting density function to construct the local model for every node is proposed in this paper. It is worth noting that it decides every decision output value according to space distribution and thus smoothes the discontinuous boundaries existed in CART algorithm. This advantage is obvious especially when the decision tree is smaller. Then a neuro-fuzzy system based on ICART algorithm, which using ICART algorithm to design neuro-fuzzy system is proposed. In this method, ICART algorithm is used to elect relevant inputs and classify the input space into adaptive tree structure, which avoids the curse of dimensionality because the total number of fuzzy rules doesn't increase exponentially with the number of input variables and neuro-fuzzy system is utilized to refine the regression and make it smooth and continuous everywhere. It can be seen that ICART and neuro-fuzzy system are complementary and their combination makes a solid approach to fuzzy modeling.

This paper is organized as follows. In section 2 we introduce the designing neuro-fuzzy system based on ICART algorithm. It consists of ICART algorithm, neuro-fuzzy system based on ICART algorithm and optimization algorithm. In section 3 the method proposed in this paper is applied to quality prediction for hydrocracking processing. Finally, section 4 contains some conclusions.

2 . DESIGNING NEURO-FUZZY SYSTEM BASED ON ICART ALGORITHM

2.1 Decision Tree

Decision trees are generated from training data in a top-down, general-to-specific direction. The initial state of a decision tree is the root node that is assigned all the examples from the training set. If it is the case that all examples belong to the same class, then no further decisions need to be made to partition the examples, and the solution is complete. If examples at this node belong to two or more classes, then a test is made at the node that will result in a split. The process is recursively repeated for each of the new intermediate nodes until a completely discriminating tree is obtained.

A typical decision tree with three-dimensional input-vector and one-dimensional output-vector is showed as Fig.1. Where x_1 , x_2 and x_3 are

respectively the three inputs and y is the output. The decision tree is a tree structure that represents a subspace of all the possible rules. It consists of internal nodes (with two children) and terminal nodes (without children). Each internal node is associated with a decision function to indicate which node to visit next, while each terminal node shows the output of a given input vector that leads the visit to this node (Duan, 2001, Jang, 1997 and Serge, 2001). Obviously the decision tree in Fig.1 classifies the input space into five non-overlapping rectangular regions. Each is assigned a constant value b_i as its decision output value, which is the output value of the given input vector. The main advantage of this decision tree is that it is a very easy-to-interpret representation of a nonlinear input-output mapping (Quinlan, 1986). They generate incomplete rules constrained to a given partitioning and offer a compact description of a given context by using only the locally most significant variables.

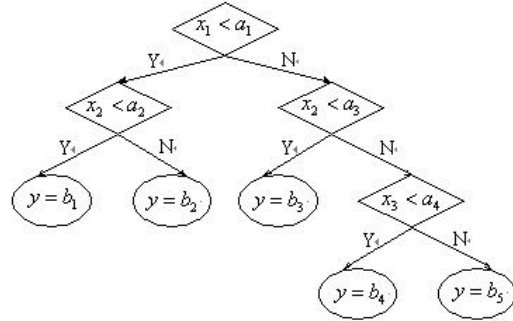


Fig. 1 The structure of decision tree

2.2 ICART algorithm

In this section, we will describe the ICART algorithm. Before proceeding, the definition of CART algorithm must be introduced. The CART technique can be generalized as involving the partitioning of training data into terminal nodes by a sequence of binary splits, starting at a parent node. The procedure searches through all values of all the independent variables to obtain the variable and the value that provides the best split into child nodes. Once a best split is found, CART repeats the search process for each child node, continuing recursively until further splitting is impossible or stopped for some reason. Splitting is not possible if only one case remains at a particular node or if all the cases at that node are identical copies of each other. When all branches from the root reached terminal nodes, the tree was considered complete. CART produces more robust results by generating what is called a maximal tree and then examining smaller trees obtained by pruning away branches of the maximal tree. The important point is that CART trees are always grown larger than they need to be and are then selectively pruned back (Ina, 1998). The final tree is picked up as the tree that performs best when the test data set is presented.

For terminal nodes with constant output values, CART can always construct an appropriate tree with a right size and, at the same time, find which inputs are irrelevant and thus not used in the tree. The

processing of determining the constant output values is stated as follows (Breiman, 1984).

For node t, the error function can be defined as:

$$E(t) = \min_{\mathbf{q}} \sum_{i=1}^{N(t)} (y_i - d_t(x_i, \mathbf{q}))^2 \quad (1)$$

Where $\{x_i, y_i\}$ is a pair of input and output data, $d_t(x_i, \mathbf{q})$ is the local model of node t, $N(t)$ is the number of input and output data pairs belonging to node t and \mathbf{q} is variable parameters.

If $d(x, \mathbf{q}) = \mathbf{q}$ is a constant function, the \mathbf{q} that can generate minimal error function $E(t)$ is

$$\mathbf{q}^* = \frac{1}{N(t)} \sum_{i=1}^{N(t)} y_i \quad (2)$$

Obviously, the CART algorithm only uses the average output of node t as its predictive output. This may cause discontinuous boundaries. In order to overcome this drawback, our improved CART (ICART) algorithm adopts the distributing density function. For node t, the predictive output is determined by the average output, the maximum output and the minimum output of this node, namely

$$\begin{aligned} \mathbf{q}^* &= (\text{MAX}_Y - \text{AVE}_Y) \exp(-\mathbf{x}_{t1} \|\text{MAX}_U - \mathbf{x}\|^2) \\ &+ (\text{MIN}_Y - \text{AVE}_Y) \exp(-\mathbf{x}_{t2} \|\text{MIN}_U - \mathbf{x}\|^2) + \text{AVE}_Y \end{aligned}$$

$$\text{AVG}_Y = \frac{1}{N(t)} \sum_{i=1}^{N(t)} y_i \quad (3)$$

Where MAX_Y is the maximum output of node t, MIN_Y is the minimum output of node t, AVG_Y the average output of node t, MAX_U and MIN_U are, respectively the input data of MAX_Y and MIN_Y . \mathbf{x}_{t1} and \mathbf{x}_{t2} are adjustable parameters. Obviously, when \mathbf{x}_{t1} and \mathbf{x}_{t2} are set to $\mathbf{x}_{t1} \rightarrow \infty$ and $\mathbf{x}_{t2} \rightarrow \infty$, Formulate (3) equate to Formulate (2). So Formulate (2) is a special case of Formulate (3).

Obviously, the main advantage of our proposed ICART algorithm is that it adopts density function to construct the local model for every crunodes and overcomes the discontinuity at the decision boundaries, which is unnatural and brings undesired effects to the overall regression and generalization.

2.3 Designing neuro-fuzzy System Based on ICART Algorithm

The decision tree in Fig.1 is equivalent to a set of crisp rules:

$$\begin{cases} \text{If } x_1 < a_1 \text{ And } x_2 < a_1 \text{ Then } y = b_1 \\ \text{If } x_1 < a_1 \text{ And } x_2 \geq a_1 \text{ Then } y = b_2 \\ \text{If } x_1 \geq a_1 \text{ And } x_2 < a_2 \text{ Then } y = b_3 \\ \text{If } x_1 \geq a_1 \text{ And } x_2 \geq a_3 \text{ And } x_3 < a_4 \text{ Then } y = b_4 \\ \text{If } x_1 \geq a_1 \text{ And } x_2 \geq a_3 \text{ And } x_3 \geq a_4 \text{ Then } y = b_5 \end{cases} \quad (4)$$

The CART procedure initially considers the data as

belonging to a single group. This group is partitioned into two relatively homogeneous subgroups. More specifically, given any input vector $(x; y)$, only one rule out of five will be fired at full strength while the other four rules are not activated at all and the output only is determined by the fired rule. Moreover, this crisp sets reduce the computation burden in constructing the tree using ICART and it also gives undesired discontinuous boundaries. Fuzzy inference, however, is the most basic human being's reasoning mechanism. The fuzzy set can smooth out the discontinuity at each split, so we use fuzzy sets to represent the premise parts of the rule set. The statement $x \geq a$ can be represented as a fuzzy set characterized by the sigmoid membership function :

$$m_{x \geq a} = \text{sig}(x; \mathbf{b}, a) = \frac{1}{1 + \exp[-\mathbf{b}(x - a)]} \quad (5)$$

Obviously, when the premise parts of the rules set in decision tree are represented by fuzzy sets, the decision tree is equivalent to a fuzzy system. On basis of this fact, we use ICART algorithm to design neuro-fuzzy system. The proposed neuro-fuzzy system based on ICART algorithm is showed as Fig.2.

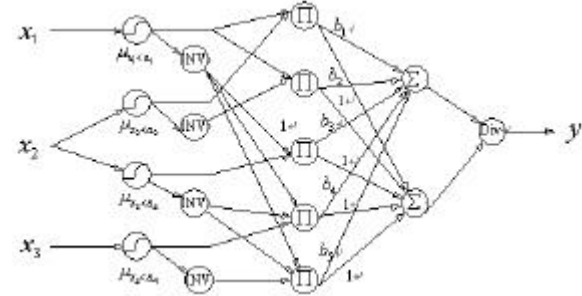


Fig. 2 The structure of neuro-fuzzy system based on ICART algorithm

The neuro-fuzzy system based on ICART algorithm consists of five layers. The first layer is input layer. Each node in this layer is called an input linguistic node and corresponds to one input variable. The node only transmits input values to the next layer directly. Nodes in second layer are called input term nodes, each of which correspond to one linguistic label of an input variable. Each node in this layer calculates the membership value specifying the degree to which an input value belongs to a fuzzy set. INV nodes represent negation operator. A sigmoid membership function is used in this layer, which is described as:

$$\begin{aligned} m_{x \geq a} &= \text{sig}(x; \mathbf{b}, a) = \frac{1}{1 + \exp[-\mathbf{b}(x - a)]} \\ m_{x < b} &= 1 - \text{sig}(x; \mathbf{b}, a) = 1 - \frac{1}{1 + \exp[-\mathbf{b}(x - b)]} \end{aligned} \quad (6)$$

where \mathbf{b} , a , b and \mathbf{h} are the adjusted parameters in membership function.

The third layer consists of N neurons, which compute the fired strength of a rule. Multiplicative inference is used, so the output of this layer is:

$$y_j^{(3)} = \prod m_{x < a} \quad (7)$$

There are two neurons in fourth layer. One of them connects with all neurons of the third layer through the weight b_j representing the consequence of the j th rule and another one connects with all neurons of the third layer through unity weights. The last layer has a single neuron to compute y . It is connected with two neurons of the fourth layer through unity weights. The integral function and activation function of the node can be expressed as:

$$y = \frac{\sum_{j=1}^5 b_j y_j^{(3)}}{\sum_{j=1}^5 y_j^{(3)}} \quad (8)$$

2.3 Parameters optimization

In parameters optimization learning phase input and output data are presented to adjust parameters and obtain better fuzzy model. Its goal is to minimize the error function:

$$E = \frac{1}{2} [y(t) - d(t)]^2 \quad (9)$$

where $y(t)$ is the current output and $d(t)$ is the desired output. For a training data pair, starting at the input nodes, a forward pass is used to compute the activity levels of all the nodes, a backward pass is used to compute $\partial E / \partial y$ for all parameters. The adjustable parameters can be adjusted as follows.

$$\mathbf{x}_i(k+1) = \mathbf{x}_i(k) - \mathbf{a} \frac{\partial E}{\partial \mathbf{x}_i} + \mathbf{b}(\mathbf{x}_i(k) - \mathbf{x}_i(k-1)), \quad i=1,2 \quad (10)$$

$$\frac{\partial E}{\partial \mathbf{x}_1} = (y-d)b_i \|\text{MAX_}_U_i - \mathbf{x}\|^2 (\text{MAX_}_Y_i - \text{AVE_}_Y_i) \exp(-\mathbf{x}_1 \|\text{MAX_}_U_i - \mathbf{x}\|^2) \quad (11)$$

$$\frac{\partial E}{\partial \mathbf{x}_2} = (y-d)b_i \|\text{MIN_}_U_i - \mathbf{x}\|^2 (\text{MIN_}_Y_i - \text{AVE_}_Y_i) \exp(-\mathbf{x}_2 \|\text{MIN_}_U_i - \mathbf{x}\|^2) \quad (12)$$

And the membership parameters can also be adjusted as above supervised algorithm.

3. PRACTICAL APPLICATION FOR MODELING JET FUEL ENDPOINT OF HYDROCRACKING PROCESSING

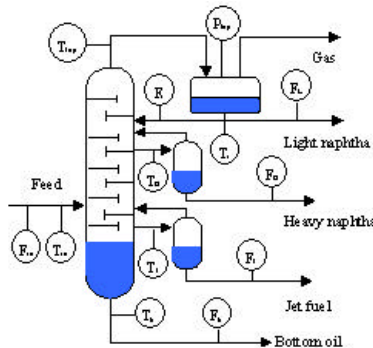


Fig.3 The schematic representation of the hydro-cracking fractionator

Hydrocracking is one of the most important processes in the petroleum industry. It upgrades

heavy oil value by making high quality products, such as gasoline or kerosene. The purpose of the main fractionator of a hydrocracking process is to split a feed that produced from the former process into three product streams of different molecular weight, that is, light naphtha, heavy naphtha and jet fuel. Their endpoints are the key indicators to value the product quality. Figure 3 shows a schematic representation of the main hydrocracking fractionator.

According to the analysis of technological mechanisms, the endpoints of the three sides (i.e., light naphtha, heavy naphtha and jet fuel) are related with the above mentioned 13 variables, which can be measured and recorded on-line. In this section, the jet fuel endpoint will be studied. The relationship between it and above-mentioned 13 variables is described as equation (13):

$$EP_J(k) = f(T_r(k), F_r(k), T_s(k), F_s(k), T_b(k), F_b(k), F_L(k)) + \mathbf{x}(k) \quad (13)$$

where $EP_J(k)$ represent the endpoint () of jet fuel, $f(\cdot)$ is the complex multivariable non-linear function, $\mathbf{x}(k)$ represents the uncertain term. The task is to find the relationship between the endpoint of jet fuel and the selected 13 secondary variables, so we can estimate the product quality of jet fuel on-line.

From equation (13) and the views of technological mechanisms, though all the 13 variables have cause-and-effect relationships with the quality variable, selecting all thirteen variables as the input of self-organizing neuro-fuzzy system is totally unnecessary because the above-mentioned variables (i.e. T_r , F_r , T_s , F_s , F_L , F_H , F_J) are highly correlated each other. By statistical regression analyzing step by step, jet fuel endpoint is mainly affected by the following six measurable variables: T_r , F_s , F_r , F_L , F_H , F_J . So its model structure is represented as:

$$EP_J = g(Tr, Fin, Fr, FL, FH, FJ) \quad (14)$$

Then the proposed algorithm is used to establish the system. There are 223 sets of sample data of thirteen operating variables in different operating states. 173 pairs of them are used as off-line training data sets and another 50 pairs are used as on-line testing data sets, which verify the fuzzy inference power of the neuro-fuzzy system designed based on ICART algorithm. In the learning phase, all training data are scaled in the intervals [-1, +1].

After the learning, 173 sets training data are clustered into 40 categories, that is the number of IF-THEN rules of neuro-fuzzy system is 40 which is less than conventional grid partitioned neuro-fuzzy system's. In order to verify the generalization of the presented fuzzy model, another 50 sets are used to test it. The estimated values are shown in Fig.4 (a). In addition, the neuro-fuzzy system based on CART algorithm is used to build a soft sensing model shown as Fig.4 (b). Table4 are about the comparison between CART algorithm and ICART algorithm. The results show that the proposed neuro-fuzzy system designed by ICART algorithm possesses better generalization ability and is smoother than CART algorithm.

In order to verify the validity of the proposed neuro-fuzzy system designed by ICART algorithm, the method proposed in paper Jia (2001), which uses clustering algorithm to construct neuro-fuzzy system, is applied to build a soft sensing model shown as Fig4 (c). Comparisons between these two models are represented in Table.1. From Table.1 we learn that the method proposed in this paper possesses simple structure and better generalization ability than the method presented in paper Jia (2001).

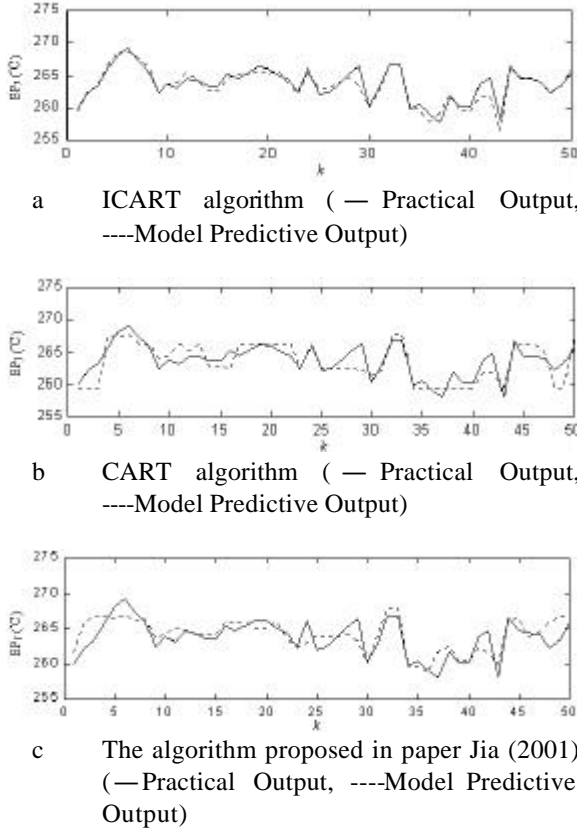


Fig.4 The comparison between CART algorithm, ICART algorithm and Method in paper Jia (2001)

Tab.1 the comparison between CART algorithm, ICART algorithm and Method in paper Jia (2001)

Algorithm	Rule	RMSE	MAX
ICART	40	0.8786	2.9812
CART	40	1.7772	4.1718
Method in paper Jia (2001)	45	1.6784	3.6864

In summary, the proposed neuro-fuzzy system designed by ICART algorithm possesses simple structure, better generalization ability and is smoother than CART algorithm. And it can be successfully applied to quality prediction for hydrocracking processing.

4. CONCLUSION

A neuro-fuzzy system based on ICART algorithm, which using ICART algorithm to design neuro-fuzzy system is proposed in this paper. It is worth noting that ICART algorithm classifies the input space into tree structure adaptively, which avoids the curse of

dimensionality because the total number of fuzzy rules doesn't increase exponentially with the number of input variables. Moreover it adopts density function to construct the local model for every crunodes in order to overcome the discontinuous boundary existed in CART algorithm. The major advantage offered by this approach is that the user can now quickly determine the roughly correct structure of a fuzzy inference through ICART, and then refine the membership functions and output functions via efficient neuro-fuzzy system architecture. It can be seen that ICART and neuro-fuzzy system are complementary and their combination makes a solid approach to fuzzy modeling. In addition, a supervised scheme is used to adjust parameters to minimize the network output error and constructer optimal fuzzy model on the basis of ICART algorithm. Finally, to illustrate the validity of the proposed method, a practical application are done. The results show that the proposed method can provide optimal model structure and parameters for fuzzy modeling, possesses high learning efficiency and is smoother than CART algorithm. And it can be successfully applied to quality prediction for hydrocracking processing.

REFERENCE

- Breiman L., Friedman, J.H., Olshen, R.A., Stone, C.J. (1984) . *Classification and regression trees*. Wadsworth, Inc., Belmont, Californiz
- Duan J.C., Chung F.L. (2001). Cascaded fuzzy neural network model based on syllogistic fuzzy reasoning. *IEEE Trans. FS*. 9(2), 293-306
- Ina S.M., Richard G.M. , Barry A.W.,(1998). A rule induction approach for determining the number of kanbans in a just-in-time production system. *Computers ind. Engng*. 34(4), 717-727
- Jang, J.S.R., Sun C.T., Mizutan E, (1997). *Neuro-fuzzy and soft computing: A computational approach to learning and machine intelligent*. Prentice Hall
- Jia, Li, Yu, Jinshou, (2001). A novel neural fuzzy network and application to modeling octane number. *Hydrocarbon Processing*. 12, 56-60
- Quinlan J.R., (1986). *Induction of decision trees*. Mach. Learn., 1, 81-106
- Mauricio, Figueiredo, Fernando, Gomide, (1999). Design of fuzzy systems using neurofuzzy networks. *IEEE Trans. Neural Networks*. 10(4), 815-824
- Meng Joo Er, (2000). Fuzzy neural networks-based quality prediction system for sintering process, *IEEE Trans. F.S.*, 8(3), 314-323
- Serge G, (2001). Designing fuzzy inference systems from data: an interpretability-oriented review. *IEEE Trans. FS*. 9(3), 426-443
- Wang, L.X., (1994). *Adaptive fuzzy systems and control*, Prentice-Hall, Englewood Cliffs, NJ
- Yin, Wang, Gang, Rong, (1999), A self-organizing neural-network-based fuzzy system, *Fuzzy sets and systems*, 103, 1-11

HYBRID CONTROL OF A FOUR TANKS SYSTEM

C. de Prada*, S. Cristea*, D. Megías, J. Serrano****

**Dpt. Systems Engineering and Automatic Control, University of Valladolid*

Faculty of Sciences, c/ Real de Burgos s/n, 47011 Valladolid, Spain

Tel. (+34) 983 423 162, Fax: (+34) 983 423 161

{prada, smaranda}@autom.uva.es

*** Dpt. Systems Engineering and Automatic Control, ETSE,*

Universitat Autònoma de Barcelona, 08193 Bellaterra, Barcelona, Spain

Tel. (+34) 935 813 027, Fax (+34) 935 813 033,

{David Megias, Javier.Serrano}@uab.es

Abstract: Many processes, even being of a continuous nature, involve in its operation signals or rules different from the classical continuous variables represented by real variables and modelled by DAE. In practice they include on/off valves or other binary actuators, are subjected to logical operational rules, or are mixed with sequential operations. As a result, classical control does not fit very well with the overall operation of the plant. In this paper we consider the problem of hybrid control from a predictive control perspective, showing in a practical non trivial example with changing process structure, how the problem can be stated and solved. *Copyright © 2003 IFAC*

Keywords: Hybrid control, predictive control, four tank system

1. INTRODUCTION

The topic of hybrid systems and hybrid control has received a lot of attention in the latest years, mainly in relation with complex distributed systems that combine continuous operating units of several nature with interconnections following logical rules. In the present paper this field is seen from a process control perspective where the core of the process is continuous, and the main variables can be represented by real numbers, but where there are also other elements that do not fit in this framework. These can be classified into four categories:

- Devices or elements that operates in an on/off way and that can be represented by binary variables instead of usual real ones. As typical examples we can mention on/off valves or motors.
- Process units that can operate or be switched off according to the production needs or constraints.
- Operational rules or constraints of logical nature that form part of the correct operation of a process. They are given usually in the form IF (situation) THEN (action).
- Process units that operate in batch mode according to a given sequence of stages. Here the timing and scheduling of the operation is a key factor.

In all these cases, the standard control approach, based on a continuous process model and continuous

manipulated variables, fails due to the discrete (integer) or logical nature of the new elements. Nevertheless, in industrial practice, if we exclude the more simple cases of SISO control loops and we navigate towards plant wide control considering the problem of controlling a complex process unit or a section of a factory, it is very likely that the above mentioned elements are present in a certain degree. Then, it is important to reformulate the control problem finding adequate representations of these hybrid systems as well as practical paths to solve and analyse them.

There are several approaches to model hybrid systems. Some of them set hierarchical levels, leaving the continuous parts in the bottom and the discrete decision variables in the upper ones (Grossmann, *et al.*, 1993). Other approaches take advantage of the fact that propositional logic expressions can be formulated in a systematic way as linear inequalities of binary variables (Clocksin and Mellish, 1981). An important contribution in this line is (Bemporad and Morari, 1999), where MLD systems are defined and analysed. Other contributions can be seen in (Colmenares, *et al.*, 2001; Zhu et al., 2000).

In this paper, within the framework of predictive control, a case study of a process with four interconnected tanks is presented. It is able to operate in different modes according to the value of a set of on/off valves. The paper is organised as follows: In section 2, a review of how to formulate hybrid models

and the associated predictive control is presented. In section 3 the process is described, while in section 4 the specific formulation for the model and MPC controller is given. Results can be seen in section 5 and, finally, some brief conclusions are drawn.

2. MLD MODELS

A natural way to represent discrete elements with two or more states (on/off type) or process units that can be switched off, is by means of integer (0–1) variables. Logical operational rules can be translated into inequalities involving binary variables in a systematic way.

If P is a logical proposition that can have the values true or false, then associating an integer variable y (1–0) to it, conjunctions and disjunctions of propositions can be translated easily:

$$\begin{aligned} P_1 \wedge P_2 & \quad y_1 + y_2 \geq 1 \\ P_1 \vee P_2 & \quad y_1 \geq 1, y_2 \geq 1 \end{aligned} \quad (1)$$

More general expressions are first converted into the so called normal conjunctive pattern:

$$Q_1 \wedge Q_2 \wedge \dots \wedge Q_n \quad (2)$$

where Q is a disjunctive proposition and then translated as before. The procedure for converting a proposition into this pattern follows three steps:

- a) Replace the logical implications by its equivalent:

$$P_1 \Rightarrow P_2 \Leftrightarrow \overline{P_1} \vee P_2 \quad (3)$$

- b) Apply Morgan's laws in order to move the negations inside

$$(\overline{P_1} \wedge P_2) \Leftrightarrow \overline{P_1} \vee \overline{P_2} \quad (\overline{P_1} \vee P_2) \Leftrightarrow \overline{P_1} \wedge \overline{P_2} \quad (4)$$

- c) Apply the distributed property in order to obtain the desired pattern

$$(P_1 \wedge P_2) \vee P_3 \Leftrightarrow (P_1 \wedge P_3) \wedge (P_2 \wedge P_3) \quad (5)$$

Activation or de-activation of real variables x linked to the existence or operation of discrete elements can be formulated as products of the type xy , but this creates a non-linearity. An alternative is to formulate them in terms of linear inequalities of the type:

$$Ly \leq x \leq Uy \quad (6)$$

where L and U are lower and upper limits of x , while y is the associated integer variable. If $y = 1$, then the standard constraint on x remains active, but if $y = 0$ the x variable is forced to 0. In (Floudas, 1995) a way of dealing with more complex situations can be seen.

A model integrating continuous dynamics, discontinuous variables and logical constraints results then in a set of equations such as:

$$\begin{aligned} \frac{dx}{dt} &= f(x, u, y) \\ h(x, u, y) &= 0 \\ g(x, u, y) &\leq 0 \\ x &\in X \subset R^n \\ u &\in U \subset R^m \\ y &\in \{0,1\} \end{aligned} \quad (7)$$

being x continuous process variables, u real decision variables and y integer ones.

The predictive control problem is then to choose u and y over a given control horizon, so that a cost index is minimised along a given prediction horizon, repeating the problem every sampling period as part of a moving horizon strategy. Unfortunately, because of the presence of the integer variables, this is a mixed integer optimisation problem which implies a heavy computational burden.

3. PROCESS DESCRIPTION

The four tanks systems is part of a lab plant at UAB used as a test bed for this kind of problems. The system to be controlled is depicted in Fig. 1 and consists of two sections: the storage section, represented by the two upper tanks and the mixing one which includes the two bottom tanks.

Liquid flows from the storage tanks to the mixing ones through four pipes which have on/off valves (V) in order to activate or block the lines, and two speed pumps. Another flows q_{BM} are added into the mixing tanks in proportion to the main currents. Input flows q_{Ev} to the storage tanks, as well as the demands of the final products q_M , are subjected to strong and frequent changes, as coming from a batch section, and can be considered as the main disturbances to the plant.

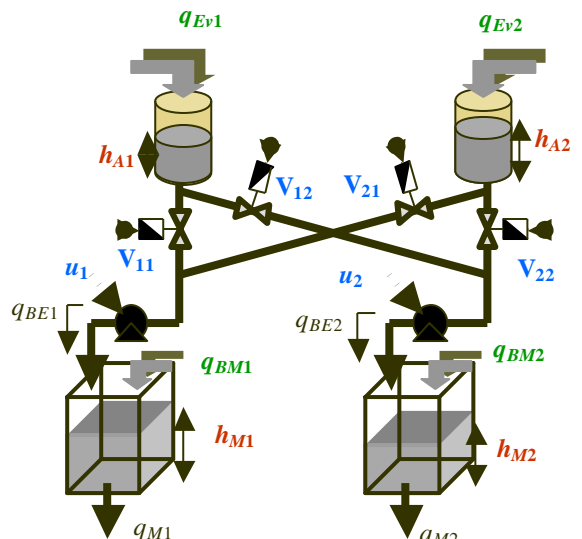


Fig. 1 Schematic Diagram

The purpose of this process is mixing the currents q_{BE} and q_{BM} in given proportions while maintaining the levels of the four tanks close to given setpoints and, on any case, within pre-specified ranges.

The storage phase can be described by the following equations:

$$S_{A1} \frac{dh_{A1}}{dt} = q_{Ev1} - q_{11} - q_{12} \quad (8)$$

$$S_{A2} \frac{dh_{A2}}{dt} = q_{Ev2} - q_{21} - q_{22} \quad (9)$$

$$q_{BE1} = ku_1 = q_{11} + q_{21} \quad (10)$$

$$q_{BE2} = ku_2 = q_{12} + q_{22} \quad (11)$$

where h represents the level in the tanks and the relation between the output flow of the pumps (q_{BE1} , q_{BE2}) and the input signal to them (u_1 , u_2) is considered linear. The inflows q_{Ev1} and q_{Ev2} are measured disturbances and the four cross flows q_{ij} are depending on q_{BE1} and q_{BE2} .

$$q_{1i} = q_{BEi} \cdot f_1(h_{A1}, h_{A2}), \quad i=1,2 \quad (12)$$

$$q_{2i} = q_{BEi} \cdot f_2(h_{A1}, h_{A2}), \quad i=1,2 \quad (13)$$

where

$$f_1(h_{A1}, h_{A2}) = \frac{\sqrt{h_{A1}}}{\sqrt{h_{A1}} + \sqrt{h_{A2}}} \quad (14)$$

and

$$f_2(h_{A1}, h_{A2}) = \frac{\sqrt{h_{A2}}}{\sqrt{h_{A1}} + \sqrt{h_{A2}}} \quad (15)$$

A simplified linear expression of relations (12) and (13), can be obtained approximating (14) and (15) by its values at the nominal operating point $(\bar{h}_{A1}, \bar{h}_{A2})$:

$$q_{1i} = \alpha_1 q_{BEi}, \quad i=1,2 \quad (16)$$

$$q_{2i} = \alpha_2 q_{BEi}, \quad i=1,2 \quad (17)$$

being

$$\alpha_1 = f_1(\bar{h}_{A1}, \bar{h}_{A2})$$

$$\alpha_2 = f_2(\bar{h}_{A1}, \bar{h}_{A2}) = 1 - \alpha_1$$

The other part of the process, the mixing tanks, is modelled by a similar set of equations:

$$S_{M1} \frac{dh_{M1}}{dt} = q_{BE1} + q_{BM1} - q_{M1} \quad (19)$$

$$S_{M2} \frac{dh_{M2}}{dt} = q_{BE2} + q_{BM2} - q_{M2} \quad (20)$$

$$q_{BM1} = Rq_{BE1} \quad (21)$$

$$q_{BM2} = Rq_{BE2} \quad (22)$$

The outflows q_{M1} and q_{M2} represent the demand of the final product which is also a known value. The

equations (21) and (22) indicate that ratio control is apply in maintaining the value of q_{BM1} and q_{BM2} .

4. PREDICTIVE CONTROL

As mentioned above, the goal is to control the levels of the four tanks in spite of the disturbances, manipulating the signals (u_1 , u_2) to the two pumps and the four on/off valves, V_{ij} , which interconnect the tanks. So, there are four controlled variables, two real manipulated variables and four integer ones, plus four disturbances.

Behind all approaches of predictive control there are a model of the plant used to predict the future evolution of the system. Based on this prediction, at each time step, the controller selects a sequence of future command inputs through an on line optimization procedure, which aims at maximizing the tracking performance subjected to given constraints. In our case, due to the on/off valves, the model is one of hybrid nature. So, in addition to continuous models used to describe the process ((8)-(22)), the behavior of the system must be completed with the operating modes imposed by the four on/off valves, which can be stated in terms of propositional logic. In this way the process can be modeled through a MLD structure. There are several ways of doing it. Here, a particular one is presented.

4.1 Representation of Logic

Note that, when taking into account the on/off valves, equations (10) and (11) are not valid in all situations and the model must be modified. The outflows from the pumps depend also on the state of the on/off valves V_{ij} , according to the following rules:

$$q_{BE1} = \begin{cases} 0 & \text{if } V_{11} = 0 \wedge V_{21} = 0 \\ ku_1 & \text{if } V_{11} = 1 \vee V_{21} = 1 \end{cases} \quad (23)$$

$$q_{BE2} = \begin{cases} 0 & \text{if } V_{21} = 0 \wedge V_{22} = 0 \\ ku_2 & \text{if } V_{21} = 1 \vee V_{22} = 1 \end{cases} \quad (24)$$

So, considering the possible combinations of the valves states (0/1), for each left and right section of the process, four possibilities are generated. The first group of compound statements is:

$$V_{11} = 0 \wedge V_{21} = 0 \Rightarrow \begin{cases} q_{11} = 0 \\ q_{21} = 0 \end{cases} \rightarrow (P_{11}) \quad (25)$$

$$V_{11} = 0 \wedge V_{21} = 1 \Rightarrow \begin{cases} q_{11} = 0 \\ q_{21} = ku_1 \end{cases} \rightarrow (P_{12}) \quad (26)$$

$$V_{11} = 1 \wedge V_{21} = 0 \Rightarrow \begin{cases} q_{11} = ku_1 \\ q_{21} = 0 \end{cases} \rightarrow (P_{13}) \quad (27)$$

$$V_{11} = 1 \wedge V_{21} = 1 \Rightarrow \begin{cases} q_{11} = k\mathbf{a}_1 u_1 \\ q_{21} = k\mathbf{a}_2 u_1 \end{cases} \rightarrow (P_{14}) \quad (28)$$

The prepositional logic expressions P_{1j} (25)-(28) can be translated into a mathematical representation by associating a binary variable $y_{1i} \in \{0,1\}$ with each clause P_{1i} . The clause P being true or false corresponds to the values $y=1$ or $y=0$.

In this way the expression for the inlet flows to the left pump has a new mathematical form:

$$\begin{aligned} q_{11} &= k u_1 y_{13} + \mathbf{a}_1 k u_1 y_{14} \\ q_{21} &= k u_1 y_{12} + \mathbf{a}_1 k u_1 y_{14} \end{aligned} \quad (29)$$

where the 0-1 y variables activate/de-activate continuous terms. As mentioned in section 2, a more efficient equivalent form of (29) is obtained by introducing inequality constraints instead:

$$\begin{aligned} 0y_{11} + 0y_{12} + q_{\min} y_{13} + \mathbf{a}_1 q_{\min} y_{14} &\leq q_{11} \\ q_{11} &\leq 0y_{11} + 0y_{12} + q_{\max} y_{13} + \mathbf{a}_1 q_{\max} y_{14} \end{aligned} \quad (30)$$

$$\begin{aligned} 0y_{11} + q_{\min} y_{12} + 0y_{13} + \mathbf{a}_2 q_{\min} y_{14} &\leq q_{21} \\ q_{21} &\leq 0y_{11} + q_{\max} y_{12} + 0y_{13} + \mathbf{a}_2 q_{\max} y_{14} \end{aligned} \quad (31)$$

where

$$\begin{aligned} q_{\max} &= k U_{\max} \\ q_{\min} &= k U_{\min} \end{aligned} \quad (32)$$

with U_{\max} and U_{\min} the upper and lower bounds on the voltage of the pumps.

Notice that one and only one of the situations (25)-(28) can be active at a time, which implies the need of the prepositional logic expression (the exclusive-or condition):

$$P_{11} \oplus P_{12} \oplus P_{13} \oplus P_{14} \quad (33)$$

which can be easily converted into a linear equality constraint in terms of the associated integer variables:

$$y_{11} + y_{12} + y_{13} + y_{14} = 1 \quad (34)$$

In a similar way, other four 0/1 variables y_{2i} ($i=1,4$) are introduced in order to model the right section of the process. The corresponding constraints are:

$$\begin{aligned} 0y_{21} + 0y_{22} + q_{\min} y_{23} + \mathbf{a}_1 q_{\min} y_{24} &\leq q_{12} \\ q_{12} &\leq 0y_{21} + 0y_{22} + q_{\max} y_{23} + \mathbf{a}_1 q_{\max} y_{24} \end{aligned} \quad (35)$$

$$\begin{aligned} 0y_{21} + q_{\min} y_{22} + 0y_{23} + \mathbf{a}_2 q_{\min} y_{24} &\leq q_{22} \\ q_{22} &\leq 0y_{21} + q_{\max} y_{22} + 0y_{23} + \mathbf{a}_2 q_{\max} y_{24} \end{aligned} \quad (36)$$

$$\sum_{i=1}^4 y_{2i} = 1 \quad (37)$$

4.2 The optimization problem

The task of the predictive controller is minimizing at every sampling time the following finite horizon objective function:

$$\min_{\Delta u_i, y} \left(\sum_{i=1}^4 \sum_{j=N1_i}^{N2_i} \left(\mathbf{g}_i (\hat{h}_i(t+j) - r(t+j))^2 \right) + \sum_{i=1}^4 \sum_{j=0}^{Nu_i-1} \mathbf{b}_i (\Delta u_i(t+j))^2 \right) \quad (38)$$

where $\hat{h}_i(t+j)$ are predicted values of the outputs (the levels of the four tanks) and $\mathbf{D}u(t) = u(t) - u(t-1)$, subjected to the model previously developed and possible constraints on the process variables. Due to the presence of integer variables, the optimization procedure is a Mixed Integer Quadratic Programming (MIQP) problem. This is a hard task from a computational point of view, mainly in the non-linear case. So, in order to keep it as simpler as possible, that is, in linear form, the optimization problem was formulated in terms of the decision variable x (39), which includes current and future values of the inlet flows to the pumps as well as the eight integer variables y_{ij} , $i=1 \div 2$, $j=1 \div 4$, instead of the more natural V and u signals.

$$\mathbf{x} = \begin{pmatrix} \Delta q_{11}(t) \\ \vdots \\ \Delta q_{11}(t+Nu_1-1) \\ \Delta q_{21}(t) \\ \vdots \\ \Delta q_{21}(t+Nu_2-1) \\ \vdots \\ \Delta q_{22}(t) \\ \vdots \\ \Delta q_{22}(t+Nu_2-1) \\ y_{11} \\ \vdots \\ y_{14} \\ y_{21} \\ \vdots \\ y_{24} \end{pmatrix} \quad (39)$$

Then, in addition to (30), (31), (34)-(37), other constraints in the controlled and manipulated variables are also taken into account:

$$\begin{cases} \underline{U}_{ik} \leq q_{ik}(t+j) \leq \bar{U}_{ik} & 0 \leq j \leq Nu_i-1; 1 \leq i \leq 4, 1 \leq k \leq 2 \\ \underline{D}_{ik} \leq \Delta q_{ik}(t+j) \leq \bar{D}_{ik} \\ \underline{L}_i \leq \hat{x}_i(t+j) \leq \bar{L}_i & N3_i \leq j \leq N4_i; 1 \leq i \leq 4 \end{cases} \quad (40)$$

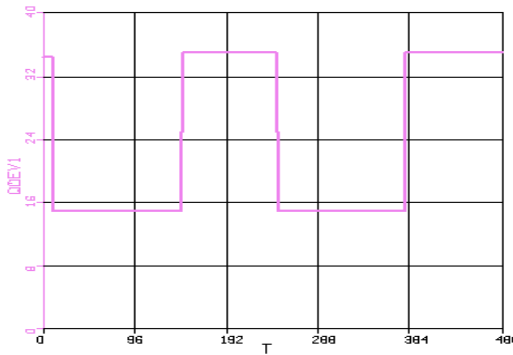


Fig.2 Evolution of inflow q_{Ev1}

Finally, a practical solution in terms of the two control signals u and the V positions can be obtained from the y_{ij} values and

$$u_1 = \frac{q_{11} + q_{21}}{k}; \quad u_2 = \frac{q_{12} + q_{22}}{k} \quad (41)$$

At each time step, this problem involves $\sum_{i=1}^4 N u_i$ continuous variables, eight integer variables and $2 * \sum_{i=1}^4 N u_i + \sum_{i=1}^4 (N_{4i} - N_{3i} + 1) + 6$ linear constraints.

The implementation of the Mixed-Integer Predictive Controller proposed in this paper has been obtained in C language by using the NAG package as a MIQP solver based on the branch and bound method.

5. RESULTS

Several tests have been carried out to investigate the performance of the controller. The nominal operating point is $(\bar{h}_{A1}, \bar{h}_{A2}) = (8.37 \text{ cm}, 11.16 \text{ cm})$ which in our plant leads to $a_1=0.46$ and $a_2=0.54$. The ratio factor from the mixing was chosen as $R=3$ and the coefficient $k = 7.5$. The sampling period was set to 5s, and the controller was tuned with the following design parameters:

- Prediction horizon: $N_1=\{1,1,1,1\}$, $N_2=\{10,10,10,10\}$;
- Constraint horizon: $N_3=\{1,1,1,1\}$, $N_4=\{10,10,10,10\}$;
- Weighting factor for the control term: $b=\{0.01,0.01,0.01,0.01\}$

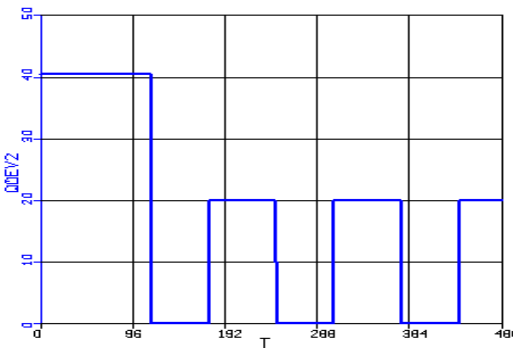


Fig.3 Evolution of inflow q_{Ev2}

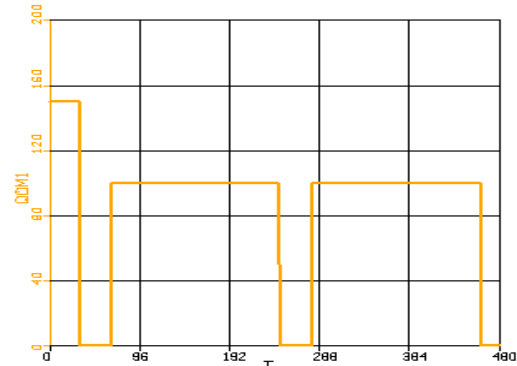


Fig.4 Demand product outflow q_{M1}

- Weights of the controlled variables in the cost index $\mathbf{g}=\{1,1,15,15\}$ which implies that preference was given to maintain the level of the mixing tanks.
- Set points for h_{A1} , h_{A2} , h_{M1} and h_{M2} were given the values: $\{8.37, 11.16, 20, 20 \text{ cm}\}$, while the input and output constraints (40) were fix to:
 - $\underline{U} = \{0,0,0,0\}$, $\overline{U} = \{75,75,75,75\} \text{ cm}^3/\text{s}$;
 - $\underline{D} = \{-15,-15,-15,-15\}$; $\overline{D} = \{15,15,15,15\}$;
 - $\underline{L} = \{0.14,0.14,0.038,0.038\} \text{ cm}$
 - $\overline{L} = \{26.5, 26.5, 30, 30\} \text{ cm}$.

The disturbances q_{Ev1} and q_{Ev2} representing the load to the storing tanks have the time evolution represented in Fig. 2 and 3, while the others two product outflows q_{M1} and q_{M2} have another periodic structure which is usual in cases where a batch section follows (Fig. 4, 5).

The first experiment considers the control horizon $Nu=\{1,1,1,1\}$ and the results are presented in Fig. 6. There we can see that the process operates according to the control objectives: keeping the levels of the mixing tanks on the set point (see the top half of the figure) and maintain the other two levels into the operating bounds (the bottom of the figure). Fig. 7 shows the manipulated variables, the two continuous signals to the pumps and the four on/off valves. A different response (Fig. 8, 9) of the process is obtained if the control horizon is increased to $Nu=\{7,7,7,7\}$. The levels of the mixing tanks are closer to the set point and the control actions present a more active form.

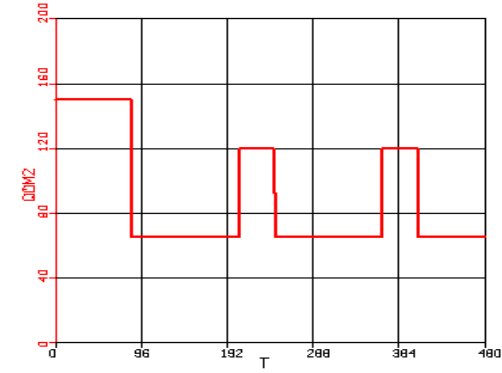


Fig.5 Demand product outflow q_{M2}

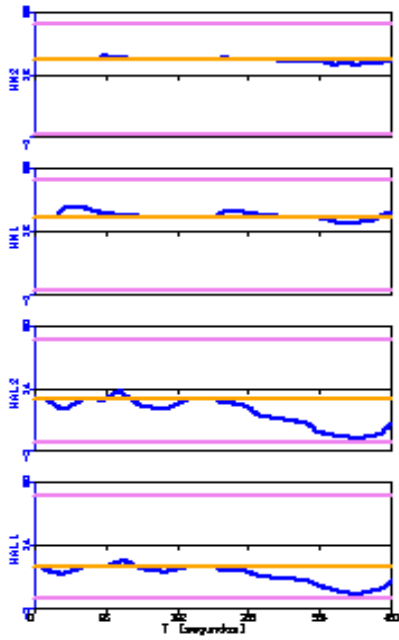


Fig. 6 Controlled variables. Short control horizon

The computation time corresponding to each sample time is approximately 0.01 seconds in a SUN workstation with 128 Mbytes of RAM.

6. CONCLUSIONS

In this paper an example of practical hybrid control have been presented. The results shows the feasibility of this approach but topics such as the best problem formulation, computational methods and closed loop properties are still open to further research.

ACKNOWLEDGEMENTS

The authors wish to express their gratitude to the Spanish CICYT for its support through the projects TAP97-1144-C02-01 and PPQ2000-1075-C02-01.

REFERENCES

- Bemporad, A. and M. Morari (1999). Control of systems integrating logic, dynamics , and constraints. *Automatica*, **35**, 407-427.
- Clocksin W. and C. Mellish (1981). *Programming in Prolog*, Springer Verlag.
- Colmenares W., S. Cristea and C. de Prada. Other (2001) MLD systems: modeling and control. Experience with a pilot process. In *IEEE CCA Conference on Control Applications*. Mexico.
- Floudas, C. A. (1995) *Non-linear and Mix-Integer Optimization*, Oxford Univ. Press.
- Grossmann R.L., A. Neorede and A.P. Ravn (1993). *Hybrid Systems*, Springer Verlag.
- Zhu G., M. Henson and B. Ogunnaike (2000). A hybrid model predictive control strategy for nonlinear plant-wide control. *Journal of Process Control*, **10**, 449-458.

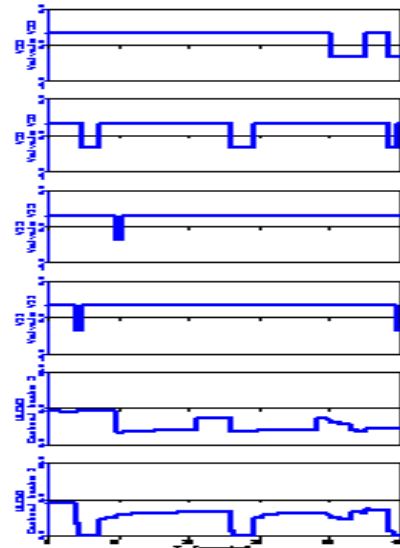


Fig. 7 Manipulated variables. $Nu=\{1,1,1,1\}$

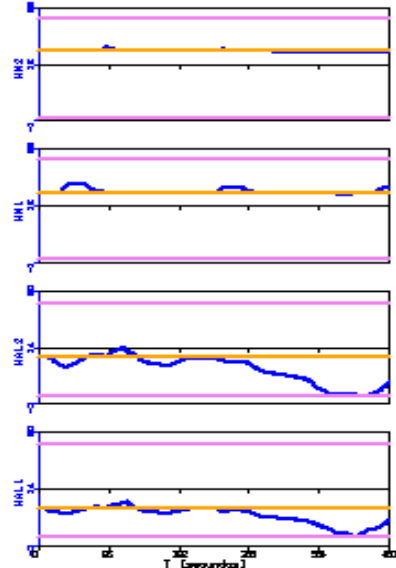


Fig. 8 Controlled variables. Longer control horizon

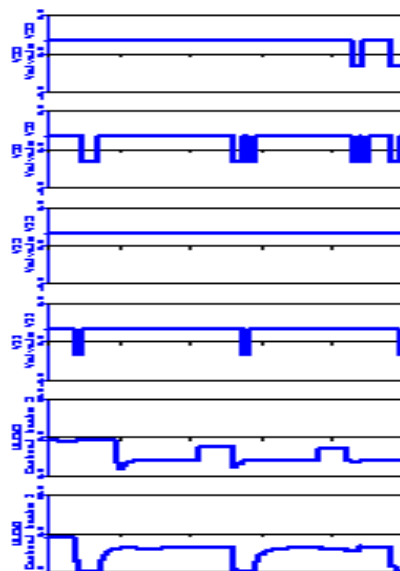


Fig. 9 Manipulated variables. $Nu=\{7,7,7,7\}$

TEMPERATURE CONTROL OF BUTYL PROPIONATE REACTIVE DISTILLATION

Shih-Ger Huang¹ and Cheng-Ching Yu²

Dept. of Chem. Eng., National Taiwan University of Sci. Tech.¹, Taipei 106-07, TAIWAN
Dept. of Chem. Eng., National Taiwan University², Taipei 106-17, TAIWAN

Abstract: In this work, we explore the temperature control of n-butyl propionate reactive distillation. Process characteristics of n-butyl propionate are explored and a systematic procedure is proposed for the design of butyl propionate heterogeneous reactive distillation. Control objective is to product specifications: high purity propionate and ppm level of acid. The control structure design procedure consists of the following steps: (1) selection of manipulated variables, (2) determine temperature control trays, and (3) find controller settings. Since two specifications on the bottoms product have to be met and stoichiometric balance has to be maintained, we have a 2x2 control problem with two obvious inputs: reboiler duty and feed ratio. The reactive distillation exhibits unique temperature sensitivities and the non-square relative gain (NRG) successfully identifies temperature control trays. It results in an almost one-way decoupled system. Therefore, decentralized PI controllers are employed. Simulation results indicate good control performance can be achieved with simple control strategy. Copyright © 2002 IFAC

Keywords: esterification, n-butyl propionate, reactive distillation, heterogeneous distillation, temperature control

1. INTRODUCTION

Reactive distillation provides an attractive alternative for process intensification, especially for reaction/separation systems with reversible reactions. The literature in reactive distillation has grown rapidly in recent years and the book by Doherty and Malone (2001) gives an updated summary. However, relatively few papers that discuss process control aspects of reactive distillation columns. These are reviewed in a recent paper by Al-Arfaj and Luyben (2000). Al-Arfaj and Luyben (2000, 2002a, 2002b) proposed several control structures for different types of reversible reactions ($A+B \leftrightarrow C+D$, $A+B \leftrightarrow C$, and $A \leftrightarrow B+C$) and consecutive reactions for the product C and by-product D ($A+B \rightarrow C$ & $A+C \rightarrow D$). They have shown that (1) reaction stoichiometric balance is crucial for system with multiple reactants, and (2) simple control strategy works satisfactorily for these complex dynamics.

Similar to the gradual replacement of methyl tert-butyl ether (MTBE) with ethyl tert-butyl ether (ETBE) (Sneesby et al., 1997), this work is a continuous effort to study the production of less volatile solvents to replace light solvents such as methyl acetate or ethyl acetate. In this work, we explore the esterification of propionic acid and n-butanol to form n-butyl propionate (Lee et al., 2002 ; Liu and Tan, 2001). n-Butyl propionate has increasing been used as a cleaning solvent for processing polymers for its relatively low volatility. The process (Huang, 2002) falls into a specific class of reactive distillations: heterogeneous reactive distillation (or three-phase reactive distillation; Chiang et al., 2002). By heterogeneous reactive distillation, we mean two-liquid phase exists in the reflux drum and a decanter

is employed to separate the aqueous product from the organic reflux.

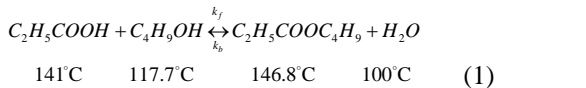
The objective of this work is to devise control structure for n-butyl propionate process and the control objective is to maintain the propionate quality at specification while keeping the acid purity at ppm (part per million) level. This would require two on-line analyzers. Instead of using expensive and less reliable on-line composition analyzers, temperature control of this three-phase reactive distillation is explored.

2. PROCESS

By heterogeneous reactive distillation, we mean two-liquid phase exists in the reflux drum and a decanter is employed to separate the aqueous product from the organic reflux. For esterification reactions, propyl acetate, butyl acetate, and amyl acetate are good examples, because they all share the following characteristics:

- (1) a large two-liquid zone exists,
- (2) the minimum boiling azeotrope is located in the two-liquid zone,
- (3) one end of all tie lines points to the direct of a pure component (typically water for esterification).

n-Butyl propionate typically is synthesized from propionic acid and n-butyl alcohol via an esterification. However, ternary azeotropes were found in the mixture of n-butanol – n-butyl acetate - water. This may lead to difficulty in down-stream separation when the conventional reactor/sePARATOR process is employed. Obviously, reaction distillation provides an attractive alternative. The esterification follows the elementary reaction:



The normal boiling points (NBP) in Eq. 1 show that the acetate is the highest boiler, the acid is the second highest boiler while water has the lowest NBP. The reaction is catalyzed by acidic cation exchange resin (Amberlyst 35). Quasi-homogeneous model with non-ideal-solution assumption (Lee et al., 2002) is used.

$$r = k_f (a_{HOPr} a_{BuOH} - \frac{a_{BuOPr} a_{H_2O}}{K_{eq}}) \quad (2)$$

where r is the reaction rate per unit volume (Kmol/m³sec), a stands for the activity of corresponding components (Kmol/m³sec). k_f is the forward reaction rate constant

$$k_f = 2.0317 \cdot 10^{11} e^{\frac{65.74}{8.314T(K)}} \quad (3)$$

with T in Kelvin and K_{eq} is the equilibrium constant with a value of 27.8. This is a reaction with negligible heat effect and the equilibrium constant is around 27.8. The catalyst price is assumed to be 18.5 \$/lb and a catalyst life of one year is assumed in this study.

Following Liu and Tan (2001), the nonrandom two liquid (NRTL) activity coefficient model is used for the vapor-liquid-liquid equilibrium (VLLE) for the quaternary system (Table 1). The Hayden-O'Connell second virial coefficient model with association parameters is used to account for the dimerization of acetic acid in the vapor phase. The Aspen Plus built-in association parameters are employed to compute fugacity coefficients.

The quaternary system has three minimum-boiling binary azeotropes (n-butanol - water, n-butyl propionate - water, and water - propionic acid) and one maximum-boiling binary azeotrope (propionic acid - n-butyl propionate). There is one ternary azeotrope for water - butanol - n-butyl propionate which corresponds the lowest boiling azeotropic temperature (92.9°C). Notice that liquid-liquid (LL) envelopes are found in three out of four ternary subsystems and, moreover, a very large LL envelope (type 2) is observed for the water - n-butyl propionate (Fig. 1) and one end of the tie lines are connected to very high purity water. This corresponds to more than 50% of the composition space as shown in Fig. 1. Figure 1 also gives the residue curve maps for these ternary systems. Following the coordinate transformation of Doherty and Malone (2001),

$$X_A = x_{HOPr} + x_{BuOPr} \quad & X_B = x_{BuOH} + x_{BuOPr} \quad (4)$$

the LL envelop can be visualized in a 2-D plot as shown in Fig. 2. This is a significant two-liquid zone and the ternary azeotrope lies within the LL envelop.

Systematic procedure is devised to design heterogeneous reactive distillation. Here, we extend the approach Chiang et al. (2002) by rearranging feed tray locations. Initially, the arrangement of feed streams is based on reaction kinetics consideration, where the heavy reactant (propionic acid) is fed to the top tray of the reactive zone and the light reactant

(butanol) comes in from the lower section of the reactive zone.

For a system with given specifications on the products and a given production rate, the design steps are:

1. Fix a number of reactive trays (N_{rxn}).
2. Place the heavy reactant feed on the top tray of the reactive zone and the light reactant feed on the lower section of the reactive section.
3. Guess the tray numbers in the rectifying sections (N_R).
4. Find the minimum number of trays of the stripping section ($N_{s,min}$) from the short-cut design with a given specification and set $N_s = 2N_{s,min}$.
5. Adjust reboiler duty until the bottom product specification (99% n-butyl propionate) is met (because organic phase is under total reflux, we have only one degree of freedom).
6. Go back to 3 and change the number of trays in the rectifying section until the total annual cost (TAC, Chiang et al., 2002) is minimized (because of the type II LLE, practically, we do not have control over water purity).
7. Go back to 2 and vary feed tray locations until TAC is minimized with acceptable acid purity in the bottom (<50 ppm).
8. Change the number of reactive trays (N_{rxn}) such that TAC is minimized.

ASPEN Plus was used to carry out steady-state simulations and the residence time of 15 s was assumed for the reactive trays. The TAC calculation was based on the cost models of Douglas (1988) (Chiang et al., 2002). The optimized design is shown in Fig. 3 and Table 2 gives parameters values and costs. The column has a total of 18 trays, with 12 stripping trays, 5 reactive trays (tray 13-17), and 1 rectifying tray (tray 18). The optimum feed tray locations are tray 15 (NF1) and tray 17 (NF2). The acid composition in the bottoms is kept to 7 ppm while maintaining propionate purity at 99%. The phase split in the decanter automatically gives rather high purity water (98.8%). Figure 4A shows most of the stripping section trying to separate propionate from butanol. The acid is consumed early in the reactive zone and its purity is kept low in the stripping section. Significant reaction is observed on trays 16 and 17 as shown in the thick long-dashed line as the fraction of the total reaction. This type of reaction rate profile is within one's expectation, because it is necessary to further react the limiting reactant (acid) in trays 13-15 in order to meet the stringent acid specification in the bottoms. Significant temperature breaks are also observed in the stripping section (trays 2-5) and the reactive zone (trays 15-17) as shown in Fig. 4B. This optimized design results in 10% less energy consumption and also 10 % less TAC as compared to the traditional feed arrangement.

2. CONTROL

The control objective is to maintain bottoms propionate purity while keeping the acid

concentration at ppm level. Instead of control the compositions directly, temperatures are used to infer product composition. This is a multivariable control problem and decentralized PI controllers are used.

A typical multivariable control system design procedure consists of the following steps: (1) selection of manipulated variables, (2) determining measurement locations, (3) variable pairing, and (4) controller tuning.

As pointed out earlier, the organic phase condensate is under total reflux and we are left with only one manipulated input, reboiler duty. The other manipulated variable naturally is the feed ratio (Fig. 3) for this double feed column, because the feed ratio has to be adjusted to maintain stoichiometric balance (Al-Arfaj and Luyben, 2000).

Before looking into measurement selection criterion, let us examine the sensitivity of temperature profiles as manipulated variables change. As the heat input changes ($\pm 1\%$), two large changes are observed (Fig. 5A). One is in the stripping section which is typical for conventional distillation and the other is in the reactive zone where significant reaction occurs (cf. Fig. 4). The later comes from the effect of increasing (or decreasing) reaction rate which has not been seen in non-reactive distillation column. Nonlinear behavior can be seen for small change in feed ratio as shown in Fig. 5B. Larger and wider temperature deviation is observed when acid is in excess ($F_{\text{butanol}}/F_{\text{acid}}=0.99$). The asymmetry in Fig. 5B comes from the fact that the excess acid activates the reaction capability in trays 13-15 and significant amount of propionate (heaviest component) is produced and, subsequently, results in much larger temperature rise. Note that this is not the result of temperature control. Similar behavior can also be seen if we choose to use direct composition control and the real reason is that we deliberately design the column asymmetrically (to maintain trace amount of acid in the bottoms).

Table 2 shows the steady-state gain matrix (K) between the temperatures and two inputs (Q_R and $F_{\text{butanol}}/F_{\text{acid}}$). The non-square relative gain (NRG) of Chang and Yu (1990) is used for measurement selection.

$$\Lambda^N = K \otimes (K^+)^T \quad (5)$$

Here, Λ^N stands for NRG, \otimes denotes element-by-element multiplication, the superscripts T and + correspond to transpose and pseudo-inverse, respectively. From the definition, the temperatures with large row sum imply the temperature profile is best maintained by holding corresponding temperatures constant. Based on the row sum of NRG, temperatures on trays 4 and 16 (T_4 and T_{16}) are selected (Table 3). These two temperatures correspond to the locations either with large temperature breaks (Fig. 4) or having high sensitivity. T_4 is located in the stripping section and T_{16} is in the place where largest fraction of total reaction occurs (Fig. 4).

Here, we have a 2x2 multivariable system. The relative gain array (RGA) is used for input-output

pairing. For this temperature controlled reactive distillation, the RGA is:

$$\Lambda = \begin{bmatrix} Q_R & F_{\text{butanol}}/F_{\text{acid}} \\ 0.999 & 0.001 \\ 0.001 & 0.999 \end{bmatrix} \begin{bmatrix} T_{16} \\ T_4 \end{bmatrix} \quad (6)$$

We have a system with RGA almost equal to 1. Actually, Fig. 5 already reveals that this is a one way decoupled system (i.e., T_{16} is not sensitive to feed ratio change). Therefore, the controller structure becomes: pair T_{16} with reboiler duty and pair T_4 with feed ratio.

Once the control structure is set, decentralized PI controllers are tuned automatically. First, the ultimate gain and ultimate are identified using sequential relay feedback of Shen and Yu (1994) and, then, PI controller settings are obtained following Tyreus and Luyben tuning rule.

Figure 6 shows that good temperature control can be achieved using simple PI controllers. For $\pm 10\%$ production rate increase, T_4 and T_{16} return to their set points in less than 100 min. However, butyl propionate composition deviates from its specification because we are controlling temperatures while the acid concentration shows little changes. For $\pm 5\%$ measurement errors in feed ratio, good control performance can also be obtained, but asymmetric responses are observed for positive and negative changes as shown in Fig. 7. The reason was pointed out earlier and it can be expected from the temperature sensitivity in Fig. 5B.

4. CONCLUSION

In this work, vapor-liquid-liquid equilibrium behavior of n-butyl propionate, a low volatility solvent, is explored and a systematic procedure is proposed for the design and temperature of the heterogeneous reactive distillation. Significant two-phase zone and a ternary minimum boiling azeotrope lead to a unique separation characteristic. Next, the issue control structure design for heterogeneous reactive distillation is studied. Since two specifications on the bottoms product (propionate purity and ppm level of acid impurity) have to be met and stoichiometric balance need to be maintained, we have a 2x2 control problem with two inputs: heat duty and feed ratio. The reactive distillation exhibits a unique temperature sensitivities, as compared to conventional distillation, and the non-square relative gain (NRG) successfully identifies temperature control trays. It results in an almost one-way decoupled system. Therefore, decentralized PI controllers are employed. The reactive distillation column may become over-capacity as production rate decreases, coordinated control is proposed by the n-butanol feed to a lower feed location. This control system over-design provides the flexibility to handle production rate variations in reactive distillation. Results show the effective control can be achieved over a reasonable range of disturbances.

ACKNOWLEDGEMENT

This work was supported by the China Petroleum Corporation of Taiwan under grant NSC88-CPC-E011-017.

REFERENCES

- [1] Al-Arfaj, M. A.; Luyben W. L. "Comparison of alternative control structures for ideal two-product reactive distillation column", *Ind. Eng. Chem. Res.*, 39, 3298 (2000).
- [2] Al-Arfaj, M. A.; Luyben W. L. "Control of ethylene glycol reactive distillation column", *AICHE J.*, 48, 905 (2002a).
- [3] Al-Arfaj, M. A.; Luyben W. L. "Design and control of an olefin metathesis reactive distillation column", *Chem. Eng. Sci.*, 57, 715 (2002b).
- [4] Agreda, V. H.; Partin, L. R.; Heise, W. H., "High Purity Methyl Acetate via Reactive Distillation," *Chem. Eng. Prog.*, 86 ,40 (1990).
- [5] Aspen Technology Inc. *ASPEN Plus User's Manual 10.2*, Aspen Technology Inc.: Cambridge, MA (2000).
- [6] Chang, D. M.; Yu, C. C.; Chien, I. L., "Coordinated Control of Blending Systems," *IEEE Trans. Control Syst. Technol.*, 6, 495 (1998).
- [7] Chang, J. W. and Yu, C. C., "The Relative Gain for Non-Square Multivariable System," *Chem. Eng. Sci.*, 45, 1309-1323 (1990).
- [8] Chiang, S. F.; Kuo, C. L.; Yu, C. C.; Wong, D. S. H. "Design Alternatives for the Amyl Acetate Process: Coupled Reactor/Column and Reactive Distillation", *Ind. Eng. Chem. Res.*, 41, 3233 (2002).
- [9] Doherty, M. F.; Malone, M. F. *Conceptual Design of Distillation Systems*, McGraw-Hill: New York, 2001.
- [10] Douglas, J. M. *Conceptual Process Design*, McGraw-Hill: New York, 1988.
- [11] Gumus, Z. H.; Ceric, A. R. "Reactive Distillation Column Design with Vapor/Liquid/Liquid Equilibria" *Comput. Chem. Eng.*, 21 (Suppl.), s983 (1997).
- [12] Lee, M. J.; Chiu, J. Y.; Lin, H. M. "Kinetics of Catalytical Esterification of Propionic Acid and n-Butanol over Amberlyst 35", *Ind. Eng. Chem. Res.*, 41, 2882 (2002).
- [13] Liu, W. T.; Tan, C. S., "Liquid-Phase Esterification of Propionic Acid with n-Butanol," *Ind. Eng. Chem. Res.*, 40, 3281 (2001).
- [14] Malone, M. F.; Doherty, M. F. "Reactive Distillation", *Ind. Eng. Chem. Res.* 39, 3953 (2000).
- [15] Sneesby, M. G.; Tade, M. O.; Datta, R.; Smith, T. N. "ETBE synthesis via reactive distillation. 2. dynamic simulation and control aspects", *Ind. Eng. Chem. Res.*, 36, 1870 (1997).

- [16] Venkataraman, S.; Chan, W. K.; Boston, J. F., "Reactive Distillation Using ASPEN PLUS," *Chem. Eng. Prog.*, Aug., 45 (1990).
- [17] Vora, N.; Daoutidis, P. "Dynamics and control of ethyl acetate reactive distillation column", *Ind. Eng. Chem. Res.*, 40, 833 (2001).

Table 1. Steady-state parameters for reactive distillation

total no. of trays (N_T)	18
stripping (N_s)/reactive(N_{rxn})/rectifying(N_R)	12/5/1
propionic acid feed tray	17
n-butanol feed tray	15
n-butanol feed flow rate (Kgmol/h)	49.991
propionic acid feed flow rate (Kgmol/h)	49.991
top product flow rate (Kgmol/h)	50.042
bottoms product flow rate (Kgmol/h)	49.941
distillate	
propionic acid (mole fraction)	0.0108
n-butanol (mole fraction)	0.0004
n-butyl propionate (m.f.)	0.0006
water (m.f.)	0.9882
bottoms	
propionic acid (ppm)	7
n-butanol (mole fraction)	0.0104
n-butyl propionate (m.f.)	0.9900
water (mole fraction)	<10 ⁻⁹
heat duty	
condenser (10 ⁷ kJ/h)	0.320
reboiler (10 ⁷ kJ/h)	0.548
column diameter (m)	1.23
heat exchanger area (m²)	
condenser	18.96
reboiler	42.87
capital cost (\$1000)	
column	232.80
trays	17.03
heat exchangers	206.12
operating cost (\$1000)	
catalyst	6.24
energy	162.02
total annual cost (\$1000)	
	333.83

Table 2. NRG and row sum

Tray No.	NRG		
	Q	F1/F2	rs(i)
T19	0.0314	0.0006	0.0320
T18	0.1032	-0.0006	0.1026
T17	0.1676	-0.0006	0.1670
T16	0.3938	0.025	0.3933
T15	0.0012	-0.0002	0.0010
T14	0.0001	0.0002	0.0003
T13	0.0002	0.0003	0.0005
T12	0.0003	0.0004	0.0007
T11	0.0002	0.0008	0.0010
T10	0.0001	0.0017	0.0018
T9	-0.0005	0.0049	0.0044
T8	-0.0028	0.0160	0.0132
T7	-0.0115	0.0540	0.0425
T6	-0.0388	0.1613	0.1225
T5	-0.0881	0.3313	0.2432
T4	-0.0579	0.3460	0.2881
T3	0.1677	0.1182	0.2859
T2	0.2323	-0.0191	0.2132
T1	0.0865	-0.0148	0.0717
T0	0.0149	-0.0028	0.0121

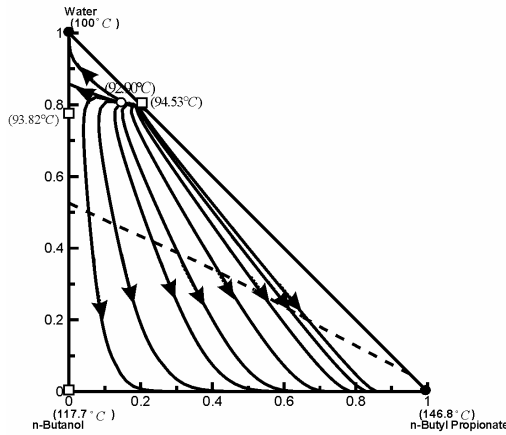


Figure 1. The residue curve maps (RCM) and LLE envelope for water - n-butyl propionate - n-butanol.

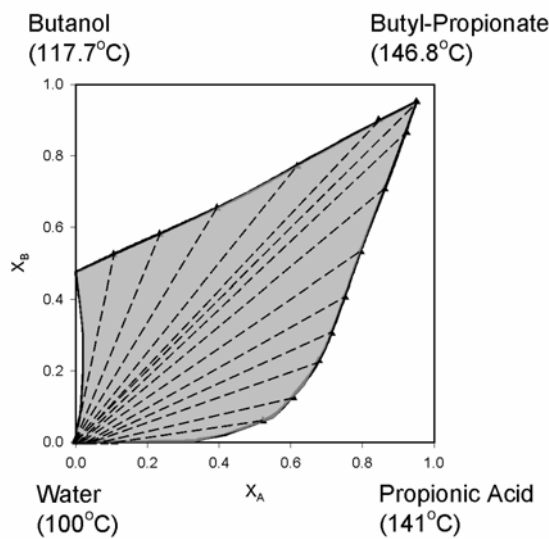


Figure 2. Two-liquid phase for the quaternary system.

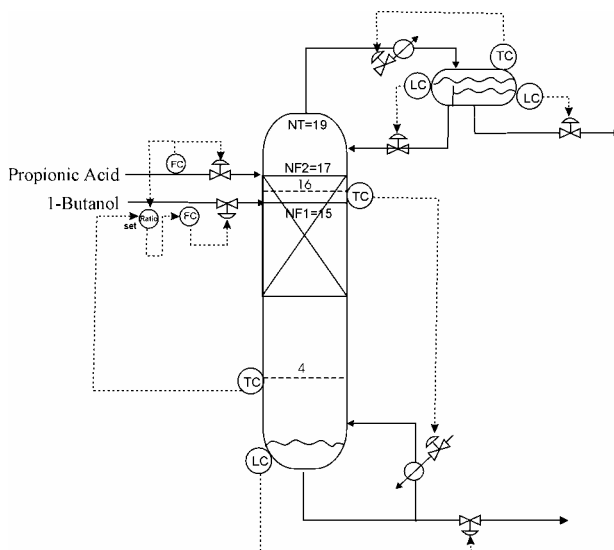


Figure 3. Temperature control scheme for the butyl propionate reactive distillation: feed trays NF1=15 & NF2=17, reactive trays 13-17, temperature control trays T4 & T16.

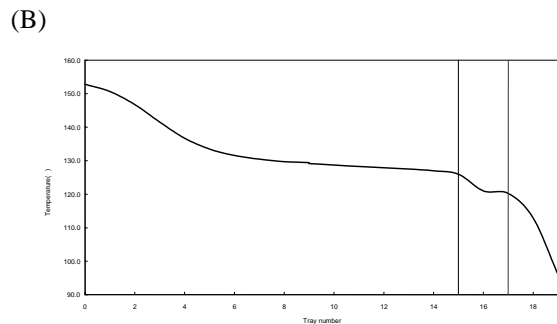
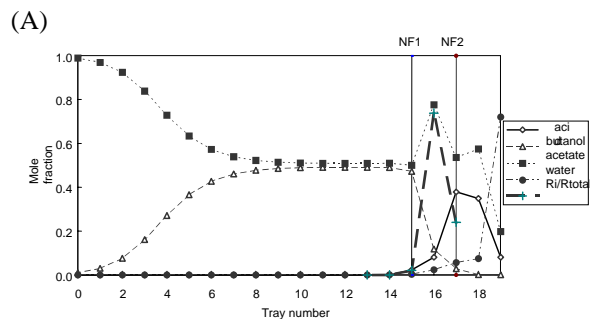


Figure 4. Composition (A) and temperature (B) profiles for optimally designed reactive distillation with $N_R/N_{rxn}/N_S=1/5/12$, $NF1/NF2=15/17$.

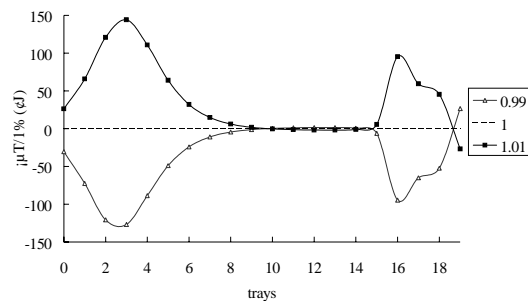


Figure 5. Steady-state gains for 1% changes in reboiler duty (QR) (top) and feed ratio (F_{BuOH}/F_{HOPr}) (bottom)

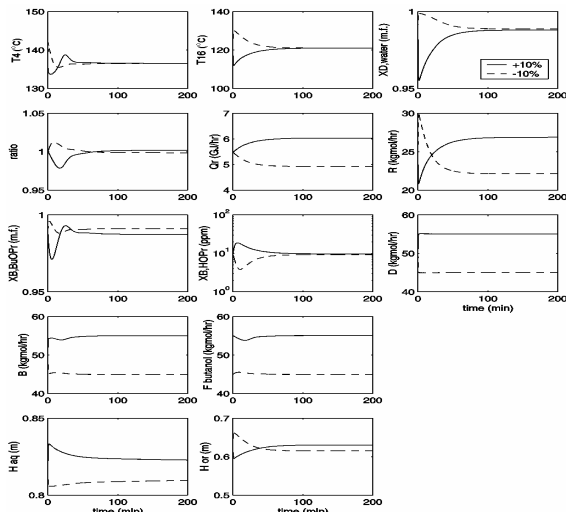


Figure 6. T_4 and T_{16} temperature control for 10% feed flow disturbances.

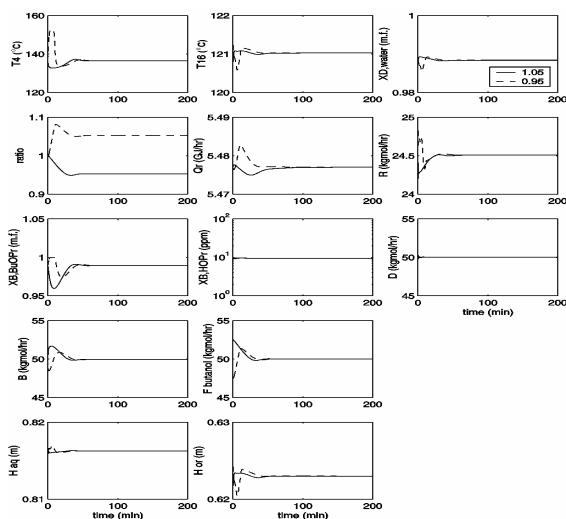


Figure 7. T_4 and T_{16} temperature control for 5% feed ratio errors.

DESIGN AND CONTROL FOR RECYCLE PROCESS WITH TUBULAR REACTOR

Yih-Hang Chen¹ and Cheng-Ching Yu^{2*}

Department of Chemical Engineering¹

National Taiwan University of Science and Technology Taipei 106-07, TAIWAN

Department of Chemical Engineering²

National Taiwan University Taipei 106-17, TAIWAN

Abstract: Interaction between design and control for gas-phase adiabatic tubular reactor with liquid recycle is studied. This generic bimolecular reaction, $\mathcal{A}+\mathcal{B}\rightarrow\mathcal{C}$, has two important features: (1) stoichimoetric balance has to be maintained and (2) reactor temperature plays an important role in design and operability. More importantly, it represents a large class of important industrial processes. Optimal reactant distribution can be obtained directly from the simplified TAC equation and effects of kinetics parameters and relative volatilities on this optimality are also explored. The results show that an increased reactor exit temperature leads to a more controllable optimal design while a high activation energy results in a less controllable one. For the operability analysis, two control structures are proposed with three different combinations of TPM. The control structure using the reactor inlet temperature as TPM gives good control performance when the reactant distribution is held constant. However, potential problem may arise as the result of high reactor exit temperature (T_{out}). For the case of biased reactant distribution, the reactant redistribution provides an extra degree of freedom and this alleviates the high T_{out} problem. The results presented in this work clearly indicate that simple material and energy balances provide useful insights in the design and control of recycle processes.

Keywords: recycle process, plantwide control, interaction between design and control, tubular reactor.

1. INTRODUCTION

Buckley's pioneer work on the plantwide control has been widely adopted in industry for many years. The first step is to lay the "material balance" control structure that handles the inventory controls. Then "product quality" loops are closed on each of the individual units. Since these loops are typically much faster than the slow inventory loops, interaction between the two is often not a problem. Steady development on the dynamics and control of recycle processes is also witnessed from 60s to 80s as can be seen in Gilliland et al. [1], Verykios and Luyben [2], and references therein. Unfortunately, progress in plantwide control is hindered by the lack of software support. During that incubation period, conceptual plantwide control design procedure is formulated, but it was difficult to validate such design procedures except for limited cases (as a result of extensive engineering manpower required for modeling and simulation). In early 90s, the increased computing power and the advent of dynamic process simulators, such as HYSYS and Aspen Dynamics, lead to renewed engineering practice.

Subsequent plantwide control research can be divided into two schools. One group tends to provide fundamental understanding of the problem [3, 4, 5].

Another group tried to provide a systematic procedure for the design of plantwide control system[6, 7, 8]. Most of the above mentioned literature addresses the control issues. Much less work has been done on the interaction between design and control. Elliott and Luyben [9] evaluate the steady-state design of a ternary system based on the total annual cost (TAC) and controllability is assessed quantitatively using capacity-based approach evaluate different designs using several control measures, e.g., relative gain array, and

relative disturbance gain. These approaches akin to a sequential control-design approach. That is controllability analysis is an add-on feature to a design problem. Luyben et al. [10] analyze the pole location of a ternary system using simple dynamic reactor model and this provides an insight into potential control problem with any given design. Chen and Yu [11, 12] extend such approach to the design of feed-effluent heat exchangers, heat-integrated reactors. Cheng and Yu [13] proposed a framework for analyzing design and control simultaneously. Ternary systems with a bimolecular reaction ($\mathcal{A}+\mathcal{B}\rightarrow\mathcal{C}$) in a CSTR and separators were studied and possible tradeoffs between design and control were explored. The objective of this work is to extend the approach of Cheng and Yu [13] to systems with simultaneous material and energy recycles.

2. STEADY-STATE DESIGN

2.1 Process

Consider a recycle process where an irreversible, exothermic reaction $\mathcal{A}+\mathcal{B}\rightarrow\mathcal{C}$ occurs in a gas phase, adiabatic tubular reactor. The process flowsheet consists of one tubular reactor, one distillation column, one vaporizer, and one furnace with two heat exchangers which was first studied by Reyes and Luyben [14] (Fig. 1). Two fresh feed streams F_{0A} and F_{0B} are mixed with the liquid recycle stream D and sent to a steam-heated vaporizer. According to the requirement of reaction temperature, the vapor from the vaporizer outlet stream is preheated first in a feed-effluent heat exchanger followed by a furnace to get proper reactor temperature as well as for the start-up purpose. The exothermic reaction takes place

in the tubular reactor and the reactor temperature increases monotonically along the axial direction with the following inlet and outlet temperatures, T_{in} and T_{out} . The hot gas from the reactor preheats the reactor feed in a feed-effluent heat exchanger, HX1, and the liquid recycle stream in a second heat exchanger, HX2, as shown in Fig. 1.

After heat recovery, via HX1 and HX2, the reactor effluent is fed into a distillation column. The two reactants, A & B, are light key (LK) and intermediate boiler (IK), respectively, while the product, C, is the heavy component (HK). The Antoine constants of the vapor pressure equation are chosen such that the relative volatilities of the components are $\alpha_A = 4$, $\alpha_B = 2$, and $\alpha_C = 1$ for this equal molar overflow system (Table 1). Only one distillation column is sufficient to separate the product (C) from the unreacted reactants (A & B). Ideal vapor-liquid equilibrium is assumed. Physical property data and kinetic data are given in Table 1. The kinetic data are shown in Table 1.

Following Reyes and Luyben [14], the following process specifications are used.

1. The product flow rate (stream B) from the base of the column is fixed at 0.12 kmol s^{-1} .
2. The product purity $x_{B,C}$ is fixed at 0.98 mole fraction C.
3. The reactor exit temperature (T_{out}) is limited to 500K at design.
4. The pressure in the reactor is assumed to be 35 bar, and the pressure drop is neglected.

At design, the following assumptions are made.

1. The minimum approach temperature differences for the heat exchangers are fixed at 10 K in HX1 and 25 K in HX2.
2. The reflux drum temperature in the distillation column is fixed at 316 K (to back-calculate column pressure)
3. Distillation columns are designed by setting the total number of trays (N_T) equal to twice the minimum number of trays (N_{min}) and the optimum feed tray is estimated from the Kirkbride equation.
4. The vapor leaving the vaporizer is at its dew point temperature, given $P=35 \text{ bar}$.
5. The ratio of furnace duty to total preheat duty is fixed at 20% ($Q_F/Q_{TOT}=0.2$).
6. The distillate composition of C is fixed at 1%.

2.2 Steady-state design and analysis

With the given specifications, we can complete the steady-state design for any given reactor conversion and reactant distribution. The steady-state conditions of all streams in the ternary recycle system are calculated from balance equations as shown in Appendix A. Next, shortcut methods are applied to find the minimum number of trays (Fenske equation) for distillation columns, locate the feed tray location (Kirkbride equation), and size the column diameter. The heat transfer areas for the reboiler and condenser are also computed from the vapor flow rates.

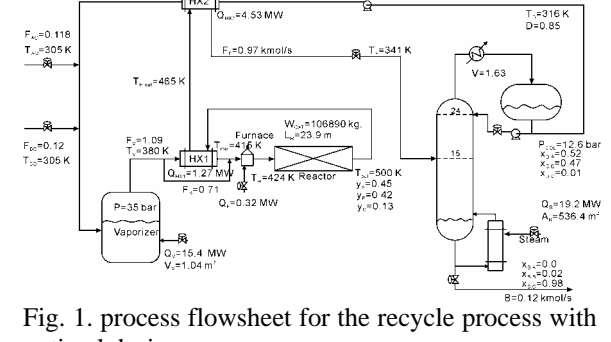


Fig. 1. process flowsheet for the recycle process with optimal design.

Table 1. Physical properties and kinetics data for steady state design

	component		
	A	B	C
Molecular weight, kg kmol ⁻¹	17.5	17.5	35
heat of vaporization at 273 K, kJ kmol ⁻¹	16 629	16 629	16 629
liquid heat capacity, kJ kmol ⁻¹ K ⁻¹	56	56	112
vapor heat capacity, kJ kmol ⁻¹ K ⁻¹	35	35	70
Antoine vapourpressureequationconstants ^a			
A_j	9.2463	8.5532	7.8600
B_j	-2000	-2000	-2000
Heat of reaction, kJ mdL ⁻¹		-23237	
Specific reaction rate, kmol bar ⁻² kg _{CAT} ⁻¹		0.3882e ^{0.07108.314T}	

^a P_j in bar and T in Kelvin: $\ln P_j = A_j + B_j/T$

2.2.1 *Simplified TAC model.* Following the approach of Malone et al. [15], the TAC model is linearized.

$$\begin{aligned} \text{TAC} = & K_0 + K_1 W_{CAT} + K_2 N_T + K_3 V_S + K_4 Q_F \quad (1) \\ & + K_5 Q_V + K_6 V_V + K_7 A_H \end{aligned}$$

For the purpose of comparison, it is useful to express the simplified TAC model in terms of process variables, e.g., conversion, reactant distribution, relative volatilities, and reaction rate constant. This can be done by substituting relevant process variables for the equipment size, tray numbers, and vapor rates in Eq.(1). From the mass balance equation, the total amount of catalyst W_{CAT} (implying reactor size, V_R) can be expressed as:

$$W_{CAT} = \frac{1}{N_R B P^2 k_o} \sum_{i=N_R}^1 \frac{F_i^2}{e^{-E/RT_i} \left[\frac{N_R-i}{N_R} + \frac{-\Delta H y_A}{C_p(T-T_o)(1+y_C)} \right] \left[\frac{N_R-i}{N_R} + \frac{-\Delta H y_B}{C_p(T-T_o)(1+y_C)} \right]}$$

where B is the production rate, N_R is no. of lumps in the reactor ($N_R=50$), F_i denotes molar flow rate in each lump, P is pressure in the reactor, y_A , y_B , y_C are mole fractions in the reactor effluence stream, $-\Delta H$ denotes heat of reaction. Next, we use Fenske equation for the minimum number of trays and set the total number of theoretical trays as $N_T=2N_{min}$. Then the vapor rate can be found from the minimum reflux ratio($V_S = (1.2R_m + 1)D$). And the minimum reflux ratio equation of Glinos and Malone [16] is used.

When the conversion (y_C) and reactant distribution (y_A/y_B) are given, we can find the TAC immediately.

2.2.2 *Optimal Paths.* The objective here is to find the optimal reactant distribution for different conversion. This locus is termed as optimal TAC trajectory. Consider the following system parameters: production rate $B = 0.12 \text{ kmol/s}$, product purity $x_{B,C} = 0.98$, reactor outlet temperature $T_{out} = 500 \text{ K}$, $Q_F/Q_{total} = 0.2$, vaporizer outlet stream temperature $T_V = 380 \text{ K}$, column feed temperature $T_F = 336 \text{ K}$. For a given y_C , the optimal reactant distribution can be found by taking the derivative of the simplified TAC (Eq.(1)). First, we substitute y_B and y_C for y_A in the

cost model and, then, take the derivative with respect to y_B . Since the fractional recoveries are fixed and K_i 's are constant. Because of $C_{PA}=C_{PB}$, the last four term of Eq.(1) can be eliminated and can be simplified to:

$$\frac{\partial TAC}{\partial y_B} = K_1 \frac{\partial W_{CAT}}{\partial y_B} + K_3 \frac{\partial V}{\partial y_B} \quad (2)$$

For any given y_C , we can find the optimal y_B by solving Eq.(2) and subsequently optimal reactant distribution along the trajectory as shown in Fig. 2. Next the TACs along the trajectory are compared and the true optimum is thus obtained. Fig. 2 reveals the changes of TAC as y_C varies and the minimum TAC corresponds to $y_A=0.45$, $y_B=0.42$, $y_C=0.13$ with a TAC of 4.21×10^7 \$/year. Table 2 gives the steady-state operating conditions for the optimal design. Note that, unlike the isothermal operation, the optimal trajectory does not reach the pure product corner as indicated by the dashed line in Fig. 2. The reason is that the lower-end of reactor inlet temperature is limited by the vaporizer temperature, a constraint imposed by the physical properties of reactants \mathcal{A} and \mathcal{B} . The optimal trajectory (Fig. 2) also reveals that, at low conversion, the separation cost dominates and a biased reactant distribution with LK in excess ($y_A/y_B > 1$) is preferred, and, as the conversion increasing, the reactor cost becomes more important and an equally distributed reactant ($y_A/y_B = 1$) is favored. The tradeoffs between reactor and separation costs are clearly illustrated in Fig. 2 for different values of y_C along the optimal trajectory.

2.3 Effect of process parameters on optimal path and true optimality

The analytical expression of Eq.(2) allows us to explore the effects of kinetics parameters and vapour liquid equilibrium on the optimal trajectory and corresponding optimal design. Fig. 2A reveals that as the maximum allowable reactor outlet temperature increases, the optimal trajectory converges to the center line at a larger y_C . The reason is that a higher reactor temperature leads to a smaller reactor costs and this, in turn, reduces the relative cost of reactor (compared to the separation cost). Moreover, the reactant distribution becomes biased (light reactant \mathcal{A} in excess) as T_{out} increases.

Next the effects of relative volatilities on the optimal trajectory are examined. Fig. 2B shows that, for fixed reactor outlet temperature, changes in the relative volatility of intermediate key (\mathcal{B}) from $\alpha_B=1.5$ to $\alpha_B=3$ do not produce significant difference. Because a larger α_B results in a lesser separation cost and, therefore, the trajectory converges to center line at a lower conversion, but not by much.

If the heat of reaction increases, the optimal trajectory converges faster toward the center line as shown in Fig. 2C. The reason is the reactor inlet temperature will become lower for system with a larger heat of reaction (this can be seen from the overall energy as will be discussed in the next section) and this in turn will lead to a higher reactor cost. This is exactly what Fig. 2C reveals, but the true optimal remains at almost the same reactant distribution.

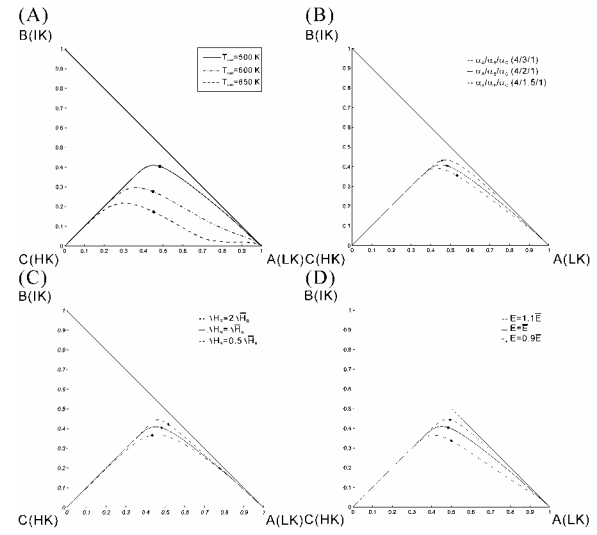


Fig. 2. Optimal TAC trajectory and design for different specifications on (A) reactor outlet temperature, (B) relative volatilities, (C) heat of reaction, (D) activation energy.

It is well known that chemical reactions with large activation energies present difficult control problems because of the rapid increase in the reaction rate as the temperature increases. It also presents difficult reactor temperature control problem when feed-effluent heat exchanger is installed as the result of large reactor gains (T_{out}/T_{in}). Fig. 2D shows that, from steady-state economic perspective, the relative reactor cost will be higher for reactions with large activation energy. Therefore, the optimal trajectory converges to the center line at a much lower y_C value and, more importantly, the true optimum is also located closer to the center line which implies equally distributed reactant.

The optimal trajectory can be computed directly from Eq.(2) and this facilitates the investigation of chemical reactions with different kinetics parameters and vapour liquid equilibrium. More importantly, the trajectories obtained provided insight to possible tradeoffs between design and control for different bimolecular reactions.

3. OPERABILITY

The material and energy balances provide the basis for steady-state operability analysis [13,17]. For a simple isomerization reaction, the production rate in terms of recycle ratio and subsequently control structure can be devised. Similar approach is taken for the case of adiabatic tubular reactor.

As pointed out earlier, for adiabatic reactor, the temperatures (T_{in} and T_{out}) play significant role in operability and energy balance has to be taken into consideration. Without loss of generality, let us use one-lump adiabatic tubular reactor to illustrate the derivation. The relationship between heat generation and the production rate can be expressed as (Luyben, 2001), and it can be derived from reactor energy balance.

The production rate for adiabatic tubular (actually, CSTR) becomes:

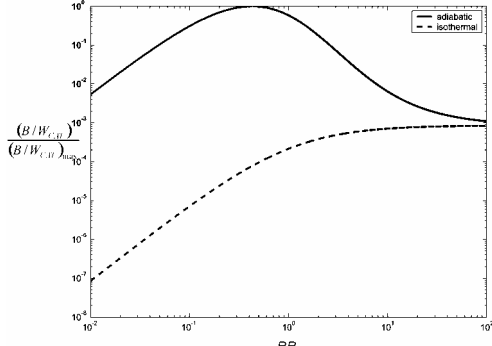


Fig. 3. Normalized production rate as a function of recycle ratio (RR) for adiabatic and isothermal operations.

$$B = W_{cat} k_o P^2 \exp \left(\frac{-E}{R \left(T_{in} + \frac{(-\Delta H)}{(1+RR)C_p} \right)} \right) \frac{x_{D,A} x_{D,B} R R^2}{(1+RR)^2} \quad (3)$$

Comparing Eq.(3) with isothermal system, one immediately observes a significant difference in the reaction rate constant where, for the case of adiabatic tubular, it is a function of recycle ratio (RR). Also shown in Eq.(3) is that the reactor inlet temperature (T_{in}), the reactor pressure (P), and the distribution of the reactant (x_{DA}/x_{DB}) also play visible roles in the production rate expression.

Insights can be gained by examining Eq.(3). Let us explore the effects of different design/operating variables on the production rate changes.

3.1 Recycle Rates (RR=D/B)

Let use kinetics data and reactant distribution of the optional design to illustrate the difference between isothermal and adiabatic operation. That is: $T_{in} = 424$ K, $P = 35$ bar, and $x_{DA}/x_{DB} = 0.52/0.47$. The normalized production per kg of catalyst, B/W_{CAT} , can be computed as the recycle ratio (RR) changes. Fig. 3 shows a non-monotonic behavior for a wide-range of recycle ratio. At low RR (corresponding to high conversion or large y_C), the production rate increases as we increase RR. However, the opposite behavior is observed at high RR region (low conversion). That is B/W_{CAT} decreases with an increase in RR and this is the typical results as seen in many of Luyben and co-worker examples. The reason for that is the temperature effect (T_{out} of the reactor) dominates the concentration effect (at high RR region). In other words, a smaller production rate will result for an increase in RR for an adiabatic reactor at low conversion with high activation energy (E) and high heat of reaction ($-\Delta H$). This can be quantified by taking the derivative of Eq.(3) with respect to RR. After some algebraic manipulation, we have:

$$\left(\frac{\partial B / \bar{B}}{\partial RR / \bar{RR}} \right)_{P, W_{cat}, y_A, y_B} = \frac{2}{1+RR} - \frac{E}{R T_{in}^2} \frac{(T_{out} - T_{in}) \bar{RR}}{1+RR} \quad (4)$$

Eq.(3) clearly indicates the competing effect between concentration and temperature. Note that, for isothermal operation, i.e., $T_{reactor}=T_{in}$, we have only the concentration effect. That is:

$$\left(\frac{\partial B / \bar{B}}{\partial RR / \bar{RR}} \right)_{P, W_{cat}, y_A, y_B} = \frac{2}{1+RR} \quad (5)$$

Fig. 3 also shows the production rate variation for isothermal operation and the “snowball effect” is also evident at high RR region.

3.2 Reactor Inlet Temperature (T_{in})

The reaction inlet temperature is an ideal candidate for the throughput manipulator (TPM) and this is especially true for reaction system with high activation energy where the RR is relatively ineffective. Again, the sensitivity of the production rate for a change in T_{in} can be derived from Eq.(3). If the reactant distribution is maintained at the nominal value, we have:

$$\left(\frac{\partial B}{\partial T_{out}} \right)_{P, W_{cat}, y_A, y_B} = \frac{\bar{B} E K_R}{R T_{out}^2} \quad (6)$$

Eq.(6) clearly shows that from steady-state viewpoint, T_{in} is a good TPM for systems with large E . Compared to the isothermal CSTR case, the sensitivity is amplified by the reactor gain K_R which is the sensitivity between the inlet and outlet temperature (i.e., $K_R = \partial T_{out} / \partial T_{in}$). As pointed out by Chen and Yu [11, 12], a heat integrated reactor via feed-effluent heat exchanger can easily become open-loop unstable for system with a high reactor gain (K_R). Therefore, controllability problem may arise when we try to recover more heat form the hot gas of the reactor effluent. Nevertheless, Eq.(6) indeed shows that T_{in} is a good candidate for TPM.

3.3 Reactor Pressure (P)

In theory, the reactor holdup is also a good candidate in handling production rate changes. And, for the case of isothermal operation, this forms the basis to overcome “snowball effect” as pointed out by Wu and Yu [18]. The problem handling capability can be quantified the taking the derivative of Eq.(3) with respect to the pressure. Thus, one obtains:

$$\left(\frac{\partial B}{\partial P} \right)_{T, W_{cat}, y_A, y_B} = \frac{2 \bar{B}}{\bar{P}} \quad (7)$$

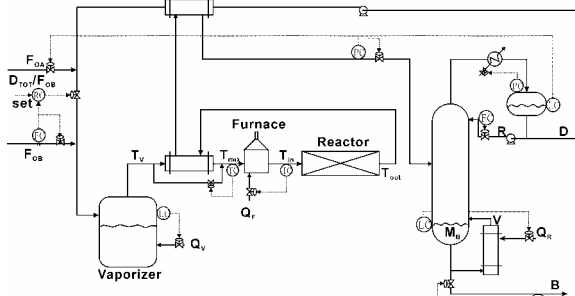
Steady-state analysis clearly shows the reactor pressure is a good choice for TPM. However, for gas-phase reactor, interaction between pressure and temperature may lead to dynamic problem. The thermal inertia may cause significant variation in the reactor inlet temperature unless a large gas-phase holdup is employed.

3.4 Reactant Distribution

Before heaving this section, we would like to look at an important design parameter: reactant distribution (y_A/y_B). The reactant distribution in some cases represents an important tradeoff between design and control as shown in the case 2 Reyes and Luyben [14] where we have a bimolecular reaction with high activation energy. The optimal (2³A)C corresponds to an almost equally distributed reactant distribution, but the operability consideration lead to a biased reactant distribution (e.g., one of the reactant is in excess). Let us consider the case where the reactant \mathcal{A} is in excess. The sensitivity in the

production rate variation for changes in y_B can be expressed as:

(A)



(B)

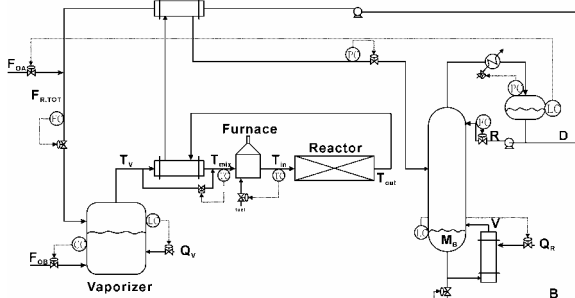


Fig. 4. Control structure fixing (A) recycle ratio (CS1) and (B) reactor exit composition (CS2).

$$\left(\frac{\partial B / \bar{B}}{\partial y_B / y_B} \right)_{P, W_{CAT}, T_{in}, RR} = \frac{(y_A - y_B)}{y_A} \quad (8)$$

It clearly shows that, a small change in the limiting reactant B can lead to significant change in the production rate and this is especially true when A is in large excess.

4. CONTROL

4.1 Control Structures

The on-going analysis provides the basis for control structure design. Two scenarios are considered. One is the optimal design as shown in Table 2 where we have a case of almost equally distributed reactant and the other case corresponds to a biased reactant distribution (also shown in Table 2). Two control structures are devised for these two cases. In the first case, the recycle ratio is fixed as shown in Fig. 4A, denoted as CS1 hereafter, and in the second case the reactant distribution is maintained by controlling one of the reactants in the vaporizer, called CS2 hereafter (Fig. 4B).

Fig. 4 shows the essential loops for these two control structures.

4.2 Throughput Manipulator

As mentioned in section 3, we have three candidate throughput manipulators. One is the reactor inlet temperature (T_{in}) which is denoted as CS1a, the second one is the reactor pressure (P) which is called CS1b, and the third one is the recycle flow rate which is the control structure CS1c. Nonlinear dynamic simulations were performed to evaluate the effectiveness of different control structures. The modeling approach of Reyes and Luyben [19] was taken and the nonlinear recycle plant was solved numerically using FORTRAN. Two different designs are tested.

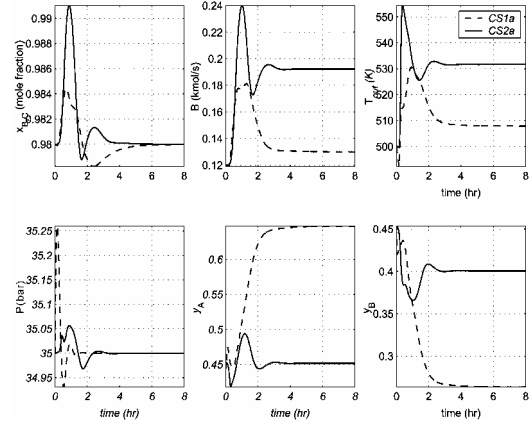


Fig. 5. Closed-loop performance using CS1 and CS2 for $\Delta T_{in} = +5$ K (case 1).

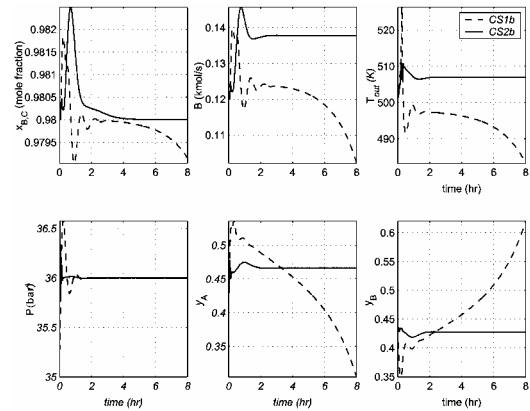


Fig. 6. Closed-loop performance using CS1 and CS2 for $\Delta P = +1$ bar (case 1).

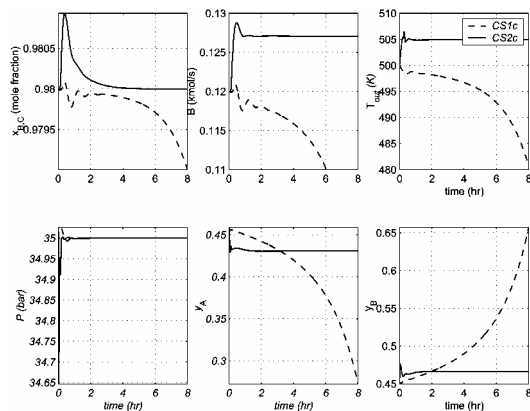


Fig. 7. Closed-loop performance using CS1 and CS2 for $\Delta D = +5\%$ (case 1).

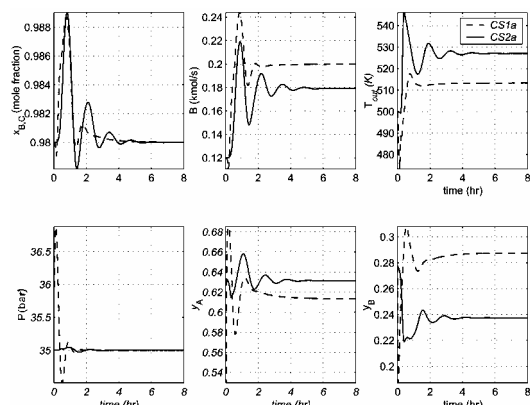


Fig. 8. Closed-loop performance using CS1 and CS2 for $\Delta T_{in} = +5$ K (case 2).

One is the optimal design (Table 2) which represents the case of almost equally distributed reactant (e.g., $y_A/y_B \approx 1$) and the other case explores the scenario of biased reactant distribution (e.g., $y_A/y_B = 2.3$). Let us compare the control performance of CS1 and CS2 for the case of equally distributed reactants. Fig. 5 shows the production rate changes for a +5 K increase in T_{in} . Despite quite similar process dynamics (e.g., settled in 4 hours), different magnitudes in production rate changes are observed. For CS2, it results in 61% production increase while, for CS1, only 8.3% production rate increased can be achieved. The reason for the smaller magnitude in production rate increase for CS2 is that the effect of T_{in} is offset by the re-distribution reactant as shown in Fig. 5. This was not seen for CS1 become the composition of B is controlled to maintain the optional reactant distribution. Similar results can also be seen when the reactor pressure and recycle flow are used as TPM. Also notice that significant change in T_{out} can be seen for CS1 when T_{in} is used as TPM and this may lead to potential problem in practice.

Finally, for the case when \mathcal{A} is in excess (e.g., $y_A/y_B = 2.3$), exactly the opposite results were obtained when comparing CS1 and CS2 (Fig. 4). Again, for a +5 K change in T_{in} , a larger production rate increase can be achieved using CS2 (50%) as compared to that of CS1 (67%) while having a lower T_{out} as shown in Fig. 8. The reason is obvious that the redistribution of reactants contributes to the production rate increase.

5. CONCLUSION

In this work, recycle process with the bimolecular reaction, $\mathcal{A}+\mathcal{B} \rightarrow \mathcal{C}$, is investigated. The total annual cost (TAC) is used to evaluate economic incentive for different designs. The simplified TAC facilitates the search for optimal reactant distribution under conversion. Similar to isothermal CSTR case, the optimal TAC trajectory starts from the light reactant corner at low conversion (where the separation cost dominated) toward the equally distributed reactant at a higher conversion (where the reactor cost dominated). Optimal design can thus be computed given different kinetics and relative volatilities provided with cost data. Next, the connection between total production and reactor temperature is derived analytically. It clearly shows the difference between adiabatic and isothermal operation. Moreover, the capability in handling production rate changes can be evaluated. Subsequently, control structures are devised. The results indicate that different control structures should be applied when the optimal reactor composition varies. More importantly, the results show that insight to the recycle process with adiabatic tubular reactor can be gained from fundamental material and energy balances.

REFERENCES

- [1] Gilliland, E. R.; Gould, Boyle, L. A.; (1964) T. J. Proc. Joint Automatic Control Conference, pp 140.
- [2] Verykios, X. E. and Luyben, W. L. (1978). Steady-State Sensitivity and Dynamics of a Reactor/Distillation column System with Recycle, **17**, pp. 31, ISA Transactions.
- [3] Luyben, W. L. (1994). Snowball Effect in Reactor/Separator Process with Recycle, **33**, pp. 299, Ind. Eng. Chem. Res.
- [4] Georgakis, C. (1986). On the Use of Extensive Variables in Process Dynamics and Control, **41**, pp. 1471, Chem. Eng. Sci..
- [5] Vinson, D. R. and Georgakis, C. (2000). A New Measure of Process Output Controllability, **10**, pp. 185, J. Process Control.
- [6] Luyben, W. L.; Tyreus, B. D.; Luyben, M. L. (1999) Plantwide Process Control, McGraw-Hill, New York.
- [7] Yi, C. K. and Luyben, W. L. (1995), Evaluation of plant-wide control structures by steady-state disturbance sensitivity analysis, **34**, pp. 2393, Ind. Eng. Chem. Res..
- [8] Semino, D.; Giuliani, G. (1997), Control Configuration Selection in Recycle Systems by Steady State Analysis, **21**, Suppl. S273, Computers Chem. Engng..
- [9] Elliott, T. R.; Luyben, W. L. (1995), A Capacity-base Economic Approach for the Quantitative Assessment of Process Controllability during the Conceptual Design Phase , **34**, pp. 3907, Ind. Eng. Chem. Res.
- [10]Luyben, M. L.; Tyreus, B. D.; Luyben, W. L. (1996), Analysis of Control Structures for Reaction/Separation/Recycle Processes with Second-Order Reactions, **35**, pp. 758, Ind. Eng. Chem. Res.
- [11]Chen, Y. H. and Yu, C. C. (2000), Interaction between Thermodynamic Efficiency and Dynamic Controllability: Heat-Integrated Reactor, **23**, pp. 1077, Comput. Chem. Eng.
- [12]Chen, Y. H. and Yu, C. C. (2003), Design and Control of Heat-Integrated Reactors, (in press) , Ind. Eng. Chem. Res..
- [13]Cheng, Y. C. and Yu, C. C. (2003) Optimal Region for Design and Control of Ternary Systems, **49**, pp. 682, AIChE J.
- [14]Reyes, F. and Luyben, W. L. (2001) Design and Control of a Gas-Phase Adiabatic Tubular Reactor Process with Liquid Recycle, **40**, pp. 3762, Ind. Eng. Chem. Res.
- [15]Malone, M. F.; Marquez, F. E.; Douglas, J. M.; Glinos, K. (1985), simple, analytical criteria for the sequencing of distillation columns, **31**, pp. 683, AIChE J.
- [16]Malone, M. F.; Glinos, K.; Marquez, F. E.; Douglas, J. M. (1985), Simple, Analytical Criteria for the Sequencing of Distillation Columns, **31**, pp. 683, AIChE J.
- [17]Wu, K. L.; Yu, C. C.; Luyben, W. L.; Skogestad, S. (2003), Reactor/Separator Processes with Recycle-2. Design for Composition Control, **27**, pp. 421, Computers Chem. Engng.
- [18]Wu, K. L. and Yu, C. C.(1996), Reactor/Separator Processes with Recycle-1. Candidate Control Structure for Operability, **20**, pp. 1291, Computers Chem. Engng.
- [19]Reyes, F. and Luyben, W. L. (2001) Extension of the Simultaneous Design of Gas-Phase Adiabatic Tubular Reactor Systems with Gas Recycles, **40**, pp. 635, Ind. Eng. Chem. Res.

OPTIMAL CONTROL OF FLUID CATALYTIC CRACKING UNIT

***JiangQingyin CaoZhikai Caijie Zhouhua**

*Department. Of Chemical Engineering. Xiamen University,
Xiamen 361005, China*

**Email: xdcds@xmu.edu.cn*

ChenZiluan WangChenglin ChenXiliang DengMingbo

*China Petroleum&Chemical Corporation Guangzhou Branch
GuangZhou 510726,China*

Abstract: This paper discusses the problem of on-line optimal control of FCCU. First a new optimal control scheme is put forward. Then some key problems to make up this optimal control system and the solving scheme are discussed. Finally, the on-line industrial running results of this system are given. *Copyright © 2003 IFAC*

Keywords:Optimal Control, Adaptive,On-line, Process.

1. INTRODUCTION

FCCU (Fluid Catalytic Cracking Unit) is one of the most important units in oil refinery. It also occupies very significant position in the refinery because of its economic benefits. So how to improve the operation level of this unit is paid a close attention by the circle of petrochemical works. No doubt one of the effective methods is to implement its online optimization and advanced control.

The Department of Chemical Engineering of Xiamen University has cooperated with Guangzhou Oil Refinery of China Petroleum&Chemical Corporation Guangzhou Branch to develop the FCCU optimal control system. This system has done a good job since it was put into practice at the beginning of 1995.

This paper will introduce this system and its application

2. FCCU PROCESS FLOW

FCCU consists of three subunits: Reactor-regenerator section, main fractionator and absorption stabilization section. The reactor-regenerator section is the most important sector in these three subunits. In which the fresh feed is atomized by superheated steam, injected into riser, and combined with high temperature (650-750) catalyst which came from regenerator. The catalyst and the hydrocarbon vapors flow up the riser and the cracking reaction is processed at the meantime. In order to prevent over reaction and improve the distribution of the product, a quick separation is adopted in the outlet of the riser. After separation, the catalyst is known as spent catalyst. At first the spent

catalyst is dropped into stripping section of the reactor. Then the spent catalyst is transported to regenerator by the slope-pipe. The reacted vapor products are sent to the main fractionator where various boiling point fractions are withdrawn such as distillate, light cycle oil (LCO), heavy cycle oil (HCO) gasoline and diesel, etc. Parts of oil that are not converted by the crack-reaction are sent back to riser reactor according to some ratio. The diesel is out of FCCU directly but the gasoline must be sent to absorption- stabilization section and then the stabilized gasoline is formed.

Regenerator is the spot where the coke of the spent catalyst is burnt off in contact with air and the activity of the catalyst is recovered. The regenerated catalyst is then recalculated back to the bottom of the riser reactor though the regenerated-slope-pipe. After that, the regenerated catalyst flows into the riser by rising steam and used again in the riser. The flux of the cycle catalyst can be controlled in the two slope-pipes where the valve location of the single slide valve is tuned. By changing the valve location of the double slide valve, which is equipped in the gas pipe of the regenerator, the pressure of the regenerator can be controlled.

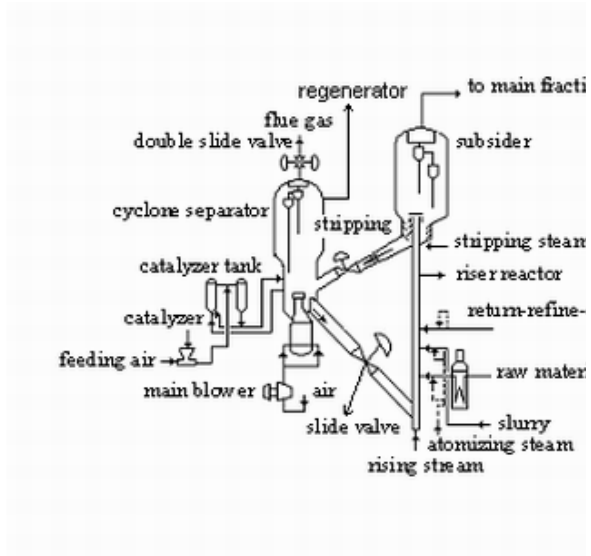


Fig 1. FCCU process flow

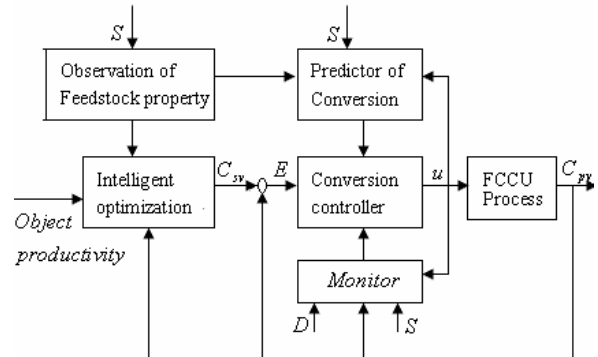
3. OPTIMAL CONTROL SCHEME

Traditional optimal control scheme in FCCU is primarily based on the control of reaction temperature. But it is the degree of reaction that influences the whole unit and the products distribution mostly. Reaction temperature doesn't represent the degree of

reaction as it is affected by many factors, so is not suitable to be used as the control variable. So the traditional scheme is an indirect method actually. To solve this problem, YuanPu(1992) put forward a scheme using reaction heat as the main control variable. The basis of it is that the reaction heat may serve as a direct measurement to the degree of reaction under the condition of unchangeableness of property of feedstock. So it doesn't fit for those units with frequently alterative feeds on property. Moreover, immeasurability of reaction heat is also a great difficulty to make the scheme going on.

Our developed optimal system is a two cascade closed-loop system which takes the conversion percentage as the optimal variable because it is the direct measurement to the degree of reaction and can be calculated online from the products distribution of FCCU. A neural network is used to predict this conversion percentage online and at real-time because there may be a large time-delay to calculate the conversion percentage. Based on this, closed-loop optimization is achieved by the uses of online observation for feeds property and adaptive intelligent optimal method.

Two cascade closed-loop optimal control schemes are shown as Fig 2:



Where C_{pv} : conversion percentage

C_{sv} : optimum set-point of conversion percentage

S: operation information

D: fault diagnosis information

E: error of controller

u: controller output

Fig 2. optimization scheme

3.KEY PROBLEMS AND SOLVING METHODS

3.1 Online observation of property of feedstock

As much oil refinery in southward China use much export oil from various countries, the oil property can not be kept stable. So it is of great importance for the optimal control system to make a quick response to the change of oil. However, the real-time analytic data on the feed oil is lacking because of the poor real-time and online analytic means. To solve this problem, we use the reaction model and the temperature distribution of riser reactor to estimate the property of the feedstock(Jiang Qingyin,1995).

$$YX = \frac{K_{CO}}{K_{AO}} H_{cr} = F(\beta_o, \Delta T_{rai}, T_{rai})$$

Simplify the reaction model, a parameter is gotten as: Where K_{CO} , K_{AO} , K_{Cr} are coke reaction rate constant, cracking reaction rate constant and cracking heat respectively. Define YX as feed factor. As YX only has relationship with the property of feedstock and the catalyst activation, it can serve as an expression for the property of oil. The right size of the equality above is a function relationship formed by riser temperature, temperature difference and catalyst-oil ratio which are all measurable or calculable. Therefore YX can be estimated online at real-time.

We can see that YX mainly indicates the heat needed by the feedstock in cracking reaction. The larger YX is, the more cracking heat is needed, and the feed oil is more difficult to be cracked.

3.2 Prediction of conversion percentage

As mentioned above, the core of conversion percentage control is its real-time prediction. To solve this problem, a BP neural network is adopted and has made a good result.

BP neural network is the most extensive kind of neural networks to be applied. It consists of an input layer L_a , several hidden layers (usually one layer) and an output layer L_c . Nonlinear mapping relationship between input variables and output variables is built up by

learning. For its structural characteristic it has good fault-tolerant capacity which is very important in the industrial process.

For the industrial online application, the BP models must have a strong generalization capability. A number of papers had discussed the generalization problem by discussing the structure and the learning algorithm of ANN, but recently, some researchers have paid attention to the problem of training samples. It has been pointed out that the basic reasons affecting the generalization capability of neural network are quality, quantity and the representation ability of the training samples.

In this Optimal Control system, we introduce a Self-organizing structure (JiangQingyin,Caijie and Cao Zhika,2002) to build up an input-output pattern base which use the continuous sample data of industrial process and automatically screen out the inputs-outputs patterns with high quality and good representation ability. Using these patterns as training samples, we can obtain a BP model of good generalization capability.

Real-time running result has shown that this BP predictor has a quite high accuracy on prediction. As shown in Fig 3, fluctuations of conversion percentage are exactly predicted. What needs to be explained clearly is that in this case the weights matrix of BP neural network was calculated some months ago when it was used. Although there are many changes in operative condition, prediction is accurate, as comes from the good adaptive capacity of this BP neural network.

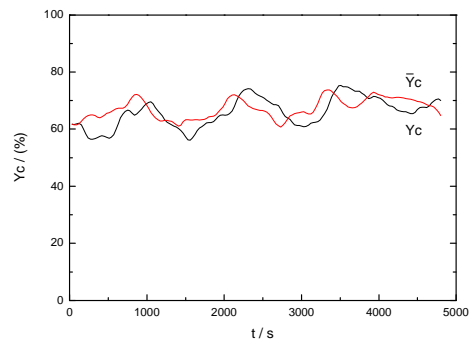


Fig 3. Online prediction of conversion percentage by BP network

3.3 Model identification-free adaptive control

Model identification-free adaptive control (MFA) is a kind of adaptive control proposed by Marsik and Strejc(J.Marsik V.Strejc,1989) which needs not process model also needs not on-line identification of model parameters. This method only needs the error of process value and the expected value in industrial process, thus can form an adaptive closed-loop control system with good dynamic characteristic. Because of the advantages such as little calculating amount, easy to carry out and strong robustness, it is very suitable for the advanced control in industrial process. But this theory can't cope with the process with large time-delay. So in our optimal control system, a predictive algorithm is introduced and a self-searching algorithm aiming at to solve the problems of inaccurate estimation on delay time and predictive error has been developed(Jiang Qingyin,1997). The improved controller works well, as shown in Fig 4. In where the C_{sv} is the optimum set-point of conversion percentage and C_{pv} is the process value of conversion percentage, Δp is the main disturbance, u the output of controller and T the reaction temperature.

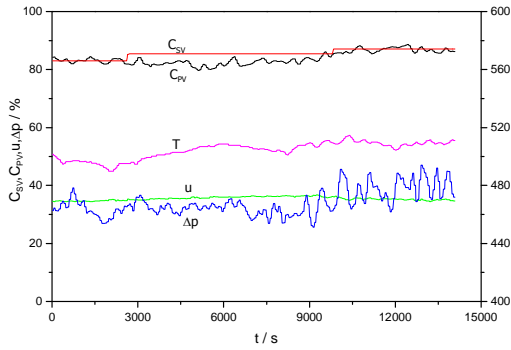


Fig 4. Online MFA control of conversion percentage

3.4 Fuzzy fault diagnosis

To assure the security of optimal control system, fault diagnosis is very important and necessary. Traditional expert system method doesn't quite fit for FCCU as it is very difficult to describe the faults in definite production rule. To make it more accurate and effective, we propose a fuzzy fault diagnosis method based on the theory of factor space (Caijie, Jiang Qingyin ,CaoZhikai and Zhouhua,2002). Besides, to solve the problem of improve on the adaptive capacity

of fault diagnosis system, the method of variable weights based on the balanced function of factor spaces is introduced into the fault diagnosis system.

3.5 Adaptive intelligent optimal method

The traditional optimal method is based on the mathematic model. That is the optimal set-point is calculated by use of a series of mathematic methods. However, traditional method is hard to be realized for the on-line closed loop optimal system, because it is difficult to develop an accurate FCC mathematic model and correct it on-line. The expert system that rose in the 1980s has offered a kind of intelligent method for optimization. But it is necessary to build a knowledge base covers the whole states of process. Meanwhile it is important to keep the knowledge base adaptive as there has been a time-variation characteristic in most industrial process. For this reason, Jiang Qingyin and Shu diqian (Jiang Qingyin and Shu diqian,1993) proposed an on-line self-organizing learning method to construct a self-organizing knowledge base which can modify the knowledge automatically by itself, therefore to realize self-adaptation of the expert system.

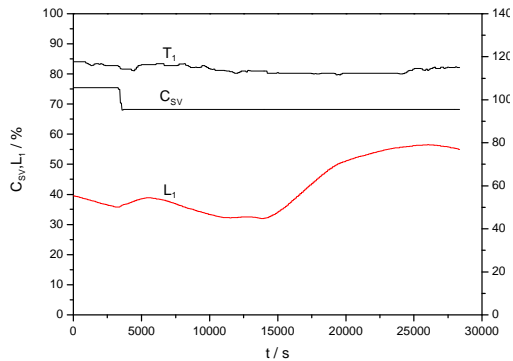
Based on it, a BP neural network is used to construct the reasoning model in order to adjust the set-point of conversion percentage in time when feedstock change. Because the building and correction of knowledge base and reasoning model are both going on automatically online, this enables a good adaptive capacity and robustness of optimal system for realizing the closed-loop optimization.

4. RUNNING SITUATION OF THE OPTIMAL CONTROL SYSTEM

This system had already been put close-loop running for years and achieved good results. After long time running, the optimal control system has shown some characteristics:

1. Security of close-loop is guaranteed. Because the optimal control system contains an integrated fault diagnosis system and adopts a series of safety measures to prevent accidents, such as instruments failure, sudden lost of power of master computer, the optimal system can all switch the closed-loop control to regular control of DCS immediately.

2. The performance of conversion percentage controller is good. It can follow the changes of given values, and has strong capacity of anti-interference, also the controller has an adaptive capacity to the change of property of feedstock and other operation condition.



Figur5 Close-loop running of optimal control system

3. This system is highly automatic and easy to use. As this optimal system has achieved closed-loop control in addition to the operational safety, the entire optimal process can be finished automatically without intervention by operators on the whole. Moreover, friendly user interface is supplied to make it easy to operate and maintain.

After being putting into effect, the optimal system has made several results as follow:

1. It makes the whole process more stable.
Degree of reaction becomes more steadily and the whole Unit of FCC includes the fractional and stabilizing systems are more steady and easier to be operated. For example, under the routine control, the liquid level of fractionating tower bottom waves up and down frequently to a high extent. While after the optimal control system working, generally flat liquid level has been maintained as degree of reaction has turned to be stable. This change has directly led to the decrease of related regulation and further the stability of whole fractionating tower. The operation state of the liquid level and the temperature of main fractionator on an eight-hour working period shift are shown in Fig 5. We can see that the stability of this unit is satisfactory.

2. The yield of light oil increases. Once we compared

the effect of optimal control system and the old control system by put into operation in day shift with that of old control system and in night shift the optimal control system, under the condition of same quantity and same property of feedstock. The yield of light oil and the liquid in night shift increase obviously, as shown in Table 1. In addition, the yield of light oil increases about 0.6% according to workshop's statistics in a long time.

5. CONCLUSION

There is a hard work to achieve closed-loop optimal control in FCCU. Our proposed new optimization scheme has been verified to be feasible and effective by the practice in Guangzhou Oils Refinery. In this scheme, many technologies arising in the 1990s have been adopted. Especially it is the first time for some of these technologies to be applied successfully into so complicated catalytic cracking process.

During the development of this optimal control system, operators, technologists and managers in Guangzhou Oils Refinery gave us great support. Thanks them for their help to make it fulfill smoothly.

References

- YuanPu(1992).*Petroleum Refining Sinica*, 23-27.
- Jiang Qingyin(1995). On-line Observation for feedstock Property of Catalytic Crack Unit, *Journal of Xiamen University (Natural Science)*, V34 pp960-964
- Jiang Qingyin and Shu diqian(1993), Adaptive Realization of Expert System for Process Control and Operation, *Chinese Journal of Automation*, V5 (1) pp.33.-37.
- Jiang Qingyin,Caijie and Cao Zhika(2002), Self-Organizing Pattern Base and Its Application in the Complicated Industrial Process, *ICCA02, IEEE ISBN: 0-7803-7413-4 p212- 215.*
- J.Marsik V.Strejc(1989), Application of Identification-free Algorithms for Adaptive Control, *Automatica*. V25 (2), pp.273-277
- Jiang Qingyin(1997), Predictive Algorithms of Identification -free Algorithms for Adaptive Control

and Its Application, *Acta Automatica Sinica*, **V23** (1) pp.107.

Caijie, Jiang Qingyin ,CaoZhiwei and Zhouhua(2002),

Diagnosis of industrial process faults based on variable weight theory of factor space. *ICCA02, IEEE ISBN: 0-7803-7413-4 p1125-1129.*

Table 1: yields comparison

shift	Processing capacity (ton)	Light dirty oil	Yield of light oil	Yield of liquid
day	837.9	77.6	75.7%	82.2%
night	838.0	76.0	77.2%	84.1%

Note:

1. The products data were read by the process instruments which values were lower than real value in both cases.
2. Temperature control was used in day shift, and closed-loop optimal control was used in night shift.

MODELLING AND ADVANCED PROCESS CONTROL (APC) FOR DISTILLATION COLUMNS OF LINEAR ALKYLBENZENE PLANT

Xiaoming Jin, Gang Rong and Shuqing Wang

National Key Lab of Industrial Control Technology, Institute of Advanced Process Control,
Zhejiang University, 310027, Hangzhou, China
email: xmjin@iipc.zju.edu.cn

Abstract: This paper introduces industrial application of model predictive control (MPC) for the series of columns in a linear alkylbenzene (LAB) complex. The APC system that is consisted of twelve controlled variables, twelve manipulated variables and eight disturbance variables is used to deal with the constrained multivariable control problem of the distillation columns. Firstly, process modelling that includes experimental test and process identification is presented. Then, the construction and implementation of the APC system for the distillation columns are discussed. Industrial application results show that the APC system can maintain the best operation for a long time and realize ultimate operating potential of the distillation columns. Copyright © 2003 IFAC

Keywords: Model predictive control, distillation process, series of columns

1. INTRODUCTION

Distillation columns have been widely used for separation processes in the petroleum and chemical industries. These columns are not only the most energy-intensive operations, but also determine the quality of products of those industries and many times limit process product rates (Kister, 1990). Recent progresses in the control theory, computer and communication have made possible extensive application of APC in process industries (Wang et al, 2001). The large economic benefit of applying APC system to the distillation columns arises from reducing the deviations of crucial process variables and pushing the steady-state operation to a better operating point (Riggs, 1998).

Distillation control has been studied extensively and poses many challenging problems since a distillation column is complex, highly non-linear, multivariable process (Shinskey, 1984, Luyben, 1992, Lundstrom and Skogestad, 1995). Recent efforts have contributed to the analysis of control properties of distillation sequences (Jimenez, et al, 2001) and comparison of control strategies for the distillation

columns (Huang and Riggs, 2002). However, the APC system that deals with whole distillation columns rather than single column via a MPC controller is lack of report in open literature.

This paper introduces industrial application via a commercial software of MPC for the distillation columns in a LAB plant, which consists of four distillation columns operated in series: HF acid stripper, benzene column, paraffin column, and LAB column. A MPC system that is constructed of twelve controlled variables, twelve manipulated variables and eight disturbance variables is developed to deal with the constrained multivariable control problem of the distillation columns. The MPC system is divided to four subsystems according to the distillation column. Each subsystem is relatively independent with the others and mainly takes charge one column. Industrial application results show that the APC system can maintain the best operation for a long time and realize ultimate operating potential of the distillation system by reducing the consumption of energy, improving product purity, and minimizing operating cost.

2. PROCESS DESCRIPTION

LAB now accounts for nearly all of the worldwide production of alkylbenzene sulfonates (LASs) that are frequently used as raw material of biodegradable household detergents. A LAB complex consists of two major steps: production of normal paraffins, and production of LAB from normal paraffins. The straight run kerosene from a refinery is used to produce normal paraffins through kerosene pre-fractionation, distillate unionfining process and Molex process. Then, the normal paraffins are dehydrogenated to corresponding mono-olefins over a highly selective and active catalyst. Lastly, benzene is alkylated with mono-olefins to LAB using hydrofluoric (HF) acid as the catalyst in alkylation process.

The alkylation process includes two major sections: alkylation section and distillation section. The distillation columns are researched in this paper. The process diagram of the distillation columns with the basic regulatory loops is shown in Figure 1. The controlled variables (CVs), manipulated variables (MVs) and disturbance variables (DVs) of the APC

system are also given in Figure 1. The distillation columns include a HF acid stripper, a benzene column, a paraffin column, and a LAB column. The columns are operated to separate multi-component mixtures of LAB stream from upstream section. The separations of various distillation columns are key variables influencing the economic performance of the alkylation process since the series of columns directly affect product quality, product rate, and utility usage.

The feed of the distillation columns is a mixed LAB stream with HF, benzene and paraffin from alkylation section, which passes through a feed heat exchanger enters at the top tray of the HF stripper. The HF vapor is vented to the HF recovery system. The hot oil to the reboiler is on flow control. The bottom level is directly controlled by adjusting bottom product flow to the benzene column. The bottom temperature is a key variable that reflects fractionation effect. The HF stripper is typically not a bottleneck, but it can be disturbed by operation of alkylation section and flooded if overloaded.

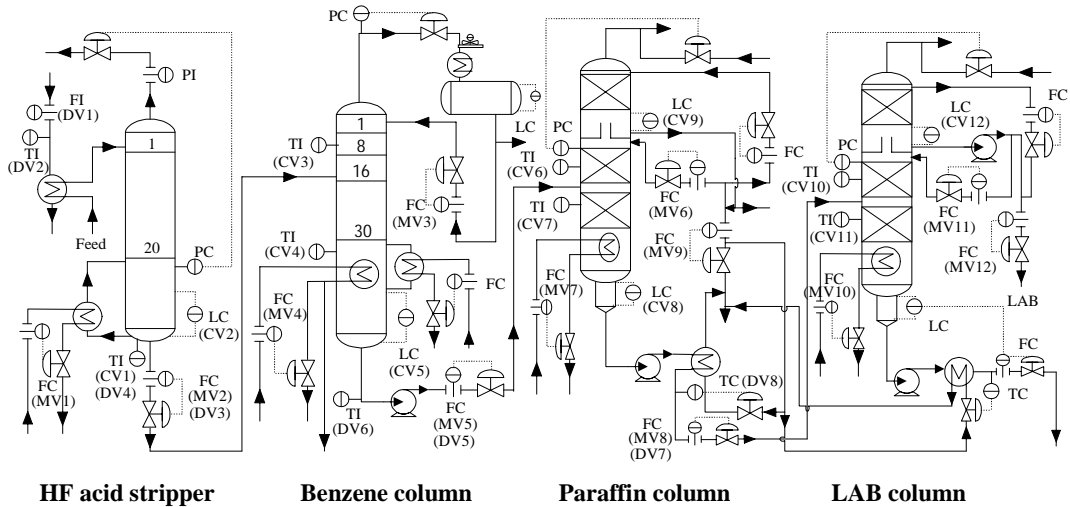


Fig. 1 Process diagram of the distillation in LAB plant

The benzene column has a whole condenser. The pressure is controlled via a hot vapor bypass around the overhead condenser. The accumulator level is controlled by adjusting top benzene product flow rate. There is a flow limit for top benzene product in that it is returned to alkylation section. The hot oil to the reboiler and reflux to column are on flow control. The bottom level is directly controlled by adjusting bottom product flow to the paraffin column. There are two important temperatures in benzene column: upper tray temperature and lower tray temperature, which reflect distillation effect and are controlled variables. The benzene column is very sensitive to feed composition disturbance. When HF stripper is overloaded or operated unsteadily the upper tray

temperature of benzene column can vary acutely and the lower tray temperature may exceed the lower limit, then influence the operation of the paraffin column.

The paraffin column is a typical packed column that is operating at a pressure slightly lower than atmospheric pressure. A jet pump is used to create and maintain the vacuum. The accumulator level is controlled by adjusting top paraffin product flow that is returned to dehydrogenation process of paraffin. The hot oil to the reboiler and hot reflux to column are on flow control, but the cool reflux to column is fixed. The bottom level is directly controlled by adjusting bottom product flow to the LAB column.

There are two important temperatures in paraffin column: upper temperature and lower temperature, which reflect distillation effect and are used to direct normal operation. The paraffin column is very important to LAB productivity of the plant since any LAB in top paraffin product will suffer losses. The paraffin column is the throughput bottleneck in the distillation columns, and can be easily overloaded.

The LAB column is also a packed column and its operation is similar to the paraffin column's. The top product is LAB that can be used to produce LASs. There are also two important temperatures in LAB column: upper temperature and lower temperature, which reflect distillation effect and are used to instruct normal operation. The LAB column is a column of finished product in which any LAB in bottom heavy LAB product will suffer losses. It is important for the LAB column to maintain steady operation.

In conclusion, the columns need to be maintained close to optimal operating conditions lay at some constraints. Nevertheless, regulatory controls of distillation column are difficult to achieve better control performance all the time for moving the column to its optimal operating point and rejecting disturbances on the controlled variables. Therefore, for the control of distillation column, especially a series of columns affected by many constraints, MPC can be used to improve control performance characterized by a reduction in the variability of the controlled variables through information gathering, process analysis, and constrained multivariable optimisation.

3. MODELLING AND MPC OF THE COLUMNS

There exist several difficulties in terms of controlling the columns of the LAB plant: 1) there are some constraints on equipment capacities and process operations. 2) The flow rate and properties of feed to distillation columns are not constant because it is dependent on the operating conditions of the upstream alkylation section. 3) There are couples among various manipulated variables of each columns, especially two-end temperature control of the column is adopted. 4) There are different time-delays in the responses of CVs versus MVs and some channels show non-linearity. The skilled operators can operate the columns based on their experience and knowledge, but they need to work intensively and can't optimise the columns. Therefore, it is necessary for the distillation columns to implement MPC system in order to realize steady operation and process optimisation. The modelling procedure and results of distillation columns and the structure and implementation of MPC system are given below.

3.1 Modelling of the columns

Dynamic models play a central role in MPC system. It has been shown that modelling is the most difficult and time-consuming work in an MPC project. Generally, the classical black-box model identification methodology is used for MPC controllers. Nevertheless, a good knowledge of the process is still required to bring out possible model structures and define an experiment design.

The modeling procedure of the distillation columns may be summarized as the following steps:

- 1) studying and understanding the columns operation from collected data sets,
- 2) determining the model structures of the columns and designing test signals,
- 3) implementing open-loop multivariable tests of the columns and dealing with the relevant data,
- 4) estimating the open-loop step response (or impulse response) models of the columns and editing these models,
- 5) validating and assessing the estimated models of the columns.

The MVs, DVs and CVs of the MPC controller for the distillation columns are listed in Table 1. The choice of CVs was fixed by specifications of the columns including tray temperatures and levels of the reboilers and/or the accumulators.

A dynamic model was developed with adding test signals in the manipulated and disturbance variables on the distillation columns and estimating model parameter from collected data. The sample time was taken to be 2 min. The data collections lasted between 48 and 72 hours. Each time, 98 variables were measured and selected. Data pretreatment and model identification were achieved using a professional off-line identification tool.

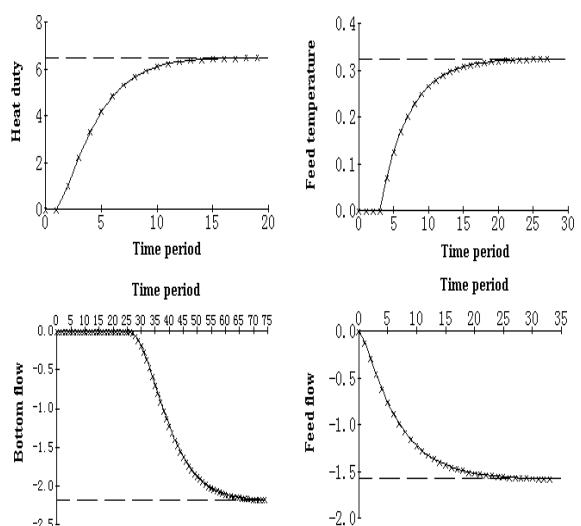


Fig. 2 Open-loop model of bottom temperature in HF stripper

The estimated model of the columns describes the multivariable relationship between 20 inputs and 12 outputs. Here, the open-loop step response models of the bottom temperature in HF stripper are shown in Figure 2 as examples. To demonstrate model validation, we use fresh data to test how well the model output agrees with the measured bottom temperature. Figure 3 shows the test result obtained over more than 900 time period.

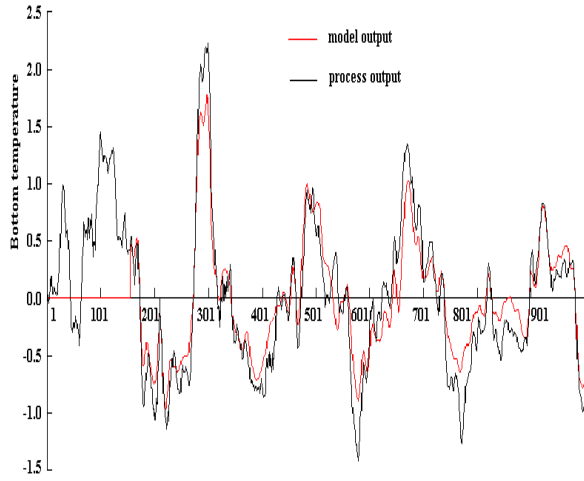


Fig. 3 Model validation of bottom temperature in HF stripper

3.2 MPC of the columns

MPC is a control strategy which predicts the future behavior of process in a control envelope from the past moves of MVs with using the dynamic models of the CVs versus MVs and determines the future moves of MVs in order that CVs will match the target values as close as possible in each control cycle. We adopted Model Algorithmic Control (MAC) to realize the overall control of the distillation columns.

The relationship between CVs and MVs of the columns is given in impulse response that can be achieved by process modelling:

$$y_m(k) = \sum_{j=1}^N \hat{h}_j u(k-j) \quad (1)$$

Where, \hat{h}_j is the coefficients of a impulse response, y is CV, u is MV, and N is number of impulse. The subscript m denotes model output. Model vector $\mathbf{h} = [\hat{h}_1 \dots \hat{h}_N]^T$ is often saved in host computer and names internal model.

The closed-loop predictive model is obtained in terms of equation (2) as follows:

$$\begin{aligned} y_p(k+i) &= y_m(k+i) + [y(k) - y_m(k)] \\ &= y(k) + [y_m(k+i) - y_m(k)] \\ &= y(k) + \sum_{j=1}^N \hat{h}_j [\Delta u(k+i-j) + \Delta u(k+i-j-1) + \dots + \Delta u(k+2-j) + \Delta u(k+1-j)] \end{aligned} \quad (2)$$

Where the subscript m denotes model predictive output, $y(k)$ is current process output.

The reference trajectory that is used to smooth expected output from $y(k)$ to setpoint y_{sp} adopts first order exponential form in MAC as follows:

$$\begin{cases} y_r(k+1) = \alpha^i y(k) + (1 - \alpha^i) y_{sp} & i = 1, 2, \dots, P \\ y_r(k) = y(k) \end{cases} \quad (3)$$

Where, $\alpha = \exp(-T/\tau)$, T is sample time and τ is constant time of reference trajectory.

To meet the above control goals, the objective function can be formulated as follows:

$$J = [\mathbf{y}_p(k+1) - \mathbf{y}_r(k+1)]^T \mathbf{Q} [\mathbf{y}_p(k+1) - \mathbf{y}_r(k+1)] + \mathbf{u}_2^T(k) \mathbf{R} \mathbf{u}_2(k) \quad (4)$$

Where,

$$\mathbf{Q} = \text{diag}[q_1, q_2, \dots, q_P]$$

$$\mathbf{R} = \text{diag}[r_1, r_2, \dots, r_M]$$

$$\mathbf{y}_r(k+1) = [y_r(k+1), y_r(k+2), \dots, y_r(k+P)]^T$$

We have combined our process control experience, design skills and process modelling capabilities into the MPC application. The MPC system shown in Figure 4 is implemented via a MPC controller and divided to four subsystems according to distillation column process. Each subsystem turns on/off independently with the others and mainly takes charge one column.

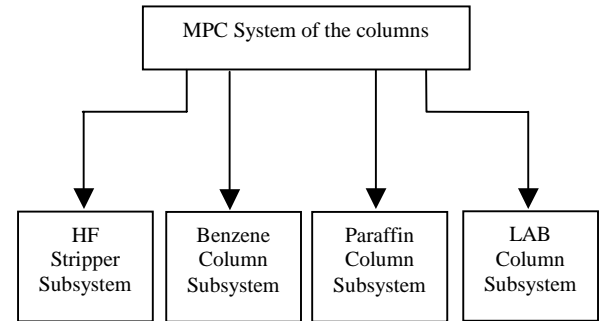


Fig.4 MPC system structure of distillation columns in LAB plant

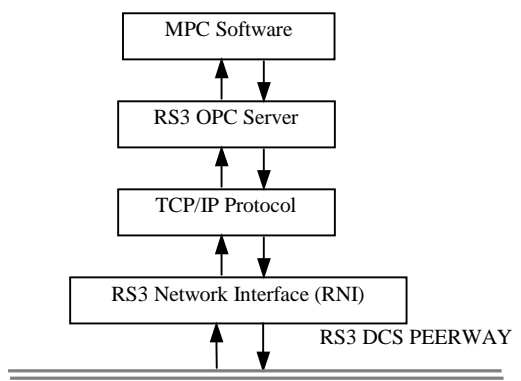


Fig.5 Connection between MPC system and DCS system

After four subsystems turn on, the over MPC system simultaneously adjusts the setpoint values for 12 regulatory loops of the distillation columns, while continuously checking the status of process and equipment limits. To handle the interactions between the different subsystems, the HF stripper bottom temperature is used as a CV in the HF stripper subsystem and its measurement as a DV in the subsequent Benzene column subsystem, the HF stripper bottom flow is a MV in the HF stripper subsystem and its measurement as a DV in the Benzene column subsystem, the downstream columns may be deduced by analogy. By integrating controls into a single controller, interactions across entire distillation columns can be better managed.

The MPC software named APC-Adcon is provided by Zhejiang Supcon Software Ltd.. APC-Adcon has two kinds of optimising functions. One is steady optimising function, which solves the steady optimal values of a CV and MV as target values for dynamic optimising. The other is the dynamic optimising function, which calculates the optimal future path of an MV. The MPC software is equipped in the host computer of an existing distributed control system (DCS) RS3 made in Fisher-Rosemount and the communication between host computer and DCS is seamless connection based on RNI for RS3 and OPC interface. Figure 5 shows the connection between MPC system and DCS system.

Table 1 Configuration for distillation columns MPC system

Controlled Variables	Manipulated Variables	Disturbance Variables
CV1-HF stripper bottom temperature	MV1-HF stripper reboiler duty	DV1-Reactor feed flow
CV2-HF stripper reboiler level	MV2-HF stripper bottom flow	DV2-Reactor feed temperature
CV3-Benzene column upper tray temperature	MV3-Benzene column reflux flow	DV3-HF stripper bottom flow
CV4-enzene column lower tray temperature	MV4-Benzene column reboiler duty	DV4-HF stripper bottom temperature
CV5-Benzene column reboiler level	MV5-Benzene column bottom flow	DV5-Benzene column bottom flow
CV6-Paraffin column upper tray temperature	MV6-Paraffin column hot reflux flow	DV6-Benzene column bottom temperature
CV7-Paraffin column lower tray temperature	MV7-Paraffin column reboiler heat duty	DV7-Paraffin column bottom flow
CV8-Paraffin column reboiler level	MV8-Paraffin column bottom flow	DV8-Paraffin column bottom temperature
CV9-Paraffin column accumulator level	MV9-Paraffin column top paraffin flow	
CV10-LAB column upper tray temperature	MV10-LAB column hot reflux flow	
CV11-LAB column lower tray temperature	MV11-LAB column reboiler heat duty	
CV12-LAB column accumulator level	MV12-LAB column top LAB flow	

4. PERFORMANCE OF THE APC SYSTEM

After the MPC controller was tuned, it had been tested on-line for three months. The comparison of the performance before and after the MPC implementation is summarized. The comparison of product quality of LAB plant and LAB in recycle paraffin is given in Table 2. The result of control performance comparison for LAB column MPC subsystem is shown in Figure 6 and Figure 7.

The MPC system is superior to human supervisory control in follow aspects:

- 1) The skill of most high experienced operator has been implemented by the MPC system.

- 2) Operation and compensation is executed at fairly frequent intervals. In case of a skilled operator, operation frequency is about 20 minutes, while, in case of the MPC system, it is 2 minutes.
- 3) Operator control manipulates the process variables in sequence. Nevertheless, the MPC control can manage several process variables in parallel.

After the implementation of the MPC system, the deviation of the main process variables became one half of that before implementation. As a result, The over economical merit from this implementation is approximately over one million Yuan by reducing the consumption of energy, improving product purity, and minimizing operating cost.

Table 2 Comparison of product quality of LAB plant

Quality Index of LAB Plant	Average Value		Standard Deviation	
	Before	After	Before	After
LAB TNP %	Base	-0.01%	0.094	0.048
LAB BR	Base	-0.37	1.580	0.820
LAB in recycle paraffin	Base	-0.01%	0.280	0.071

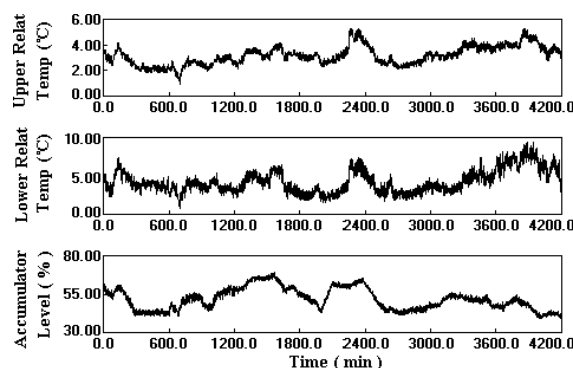


Fig. 6 Performance of the CVs of LAB column before MPC implementation

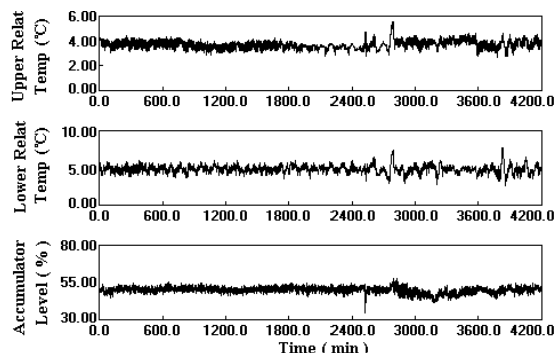


Fig. 7 Performance of the CVs of LAB column after MPC implementation

5. CONCLUSION

This paper presents process modelling and APC system of the distillation columns in LAB plant. Industrial application results show that the APC controller is superior to conventional control. The APC control can maintain the best process operation for a long time and realize ultimate operating potential of the distillation columns. Economic benefits are achieved by using the APC system when the process model is constructed correctly and MPC controller is set compatibly.

Kister, H.Z.(1990). *Distillation Operation*, McGraw-Hill, New York.

Wang, S.Q. et al, (2001). *Advanced Process Control and its Applications*, Chemical Industry Press (in Chinese), Beijing.

Riggs, J.B. (1998) Improve distillation column control. *Chemical Engineering Progress*, 10: 31-47.

Shinskey, F.G. (1984) *Distillation control*, 2nd Edition, McGraw-Hill, New York.

Luyben, W.L. (1992) *Practical distillation control*, Van Nostrand Reinhold, New York.

Lundstrom, P., S. Skogestad, (1995) Opportunities and difficulties with 5 × 5 distillation control. *Journal of Process Control*, 5(4): 249-261.

Jimenez, A. et al, (2001) Analysis of control properties of conventional and nonconventional distillation sequences. *Ind. Eng. Chem. Res.*, 40: 3757-3761.

Huang, H.T., J.B. Riggs, (2002) Comparison of PI and MPC for control of a gas recovery unit. *Journal of Process Control*, 12: 163-173.